Biophysical Journal
Article

Biophysical Society

Inhibition of platelet-surface-bound proteins during coagulation under flow I: TFPI

Kenji Miyazawa,[1] Aaron L. Fogelson,[2,3] and Karin Leiderman[4,5,*]
[1]Quantitative Biosciences and Engineering, Colorado School of Mines, Golden, Colorado; [2]Department of Mathematics, University of Utah, Salt Lake City, Utah; [3]Department of Biomedical Engineering, University of Utah, Salt Lake City, Utah; [4]Mathematics Department, University of North Carolina at Chapel Hill, Chapel Hill, North Carolina; and [5]Computational Medicine Program, University of North Carolina at Chapel Hill, Chapel Hill, North Carolina

ABSTRACT Blood coagulation is a self-repair process regulated by activated platelet surfaces, clotting factors, and inhibitors. Tissue factor pathway inhibitor (TFPI) is one such inhibitor, well known for its inhibitory action on the active enzyme complex comprising tissue factor (TF) and activated clotting factor VII. This complex forms when TF embedded in the blood vessel wall is exposed by injury and initiates coagulation. A different role for TFPI, independent of TF:VIIa, has recently been discovered whereby TFPI binds a partially cleaved form of clotting factor V (FV-h) and impedes thrombin generation on activated platelet surfaces. We hypothesized that this TF-independent inhibitory mechanism on platelet surfaces would be a more effective platform for TFPI than the TF-dependent one. We examined the effects of this mechanism on thrombin generation by including the relevant biochemical reactions into our previously validated mathematical model. Additionally, we included the ability of TFPI to bind directly to and inhibit platelet-bound FXa. The new model was sensitive to TFPI levels and, under some conditions, TFPI could completely shut down thrombin generation. This sensitivity was due entirely to the surface-mediated inhibitory reactions. The addition of the new TFPI reactions increased the threshold level of TF needed to elicit a strong thrombin response under flow, but the concentration of thrombin achieved, if there was a response, was unchanged. Interestingly, we found that direct binding of TFPI to platelet-bound FXa had a greater anticoagulant effect than did TFPI binding to FV-h alone, but that the greatest effects occurred if both reactions were at play. The model includes activated platelets' release of FV species, and we explored the impact of varying the FV/FV-h composition of the releasate. We found that reducing the zymogen FV fraction of this pool, and thus increasing the fraction that is FV-h, led to acceleration of thrombin generation.

SIGNIFICANCE We developed a novel mathematical model of flow-mediated coagulation that was sensitive to changes in TFPI levels, especially at low tissue factor densities, which is consistent with experimentally observed effects of TFPI under flow. The sensitivity of the system was entirely due to inhibition reactions that occurred on activated platelet surfaces. TFPI is a potential therapeutic target to rescue thrombin generation in bleeding disorders; thus, our model, which is based on recent discoveries about its inhibitory mechanism, could serve as powerful tool to explore the role of TFPI as a modifier of thrombin generation.

INTRODUCTION

Hemostasis is a self-defense mechanism initiated by a vascular injury, whereby a blood clot forms to stop bleeding. It consists of two intertwined processes, platelet aggregation and coagulation, that begin when the injury exposes subendothelial collagen and tissue factor (TF), respectively. Platelets adhere to the collagen and become activated, which enhances their ability to aggregate and plug the injury. They also expose phospholipid binding sites on their surfaces to which plasma proteins, called clotting factors, can bind. Activated platelets release proteins from internal stores, including additional clotting factors, inhibitors, and agonists that further platelet activation (1,2). Coagulation is a network of enzymatic reactions that involves clotting factors and inhibitors and culminates in the production of the enzyme thrombin. Thrombin cleaves the soluble plasma protein fibrinogen to form insoluble fibrin, which polymerizes to form a cross-linked hydrogel that physically stabilizes the growing platelet aggregates.

Submitted January 8, 2022, and accepted for publication November 15, 2022.

*Correspondence: karin.leiderman@unc.edu

Editor: Mark Alber.

https://doi.org/10.1016/j.bpj.2022.11.023

Thrombin generation is necessary to the clotting process and is accomplished by the sequential formation of three enzyme-cofactor complexes. One is formed on the injured vascular wall by TF (cofactor) and activated coagulation factor VIIa (FVIIa), and the other two are formed on the surfaces of activated platelets by coagulation factors VIIIa (cofactor) and IXa (the FVIIIa:FIXa "tenase" complex) and by coagulation factors Va (cofactor) and Xa (the FVa:FXa "prothombinase" complex). It is the prothrombinase complex that enzymatically converts the plasma protein prothrombin into thrombin. Because of the essential roles of the platelet-bound enzyme complexes, the availability of binding sites on the surfaces of activated platelets for the coagulation factors that form these complexes is an important regulator of coagulation; robust thrombin generation does not occur if these complexes cannot form. Furthermore, the requirement that important coagulation reactions occur on activated platelets helps localize coagulation to the site of injury instead of it being spread throughout the vasculature by the flowing blood. The coagulation process involves positive and negative feedback loops, which enable thrombin generation to exhibit threshold-like behavior; substantial thrombin generation occurs only after a sufficient level of TF is exposed. On the other hand, a lack of sufficient inhibitors, which take part in the negative feedback loops, may lead to excessive clot growth and thrombosis, while abnormally high concentrations of inhibitors may impede coagulation and lead to excessive bleeding. The many regulators of clotting normally work together to maintain a proper balance between promoting and inhibiting processes. Bleeding and clotting disorders that manifest as deficiencies or mutations in clotting proteins, such as hemophilia, can disrupt this balance, with serious consequences.

Tissue factor pathway inhibitor (TFPI) has long been regarded as a key inhibitory regulator of coagulation. It is best known for its inhibition of TF:VIIa activity owing to formation of a quaternary complex that includes TF:VIIa, TFPI, and FXa, but more recently has become known to inhibit through FV (more details of this are given below). In humans, there are two TFPI types: TFPIα and TFPIβ (3,4). In this study, we focus only on TFPIα. TFPIα is found in human plasma (4) and is also released from platelets upon the platelets' activation (5). TFPIα contains three Kunitz domains and a C-terminus tail. TFPI binds to TF:VIIa and FXa through its Kunitz 1 and 2 domains, respectively (6,7), and to protein S via Kunitz 3 domain (3). It binds to some FV variants through the C-terminus tail, which is important for its inhibitory action.

Coagulation factor V (FV) is another essential protein for thrombin generation. In its fully cleaved/activated form (FVa), it serves as the cofactor for FXa within the prothrombinase complex that converts prothrombin to thrombin (8,9). In 2001, a novel bleeding disorder was discovered in a family from East Texas (10) that was related to FV (11). A genetic mutation caused increased expression of an alternative form of FV that was "partially" cleaved and thus named FV-short. Later, FV-short was shown to bind tightly to TFPIα, which was in line with the observed increased levels of TFPIα in the East Texas family. It is now believed that the increased TFPIα levels are the cause of their bleeding phenotype (12). Since the FV-short discovery, it has been recognized that normal FV is physiologically cleaved into two different forms through distinct mechanisms: FXa cleaves what is called the basic region of the B domain, leading to what we call the partially cleaved/activated form (13,14), and thrombin cleaves the entire B domain, leading to the fully cleaved/activated form (15). There is some evidence that FXa can fully cleave FV into FVa, but it does so rather inefficiently (16,17).

Variants of FV are stored in a platelet's α-granules and secreted after the platelet is activated. (8,18,19). Platelet-secreted FV may be partially or fully cleaved, but there are little data in the literature on the detailed make-up of platelet-secreted FV molecules or on their susceptibility to be bound by TFPIα. In the rest of this paper, we denote the partially cleaved or platelet stored FV as FV-h, for half-cleaved/activated, and FVa as the fully activated form. Of note, FV-short, FV-h, and FVa possess similar cofactor activity within the prothrombinase complex, but only FV-short or FV-h can bind to TFPIα (20).

Early biochemical studies showed that TFPIα has varying effects on thrombin generation depending on the forms of FV that are present. Mast and Broze (21) performed prothrombin activation assays with mixtures containing prothrombin, FXa, lipids, TFPIα, and varying forms of FV. With FVa and FXa, addition of TFPIα produced modest inhibition of thrombin generation. With FV and FXa, however, addition of TFPIα substantially impeded thrombin generation. Interestingly, when FV was preincubated with FXa, subsequent addition of TFPIα had a decreased inhibitory effect (i.e., more thrombin was generated) in comparison with the case in which FV, FXa, and TFPIα were added at the same time. These results suggest that TFPIα inhibits thrombin generation through a variety of mechanisms that could act before and/or after the formation of prothrombinase (with either FV-h or FVa). The presence of lipids may also have enhanced or mediated the inhibitory mechanisms in that study. In later biochemical studies, TFPIα was shown to inhibit prothrombinase early in thrombin generation via FV-h (13,22). It was suggested that TFPIα inhibits thrombin generation through multiple mechanisms, including direct binding of TFPIα with FV-h, interactions with FV-h in ways that either prevent FXa from binding FV-h or that cause it to bind in a way that does not promote thrombin generation, and of course the well-known binding interaction between TFPIα and FXa (22). The relative importance of these various mechanisms and

interactions, along with the effects of lipid or platelet surfaces on them, remains unclear.

Mathematical models are powerful tools that can be used to gain insight into complex biological systems. Our group has developed mechanistic, experimentally validated mathematical models of flow-mediated coagulation that have led to novel insights related to phenotypic variation observed in bleeding and thrombotic disorders (23–28). These models include activated platelet surfaces as the site of many coagulation reactions, thus allowing the availability of these surfaces and their properties to regulate coagulation. In simulations with our previous models, procoagulant platelet-surface reactions are critical to the production of thrombin. The availability of binding sites on the procoagulant surfaces of platelets deposited onto the injury play an important regulatory role. Other mathematical models that simulate thrombin generation in the absence of flow (29) have also shown that thrombin generation is sensitive to variation in normal levels of clotting factors in healthy individuals (30) and in hemophilia (31); these models generally assume that the reactions occur in the presence of an excess of lipid surfaces and do not look specifically at events on limited platelet surfaces as regulators of coagulation.

Collectively, these experimental and mathematical findings raise the question: would blocking the binding of TFPIα to FXa and/or FV-h on the platelet surface rescue thrombin generation in hemophilia? Platelet-surface-dependent, TFPIα-mediated inhibition has not yet been included in any mathematical models of coagulation. We extended our previous model of flow-mediated coagulation to include a detailed description of platelet-surface-mediated TFPIα inhibition, via platelet-bound FXa and FV-h. In our previous model, TFPIα was assumed to bind FXa in the plasma phase and the TFPIα:Xa complex could subsequently bind to TF:VIIa. However, TFPIα had very little impact on thrombin generation through this mechanism because the overwhelmingly dominant inhibitor was dilution of fluid-phase enzymes and active cofactors as flow carried them downstream away from the injury. This was true for all shear rates examined with the model (23). An alternative mechanism of TFPIα inhibition of TF:VIIIa, in which TFPIα binds to TF:VIIa:Xa, was also investigated in this model, and it was found that for this mechanism to work, FXa would have to remain bound to TF:VIIa for a long time, in which case its own presence could inhibit TF:VIIa without a role for TFPIα (24).

A major motivation for the current study is to explore the effectiveness of platelet-surface anticoagulant reactions in the regulation of thrombin generation under flow. To our knowledge, our studies are the first to examine the effect of TFPI- and antithrombin (AT)-mediated inhibition occurring directly on platelet surfaces with modeling (we studied AT inhibition with and without heparin in a companion study (32)). The key new additions to the model in this paper are that 1) FV can be partially activated to FV-h by FXa, 2) FV-h can bind FXa to form active prothrombinase on the platelet surface, 3) TFPIα can directly bind to FV-h in the fluid or bound to the platelet surface, and 4) TFPIα can bind directly to FXa that is bound to the platelet surface. The aforementioned experiments suggested that early in the coagulation reactions, before much thrombin has been generated, active prothrombinase forms on activated platelet surfaces by binding of FXa and FV-h, and that the activity of FXa, FV-h, and/or the prothrombinase formed from them is significantly impacted by TFPIα.

The assumptions regarding TFPIα resulted in many binding combinations that either interfered with the formation of prothrombinase or directly inhibited the already formed complex. We studied how the additional TFPIα inhibition affected the TF threshold for various shear rates and whether inhibition via FXa or FV-h had a larger inhibitory effect. Our results demonstrated new and significant sensitivity of simulated thrombin generation to TFPIα levels that was entirely due to inhibition reactions occurring on platelet surfaces. Direct binding of TFPIα to FXa on the platelet surface had a somewhat stronger inhibitory effect than binding to FV-h when each was considered in isolation, but the greatest inhibitory effect occurred when both mechanisms were at play.

MATERIALS AND METHODS

Previous mathematical model review

Here we give a brief review of our previously developed mathematical model of flow-mediated coagulation (23–25) More details about this model and its sensitivity to parameters can be found elsewhere (27). The model simulates the coagulation reactions occurring in a small reaction zone (RZ) above an injury where TF in the subendothelium (SE) is exposed (Fig. S1). Clotting factors and platelets are transported into and out of the RZ by a combination of flow and diffusion, using a mass transfer coefficient whose value is a function of vessel and injury size, the flow's shear rate, and the species' diffusivity. Clotting factor concentrations in the RZ change owing to their involvement in the coagulation reactions, their binding with activated platelets, and transport in and out of the zone. Similarly, platelet concentrations change as platelets adhere to the injured wall and become activated, and as other platelets are transported in and out of the zone. As platelets build up in the RZ, the height and volume of the RZ increase with the volume of plasma and concentration of platelets in it changing accordingly. Deposition of platelets also blocks the activity of TF:VIIa on the subendothelium in proportion to the fraction of the subendothelium which the platelets cover. The concentration of each species in the RZ plasma is tracked with an ordinary differential equation; this choice relies on the assumption that each species is uniformly distributed (well-mixed) within the reaction zone. An additional well-mixed endothelial zone (EZ) is located adjacent to the RZ, in the direction perpendicular to the flow, with height equal to that of the RZ and width dependent on the flow shear rate and protein diffusion coefficients. The EZ is where active protein C (APC) is produced by a complex formed by thrombomodulin in that zone and thrombin that has diffused to the EZ from the RZ. This APC either diffuses into the RZ or is carried away by the flow.

There are three forms of platelets in the model: unactivated platelets that exist in the plasma phase, activated platelets that are directly attached to SE, and activated platelets in the thrombus that are not directly attached

to SE. Activation of platelets is achieved by contact with the SE, interaction with thrombin, or by exposure to already activated platelets (this is an indirect way to model release of agonists from platelet stores). Activated platelets provide the membrane surface necessary for coagulation factors to bind and react. Each activated platelet expresses specified types and numbers of binding sites to which coagulation proteins can selectively bind.

New model extensions

The key new extensions to the model are described in the next few sections. They involve partially activated FV (FV-h) and its interaction with FXa and TFPIα. The additional reactions describe the generation of FV-h, TFPIα binding to FV-h and FXa, direct inhibition of FV-h or FXa within prothrombinase by TFPIα, inhibition of FV-h:FXa prothrombinase assembly, and full activation of FV-h by thrombin. All of these additional reactions involving FV-h, FXa, and TFPI are sketched in Fig. 1 and listed in Table 1 with any available kinetic rate constants from the literature. In Eq. 1, we show the evolution equation for the concentration of one of the new species as an example of the nature of the model's equations. A full listing of the model equations and parameter values is given in the section S2 of supporting material. Note that for this paper, the ordinary differential equations labeled 1–104 comprise the model. The remaining equations are added for the companion paper.

The model uses the following notation: Z_i and E_i to refer to a specific zymogen or pro-cofactor species and the corresponding enzyme or cofactor species when they are in the plasma, and Z_i^m and E_i^m refer to the surface-bound versions of these proteins (e.g., E_7^m refers to the TF:VIIa complex on the subendothelium, and E_5 and E_5^m refer to factor Va in the plasma and bound to a platelet surface, respectively). The new species, partially cleaved factor V is denoted E_5^h. The concentrations of the proteins are denoted similarly, but with lowercase z and e. Therefore, e_5^m is the concentration of platelet-bound factor Va. The symbols TF,P_2,P_5,P_8,P_9,P_{10}, and P_{11} are used to denote TF and the platelet binding sites for prothrombin, FV/FVa, FVIII/FVIIIa, FIX/FIXa, FX/FXa, and FXI, respectively. For the platelet binding sites specific to thrombin, factor IXa, and factor XIa, we use the symbols P_2^*, P_9^*, and P_{11}^*. The concentrations of binding sites are indicated similarly but with lowercase p. We denote the complex of Z_i and E_j by $Z_i : E_j$ and its concentration by $[Z_i : E_j]$, so, for example, $TFPI\alpha : E_{10}^m$ denotes TFPIα bound to platelet-bound factor Xa, and $[\text{TFPI}\alpha : E_{10}^m]$ refers to its concentration.

Generation and activation of FV-h

We assumed there are two major sources of FV-h: activation of FV by FXa (reaction 25 from Table 1) and secretion by platelets upon their activation. We assume here that FXa can only partially activate FV to FV-h. We also assume that a total of 3000 FV and FV-h molecules are released per activated platelet (33), and denote by h_5 the fraction of these which are FV-h molecules. For most of the simulations in this study we fixed $h_5 = 0.5$, but we also reported on simulations examining the model result's sensitivity to variations in h_5. We assumed that FV and FV-h bind to the same platelet binding sites (P_5) and that platelet-bound FV-h and FXa can bind to one another to produce an early form of prothrombinase FV-h:FXa. We assumed that FV-h can be fully activated by thrombin, in the plasma, on the platelet surface, and within the FV-h:FXa complex (reactions 2, 6, and 9 in Table 1).

TFPIα binding to FV-h and FXa

In our previous model (23–25), TFPIα could bind only to fluid-phase FXa. Here, we also allowed TFPIα to bind directly from the plasma to platelet-bound Xa (reaction 22 in Table 1) and to FV-h in the plasma or bound to a platelet (reactions 1 and 5 in Table 1). We assumed that TFPIα cannot bind to FVa because the FV's B domain is completely removed upon full activation. This assumption is supported by the fact that TFPI binds FV in a form where only part of the B domain is cleaved upon activation by FXa, leaving the acidic region to bind the C-terminus of TFPI (13). We assumed that the entire 20% of plasma TFPI is the full-length form, which can interact with both FV-h and FXa. Differentiation between the truncated form and full-length forms of TFPI in the plasma is the subject for future research. Furthermore, we assumed that when FXa or FV-h is bound to TFPIα, it cannot subsequently form an FV-h:FXa prothrombinase complex. We based this assumption on the proximity of the binding sites on FV-h, FXa, and TFPIα for each other, the large size and flexibility of a TFPIα molecule, and the previous suggestion that this reaction is blocked (13,22,34). We do not consider the secretion of TFPIα from platelets in this model extension.

Direct inhibition of prothrombinase

We assume that prothrombinase is formed by the binding of platelet-bound FXa to platelet-bound FVa (FVa:FXa), as in our previous model, or to

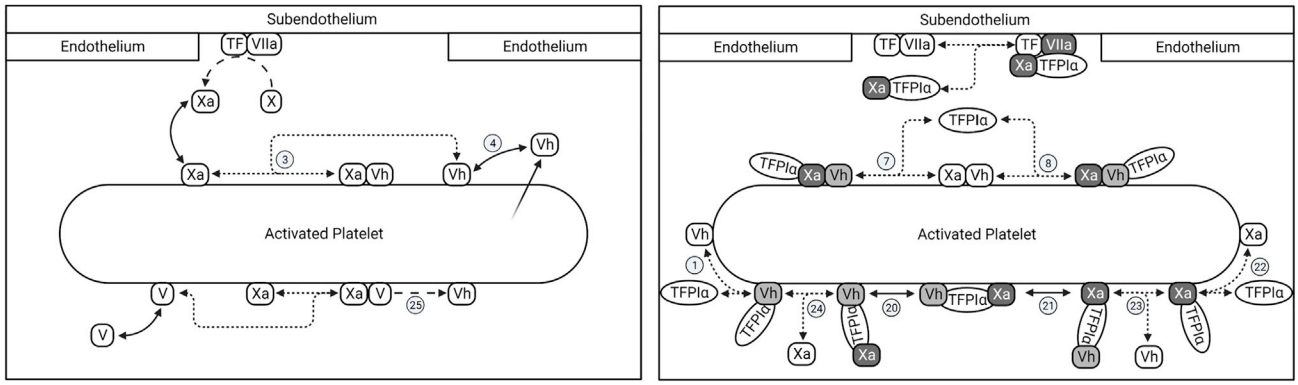

FIGURE 1 Newly added reactions involving FV-h, FXa, and TFPIα. (*Left*) Generation of FV-h through the activation of FV by FXa and secretion from platelet stores, binding/unbinding of coagulation factors to the platelet surface, and the assembly of prothrombinase. (*Right*) Binding of TFPIα to platelet-bound FXa, FV-h, and prothrombinase, and inhibition of prothrombinase assembly by TFPIα. Line styles indicate different interactions: dense dashed lines, binding and unbinding of protein pairs; longer dashed lines, catalytic reaction steps; solid double arrow, binding and unbinding of proteins with platelet surface; arrow with faded tail, secretion of protein from platelet. Light shade with black font indicates TFPI-bound and inhibited cofactors, and heavier shade with white font indicates TFPIα-bound and inhibited enzymes. FV is also secreted from platelet stores and can be activated by thrombin, but this is not shown because they were included in an earlier model. Circled numbers indicate reaction number listed in Table 1. To see this figure in color, go online.

TABLE 1 List of reactions added to the model and their kinetic rate constants, with literature references (k^+ shows forward reaction rate, k^- shows backward reaction rate, and k^{cat} indicates catalytic reaction rate)

Reaction list							
Reaction no.	Reactants	Catalytic intermediate	Products	k^+ (M^{-1} s^{-1})	k^- (s^{-1})	k^{cat} (s^{-1})	Note
1	E_5^{hm} + TFPI		TFPI:E_5^{hm}	$5.0(10)^7$	$4.5(10)^{-3}$		a
2	E_5^{hm} + E_2^m	E_5^{hm}:E_2^m	E_5^m + EE_2^m	$1.73(10)^7$	1	0.23	b
3	E_5^{hm} + E_{10}^m		E_{10}^m:E_5^{hm}	$1.0(10)^8$	0.01		c
4	E_5^h + P_5		E_5^{hm}	$5.7(10)^7$	0.17		d
5	E_5^h + TFPI		TFPI:E_5^h	$5.0(10)^7$	$4.5(10)^{-3}$		a
6	E_5^h + E_2	E_5^h:E_2	E_5 + E_2	$1.73(10)^7$	1.0	0.23	b
7	E_{10}^m:E_5^{hm} + TFPI		TFPI:E_{10}^m:E_5^{hm}	$1.6(10)^7$	$3.3(10)^{-4}$		e
8	E_{10}^m:E_5^{hm} + TFPI		E_{10}^m:E_5^{hm}:TFPI	$5.0(10)^7$	$4.5(10)^{-3}$		a
9	E_{10}^m:E_5^{hm} + E_2^m	E_{10}^m:E_5^{hm}:E_2^m	E_{10}^m:E_5^m + E_2^m	$1.73(10)^7$	1.0	0.23	b
10	E_{10}^m:E_5^{hm} + Z_2^m	Z_2^m:E_{10}^m:E_5^{hm}	E_{10}^m:E_5^{hm} + E_2	$7.13(10)^7$	1.0	27.5	f
11	TFPI:E_5^{hm} + E_{10}^m		E_5^{hm}:TFPI:E_{10}^m	$1.6(10)^7$	$3.3(10)^{-4}$		e
12	TFPI:E_{10}^m + E_5^m		E_5^{hm}:TFPI:E_{10}^m	$5.0(10)^7$	$4.5(10)^{-3}$		a
13	TFPI:E_{10} + P_{10}		TFPI:E_{10}^m	$1.0(10)^7$	0.025		d
14	TFPI:E_5^h + P_5		TFPI:E_5^{hm}	$5.7(10)^7$	0.17		d
15	E_5^{hm} + APC	APC:E_5^{hm}	APC + $E_{5,dead}^{hm}$	$1.2(10)^8$	1.0	0.5	g
16	TFPI:E_{10} + E_5^h		E_5^h:TFPI:E_{10}	$5.0(10)^7$	$4.5(10)^{-3}$		a
17	TFPI:E_5^h + E_{10}		E_5^h:TFPI:E_{10}	$1.6(10)^7$	$3.3(10)^{-4}$		e
18	E_5^h:TFPI:E_{10} + P_5		E_5^{hm}:TFPI:E_{10}	$5.7(10)^7$	0.17		d
19	E_5^h:TFPI:E_{10} + P_{10}		E_5^h:TFPI:E_{10}^m	$1.0(10)^7$	0.025		d
20	E_5^{hm}:TFPI:E_{10} + P_{10}		E_5^{hm}:TFPI:E_{10}^m	$1.0(10)^7$	0.025		d
21	E_5^{hm}:TFPI:E_{10}^m + P_5		E_5^h:TFPI:E_{10}^m	$5.7(10)^7$	0.17		d
22	TFPI + E_{10}^m		TFPI:E_{10}^m	$1.6(10)^7$	$3.3(10)^{-4}$		e
23	TFPI:E_{10}^m + E_5^h		E_5^h:TFPI:E_{10}^m	$5.0(10)^7$	$4.5(10)^{-3}$		a
24	TFPI:E_5^{hm} + E_{10}		E_5^{hm}:TFPI:E_{10}	$1.6(10)^7$	$3.3(10)^{-4}$		e
25	Z_5^m + E_{10}^m	E_{10}^m:Z_5^m	E_5^{hm} + E_{10}^m	$1.0(10)^8$	1.0	0.046	h

Notes: (a) Binding of TFPIα to FV-h, $K_D = 9$ pM from Jeremy et al. (15). (b) Activation of FV by thrombin, $K_M = 7.1(10)^{-8}$ M from Monković and Tracy (35). (c) Binding between FV-h and FXa, $K_D = 1(10)^{-10}$ M from Mann (36). (d) FV-h binding platelet surface, $K_D = 3(10)^{-9}$ M from Krishnaswamy et al. (37). (e) TFPIα binding FXa, $K_D = 2(10)^{-11}$ M from Jesty et al. (38). (f) Prothrombin activation by prothrombinase that has FV-h, $K_M = 0.4$ μM from Petrillo et al. (20). (g) Inactivation of FV-h by activated protein C, $K_M = 12.5(10)^{-9}$ M from Solymoss et al. (39). (h) Generation of FV-h by FXa, $k_5^{cat} = 0.046$ s^{-1} and $K_M = 10.4(10)^{-9}$ M from Monković and Tracy (35).

platelet-bound FV-h (FV-h:FXa, reaction 3 in Table 1). Since FXa and FV-h can both be bound to TFPIα, via its Kunitz 2 domain and C-terminus region, respectively, we assume that FV-h:FXa can be directly inhibited by TFPIα binding either to FXa or to FV-h in the complex (reactions 7 and 8, respectively in Table 1). This is illustrated by the reactions shown on the top surface of the activated platelet in Fig. 1 (*right*). The binding kinetics for TFPIα binding to FXa or FV-h in the FV-h:FXa complex are considered to be the same as those for TFPIα's binding to FXa or FV-h outside of the complex. Both forms of prothrombinase (FVa:FXa and FV-h:FXa) are assumed to be active and able to cleave prothrombin (20), but the enzymatic function of FV-h:FXa is assumed to stop when TFPIα is bound to either the FV-h or FXa part of the complex. TFPIα does not inhibit the enzymatic function of standard prothrombinase FVa:FXa.

Inhibition of prothrombinase assembly

As mentioned above, we assume that TFPIα can be bound to both FXa and FV-h at the same time via its Kunitz 2 domain and C-terminus, respectively, but binding interactions between FXa and FV-h in that case are blocked. In this situation, TFPIα is inhibiting the assembly of FXa and FV-h into prothrombinase. The inhibition of assembly can occur through two different, two-step reactions: TFPIα binds to FV-h via its C-terminus first and then binds to FXa via its K2 domain (reaction 11 in Table 1), or TFPIα binds to FXa via its K2 domain first and then binds to FV-h via its C-terminus (reaction 12 in Table 1). This is illustrated by the reactions shown on the bottom surface of the activated platelet in Fig. 1 (*right*). Each coagulation factor to which TFPIα is bound can either be platelet bound or in the fluid. Thus, there are multiple situations to consider, including ones in which one of the coagulation factors in the FV-h: TFPIα:FXa complex is bound to the platelet membrane and the other factor is not bound to the membrane, but is held close to the platelet through its interaction with TFPIα (reactions 16–21 in Table 1). In such cases, the free end of the ternary complex can become attached to the membrane, or the membrane-bound end can detach from the surface and release the entire ternary complex into the fluid. The fluid-phase ternary complex can rebind to a platelet surface by either its FV-h or FXa, or it may be washed away by the flow.

Model equations

The reactions in Table 1 are translated into mathematical equations using the law of mass action. Equation 1 is an example of the type of equations that constitute the model. It describes the rate of change of the concentration of FV-h in the fluid by the processes of the binding and unbinding of FV-h from the platelet surface, its delivery or removal due to flow, its secretion from the platelet, its full activation by thrombin, and its binding to and unbinding from TFPIα:

$$\frac{de_5^h}{dt} = \underbrace{-k_5^{\text{on}} e_5^h\, p_5^{\text{avail}}}_{\text{FV-h binding to platelet}} + \underbrace{k_5^{\text{off}} e_5^{hm}}_{\text{FV-h unbinding from platelet}} + \underbrace{k_{\text{flow}}\left(e_5^{h,up} - e_5^h\right)}_{\text{FV-h flowing in/away from RZ}} + \underbrace{h_5 \cdot n_5 \cdot \frac{d}{dt}\left(\left[PL_a^s\right] + \left[PL_a^v\right]\right)}_{\text{FV-h secretion term}} - \underbrace{k^+_{e_5^h:e_2} e_2 e_5^h}_{\text{binding of FV-h to thrombin}} + \underbrace{k_{e_5^h:e_2}{}^- \left[E_5^h : E_2\right]}_{\text{dissociation of FV-h from thrombin}} - \underbrace{k^+_{e_5^h:\text{TFPI}} \cdot e_5^h \cdot TFPI}_{\text{TFPI binding FV-h}} + \underbrace{k_{e_5^h:\text{TFPI}}{}^- \cdot \left[E_5^h : TFPI\right]}_{\text{TFPI unbinding FV-h}}. \quad (1)$$

In this equation, p_5^{avail} denotes the concentration of platelet binding sites for FV, FV-h, and FVa that are not already bound to one of these species, n_5 denotes the total number of FV and FV-h molecules released by a platelet when it is activated, $e_5^{h,up}$ is the concentration of FV-h in the bulk plasma (generally set to 0), and $\frac{d}{dt}([PL_a^s]+[PL_a^v])$ is the rate at which platelets are activated. The other quantities are defined in Table 1.

RESULTS

Tissue factor and shear rate dependency

Here we examined how the variation in TF density and shear rate affected thrombin production with the additional TFPIα inhibitory mechanisms and compared the outcomes with those from our previous model. We focused on how TF and shear rate dependency differ for low (0.5 nM) and high (2.5 nM) TFPIα plasma concentrations. For various TF densities in the range 0–20 fmol/cm^2 and for shear rates 100/s, 500/s, and 1500/s, we performed simulations with the old and new models. We looked at two output metrics: the lag time, which we define as the time point at which the thrombin concentration first reaches 1 nM, and the thrombin concentration at 10 min. Fig. 2, *A* and *C* show the lag times and Fig. 2, *B* and *D* show the thrombin concentrations at 10 min. For both old and new models and for both TFPIα levels, the lag time decreased as the TF density increased and/or the shear rate decreased. The reason for these behaviors is that a higher TF density provides a larger initial stimulus and decreasing the shear rate slows the loss of essential enzymes from the RZ. Also, the thrombin concentrations at 10 min increased with the TF density, sharply at low TF densities and more gradually at high ones. In fact, the results indicated a threshold dependence on TF density in all cases examined. (We refer to curves of thrombin at 10 min versus TF density as threshold curves.) The thrombin concentration at 10 min was also affected by the shear rate; in particular, the level of TF necessary to achieve a high thrombin concentration depended on the shear rate and, for high TF, the thrombin concentration at 10 min was somewhat higher for lower shear rate.

In Fig. 2, results for the old and new models are indicated by gray and black lines, respectively. In Fig. 2, *A* and *C* we see that, for a given TF density, the newly added TFPIα inhibition increases the lag time, and that to achieve a particular lag time a larger TF density was needed with the new model. This is because the additional inhibition reactions made it more difficult for the system to accumulate FXa on platelet surfaces, and this slowed prothrombinase formation and thrombin generation. We see for both TFPIα levels that the change in lag time between the two models was greater at higher shear rate. For the low TFPIα level (Fig. 2 *A*), we see that for each shear rate, the curves for the two models converged as the TF density was increased, indicating that the effect of the additional inhibition is more pronounced at low TF densities. Compared with these results, we see that for the higher TFPIα level (Fig. 2 *C*), the differences between the two models were greater for each TF density and that a substantial effect of the additional inhibition persisted to much higher TF densities.

Turning to Fig. 2, *B* and *D*, we look at how the thrombin concentration at 10 min differs between the two models for different TF densities and shear rates. For each shear rate, the threshold TF density was increased by the additional TFPIα inhibition reactions, that is, the threshold curves were shifted to the right. For low TFPIα, the effect was small for shear rate 100/s and progressively increased as the shear rate was increased first to 500/s and then to 1500/s. For the range of TF densities that were above threshold for the old model and below threshold for the new one, there was a notable difference in the thrombin concentrations at 10 min. For TF densities that were below threshold for both models or above threshold for both models, there was little effect of the additional inhibition reactions. In particular, at high TF densities the thrombin concentrations at 10 min are very similar. For high TFPIα, the effects of the model changes are more dramatic. There is a much broader range of TF densities which for the old model are above threshold and for the new model are below threshold, and for TF in this range there was a substantial difference in the thrombin concentrations achieved with the two models.

In summary, a major effect of the additional platelet-surface-mediated TFPIα inhibition reactions was to increase the TF threshold for substantial thrombin production to a degree that increased with increasing plasma TFPIα levels. For TF densities that were above threshold for both models, the lag time was larger with the additional reactions. The magnitude of the extra delay in thrombin production engendered by the additional inhibition varied with the TF density and shear rate and was substantial for a range of TF densities and shear rate 1500/s for low TFPIα and for a much broader range of TF densities and all shear rates considered for high

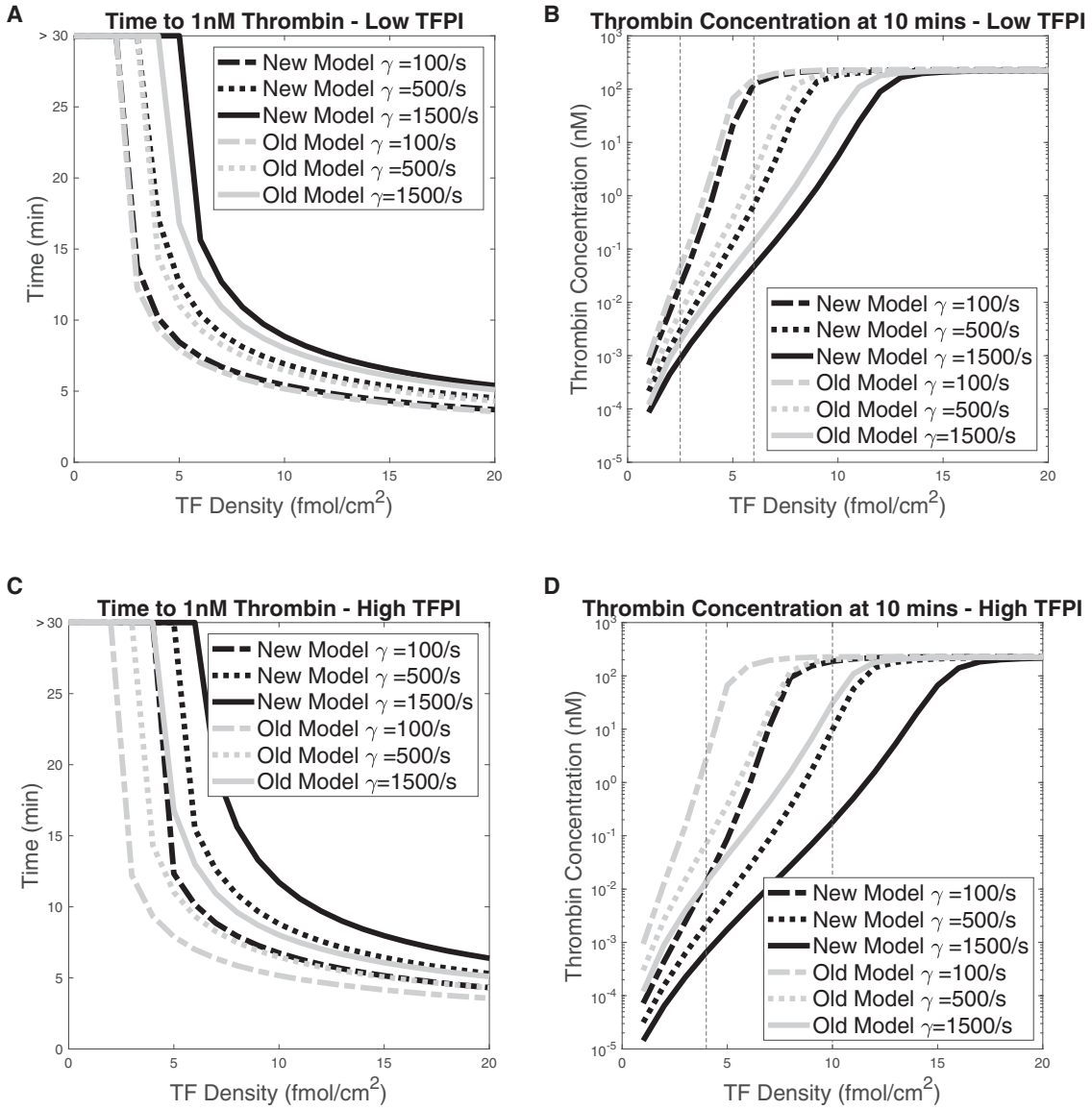

FIGURE 2 Effects of the TF level and shear rate on the lag time and the thrombin concentration threshold behavior. (*A* and *C*) Lag times and (*B* and *D*) thrombin concentration after 10 min for a range of TF densities and three different shear rates. Black curves represent the results from the new model, which includes the additional TFPIα-mediated inhibition reactions, and gray curves represent the results from the old model, where TFPIα could only bind to fluid-phase FXa and then to TF:VIIa. All simulations were run with [TFPIα] = 0.5 nM. Vertical dashed lines indicate TF densities of interest. The flat horizontal lines in (*A*) and (*C*) at lag time >30 indicate that the thrombin concentration did not reach 1 nM within 30 min for the corresponding TF density.

TFPIα. The thrombin after 10 min for a sufficiently high TF density was affected little by the additional reactions for both TFPIα levels and all shear rates considered.

Impact of TFPIα concentration on thrombin generation

The previous results were based on variations in TF and shear rate for two fixed plasma concentrations of TFPIα. Next, we fixed the TF density at 2.5 fmol/cm^2 or 10 fmol/cm^2 and the shear rate at 100/s, and studied how varying the TFPIα levels from 0 to 2.5 nM in increments of 0.5 nM affected thrombin generation. We did this only with the new model, as the old model's results varied negligibly with the TFPIα level. The variation of thrombin with time for these experiments is shown in Fig. 3. In Fig. 3 *A*, two qualitatively different outcomes are seen for a TF density of 2.5 fmol/cm^2 depending on the TFPIα level. As the TFPIα concentration was increased from 0 nM to 0.5 nM and then to 1.0 nM, there was a substantial prolongation of the lag time from 923 s to about 1400 s to about 1980 s. The thrombin concentrations at 40 min in these simulations were 333, 303, and 261 nM for TFPIα concentrations of 0, 0.5, and 1.0 nM, so the new inhibition reactions also affected, albeit modestly, the thrombin concentrations at this time. For higher TFPIα concentrations (1.5, 2.0, and

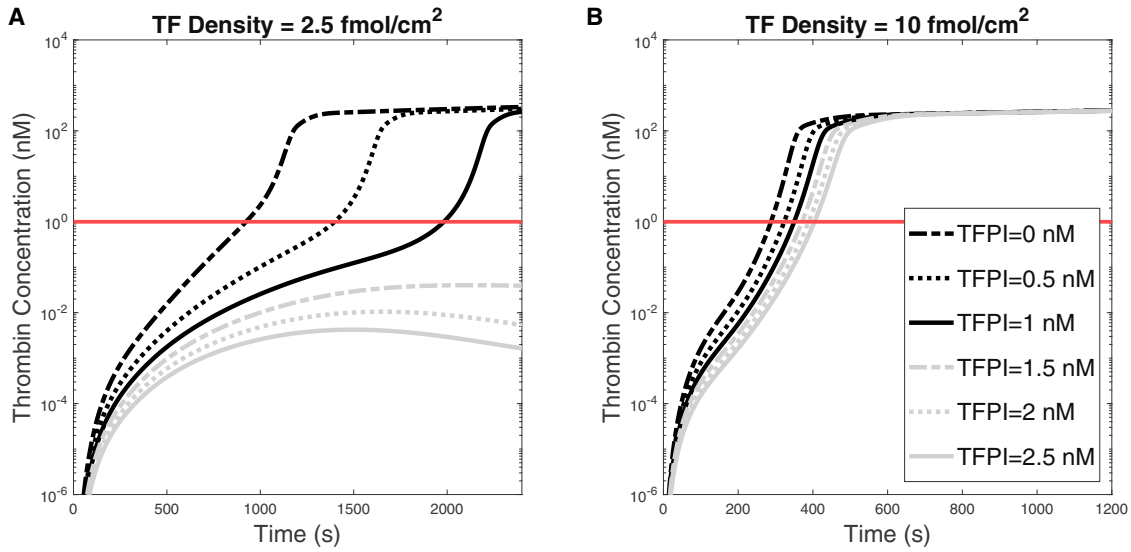

FIGURE 3 Thrombin concentration versus time for the indicated TFPIα levels for shear rate 100/s and with (*A*) TF = 2.5 fmol/cm^2 and (*B*) TF = 6 fmol/cm^2. Note the different timescales. To see this figure in color, go online.

2.5 nM) the thrombin curves peaked at levels below 1 nM and were in decline during the latter part of the simulations, indicating that robust thrombin production would never occur. These results are reflected in and explained by the concentration time course of FXa, FV-h, and their complexes with TFPIα under different TF, shear rate, and TFPI levels, as shown in Fig. S7. Similar to what we observed for thrombin, higher TF levels lead to higher concentrations of platelet-bound FXa and FV-h, whereas responses to increases in shear rate are more sensitive at low TF levels (see Fig. S7).

The thrombin curves for a TF density of 10 fmol/cm^2 are shown in Fig. 3 *B*. At this TF density, the variations in TFPIα levels prolonged the lag time modestly and robust thrombin production occurred for all the TFPIα concentrations examined. These results reinforced our earlier observation that the additional TFPIα-mediated inhibition reactions can strongly influence thrombin dynamics with the greatest impact occurring for low TF densities. These results are in line with experimental ones showing that the major inhibitory effects of TFPI under flow occur at low TF (40). In that study, Thomassen et al. showed that TFPI antagonism decreases the lag time of fibrin deposition at low TF and to a lesser extent at higher TF levels. Our results for thrombin generation with TFPI = 0 and 0.5 nM, plotted on a linear scale (Fig. S4), compare well with their time courses of fibrin deposition and differences they see in lag times with and without TFPI antagonism and under different TF levels.

Examination of the major inhibitory reaction step(s)

Our model included two new ways that TFPI could impede thrombin generation: through direct binding with platelet-bound FXa and through interactions with FV-h. To investigate whether one binding reaction more greatly affects the lag time and to determine for which TF levels that occurred, we computed the lag times as we varied the TF density and the TFPIα concentration with and without the binding of TFPIα to FXa and FV-h. The results are shown in the four heatmaps in Fig. 4. In the heatmaps, the color indicates the lag time in minutes (white cells indicate that the thrombin concentration did not achieve 1 nM within 40 min), a minus sign indicates that the binding reaction is "turned off," and a plus sign indicates that the binding reaction is "turned on." To "turn off" the binding of TFPIα to FXa, we set all association rates between TFPIα and FXa to zero (reactions 7, 11, 17, 22, and 24 in Table 1). Similarly, to "turn off" TFPIα binding with FV-h, we set all association rates between TFPI and FV-h to zero (reactions 1, 5, 8, 12, 16, and 23 in Table 1).

As expected, when we turned off TFPIα binding to both FXa and FV-h, shown in Fig. 4 *A*, we observed that the lag time was dependent only on TF (displaying threshold dependence) and was independent of the TFPIα concentration. For simulations in which we turned on only the binding between TFPIα and FV-h, the lag time exhibits dependence on TFPIα, but this effect saturated at a TFPIα concentration greater than about 3 nM (Fig. 4 *B*). Also, the influence of the TFPIα concentration on the lag time was much diminished for TF densities higher than about 6 fmol/cm^2.

If instead we turned on only the binding of TFPIα to FXa, there was a slightly greater dependence of lag time on both TFPIα and TF, and this effect did not saturate with TFPIα level, at least up to 5 nM (Fig. 4 *C*). Turning on both binding reactions, as seen in Fig. 4 *D*, the lag time threshold was shifted to a higher TF level than in either of the previous cases, consistent with the shift in

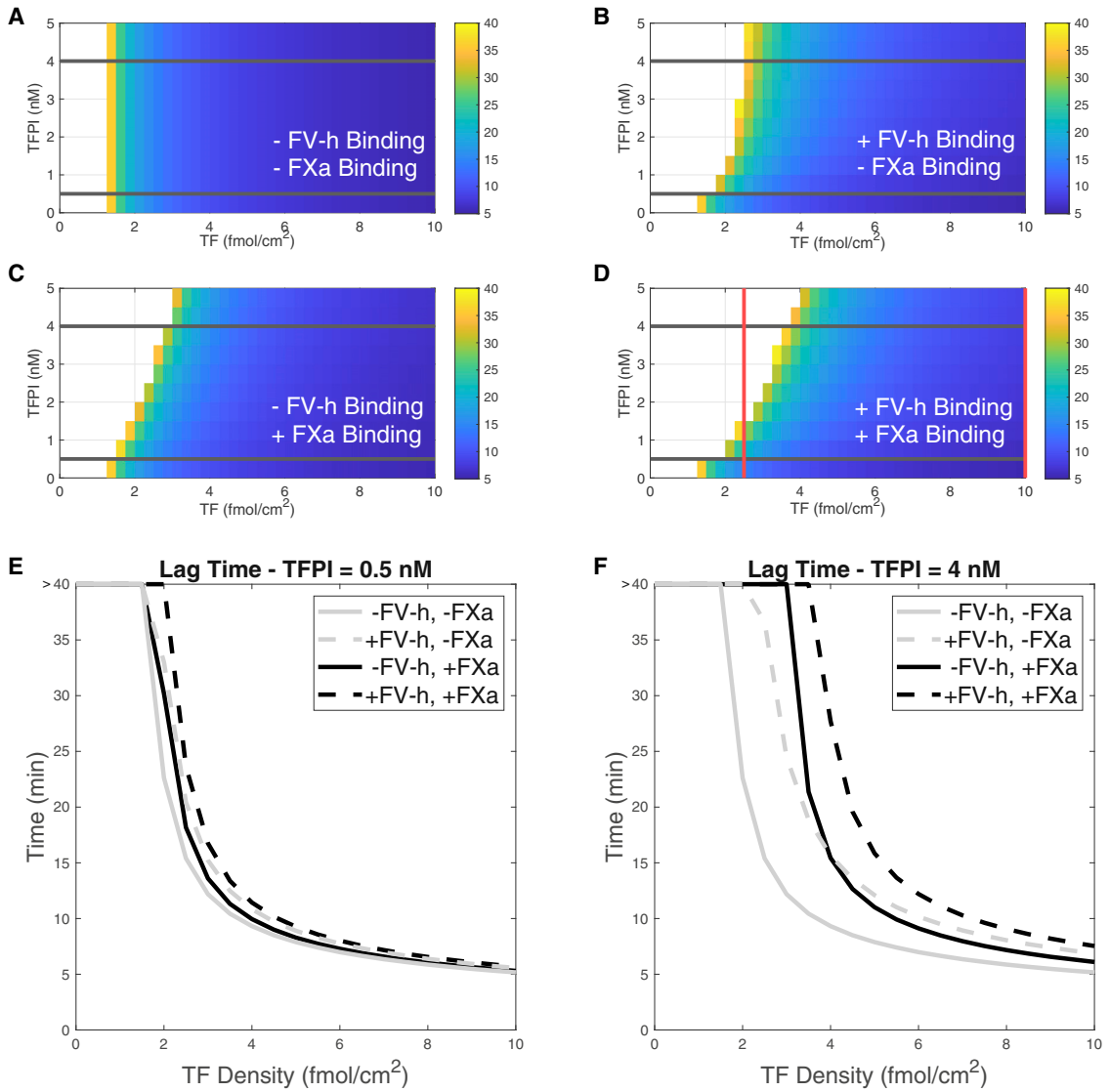

FIGURE 4 Lag times as functions of TF and TFPIα levels with the specified TFPIα binding reactions. Lag times for cases in which (*A*) TFPIα binding with both FV-h and FXa are turned off, (*B*) TFPIα binding with FV-h is turned on and TFPIα binding with FXa is turned off, (*C*) TFPIα binding with FXa is turned on and TFPIα binding with FV-h is turned off, and (*D*) TFPIα binding to both FV-h and FXa are turned on. For parameter values in the region without color, the thrombin concentration did not reach 1 nM thrombin within 40 min. Lag time versus TF density for TFPIα = 0.5 nM with and without TFPIα binding FV-h or/and FXa for (*E*) TFPIα = 0.5 nM and (*F*) TFPIα = 4.0 nM. These curves correspond to the slices in the heatmap indicated by the horizontal lines in (*A*)–(*D*). Shear rate is fixed to 100/s. To see this figure in color, go online.

the TF threshold in the new model revealed in Fig. 2. Note also that the red vertical line at TF 2.5 fmol/cm^2 represents the same information as that at the intersections of the thrombin curves and the 1 nM level line (*red horizontal line*) in Fig. 3, where the TF density was fixed to 2.5 fmol/cm^2. Comparing the heatmaps in Fig. 4, *B* and *C*, we conclude that binding of TFPI to one of either FV-h or FXa significantly altered the lag time but that the TFPIα-FXa binding had a stronger influence.

For a more detailed comparison of the lag times for the four cases at specific TFPI levels, Fig. 4, *E* and *F* show plots of the lag times as a function of TF density for two specific TFPIα concentrations, 0.5 nM and 4 nM, indicated with horizontal black lines in the heatmaps. These plots allow a clearer comparison of the effects of each of the binding reactions on lag times. In particular, Fig. 4 *E* shows that at the lower TFPIα, lag times are increased in the order of adding TFPIα/FV-h reactions alone, adding TFPIα/FXa reactions alone, and finally both reactions together (the curves shift slightly to the right and never cross). However, for the higher TFPIα shown in Fig. 4 *F*, the larger lag times are clearer but, additionally, a larger effect of one of the individual reactions alone depends on the TF density (*gray dashed line* and *black solid line* cross at TF 4 fmol/cm^2). The greatest increase in lag time occurred when both reactions were at play (Fig. 4 *D*).

Significance of platelet-derived FV

To further investigate the importance of FV-h in the coagulation system, we explored the effect of the FV-h derived from platelets that is secreted upon activation. We did this by varying the parameter h_5 that denotes the fraction of all of the FV-type molecules released by the platelet that are half-activated FV-h. This parameter is used in Eq. 1. Fig. 5 shows the thrombin generation over time for various h_5 and TF values for low (0.5 nM) and high (2.5 nM) TFPIα plasma concentrations. We vary h_5 among 0, 0.5, and 1, which correspond, respectively, to only zymogen FV, a mixture of half FV, and half partially activated FV-h, and only FV-h being released from platelets upon activation. At the low TFPIα concentration, we considered TF densities 2.5 and 6.0 fmol/cm^2 and for the high TFPIα concentration, we ran simulations at TF densities 4.0 and 10.0 fmol/cm^2. These values, indicated by vertical lines in Fig. 3, *B* and *D*, bracket the range of TF values over which the thrombin concentration at 10 min changed rapidly as the TF density was varied for shear rate 100/s and the low and high TFPIα concentrations, respectively.

For both TFPIα concentrations, the resulting behaviors were qualitatively similar but differed in magnitude. In Fig. 5 *A*, we see that for TFPI$\alpha = 0.5$ nM and for the higher TF density (6.0 fmol/cm^2), there was little difference in the thrombin curves for the different h_5 values. In contrast, for the lower TF density (2.5 fmol/cm^2), the effect of increasing h_5 was to shorten the lag time, from 1419 s when only zymogen is released by the platelets, to 1080 s for the 50:50 mixture, to 914 s when only partially activated FV-h was released. For both TF densities, the thrombin concentration at 40 min changed little with changes in h_5. Fig. 5 *B* shows that for TFPI$\alpha = 2.5$ nM, there was almost negligible difference in the thrombin curves for the higher TF density (10.0 fmol/cm^2) and that, while the variation in lag time with h_5 was greater for TF density (4.0 fmol/cm^2), it was much less than for the combination of low TFPIα concentration and low TF density shown by the black curves in Fig. 5 *A*. To summarize, an increase of FV-h content within the platelets shortened the lag times. When TFPIα was low, the effect was the greatest for a low TF density.

Local sensitivity analysis

We performed a local, one-at-a-time, sensitivity analysis (SA) of the new model to the new parameters relating to TFPI binding with FV-h. All of the details and the results are shown in the section 4 of the supporting material and in Figs. S2 and S3, and we will give only a brief summary of them here. The SA methods were based on those developed by Saltelli and colleagues (41,42) and those we used to analyze our previous model (27). We chose three thrombin metrics: lag time, maximum rate of thrombin generation, and final thrombin concentration, as the quantities of interest and then ranked the sensitivities of these quantities to levels of all clotting factors and inhibitors except for TFPIα, as in our previous work (27). The lag times in the new model showed a higher sensitivity to TFPIα levels than in our old model, as expected from the previous results shown above; the effects of TFPIα on the maximum rates and final thrombin concentration were negligible, as they were with the previous model. However, in comparison with our previous SA results, FX became increasingly important for the lag times and maximal rates with the new model, which makes sense given the direct inhibition of FXa on platelet surfaces by TFPIα. Next, a local SA

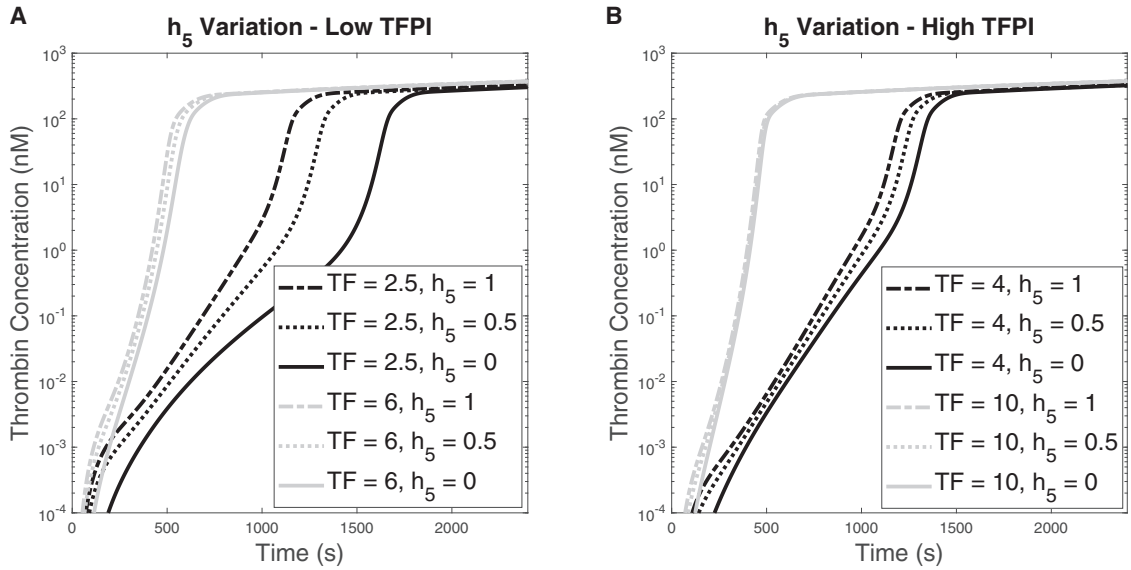

FIGURE 5 Thrombin generation for $h_5 = 0, 0.5, 1.0$ for shear rate 100/s. (*A*) The TFPIα concentration is 0.5 nM and the TF density was either 2.5 or 6 fmol/cm^2. (*B*) The TFPIα concentration is 2.5 nM and the TF density was either 4 or 10 fmol/cm^2.

was performed on the kinetic rates. Forward and reverse kinetic rates for each of the TFPIα/FV-h reactions were varied by 10%, and the changes in the three thrombin metrics were measured. These small perturbations in reaction rates had minimal effects on all thrombin metrics; none of the perturbations led to more than a 1% change from baseline metric values.

DISCUSSION

Our previous mathematical model, in which TFPIα acts only through FXa and TF:VIIa, showed minor inhibitory effects of TFPIα on thrombin generation. In that model, most FXa that was produced on the subendothelium and subsequently bound to TFPIα in the fluid was quickly washed away by the flow before it could rebind to the TF:VIIa in the small injury zone. It is possible that for a longer injury, the fluid-phase FXa: TFPIα complexes might bind to TF:VIIa downstream and inhibit its action. Other reaction schemes for this pathway have been considered (24,38,43–45), which has led to some disagreement regarding the effects of TFPIα under flow. Further mathematical investigation of different schemes and injury sizes is warranted to better understand TFPIα inhibition via TF:VIIa under flow.

To the best of our knowledge, the current study is the first mathematical modeling approach to investigate TFPIα inhibition on the surface of activated platelets. We extended our previous model to include generation and activation of FV-h as well as its inhibition by TFPIα on activated platelet surfaces. Additionally, we included TFPIα binding to FXa bound to an activated platelet surface that leads to its inhibition. These extensions relate solely to platelet-surface reactions, and essentially all of the inhibitory effects of TFPIα we observe in the extended model are due to these reactions, since TFPIα had very little influence in our earlier model. We studied how the newly added TFPIα inhibition pathways affected thrombin generation related to the TF threshold behavior, thrombin lag times, the system's sensitivity to shear rate, and how thrombin generation was affected by varying TFPIα levels at low and high TF densities. In general, we found that the newly added TFPIα reactions created a new sensitivity of the model system to TFPIα levels, especially at low TF levels. At high TF densities, the same TFPIα concentration increased the lag time but still led to a robust thrombin response. In fact, when a strong thrombin response was generated, under variations of TFPIα from 0 to 5 nM, the system produced approximately the same final thrombin concentrations.

Our general results about TFPIα inhibition under flow are in line with previous experimental studies performed with microfluidics (40). In those studies, it was observed that TFPIα antagonism enhanced fibrin formation (thrombin generation in our model can be thought of as a surrogate for fibrin formation) when normal blood or plasma was flowed over TF/collagen microspots, but this effect was seen only at low TF densities. The experiments did not run long enough to find out whether the final fibrin fluorescence achieved was similar with and without TFPIα antagonism; however, there was a significant fibrin response that was delayed with TFPIα. Taken together with our results, this suggests that platelet-surface-dependent TFPIα inhibition affects the timing but not the magnitude of a thrombin response and that these effects are most pronounced at low TF densities. TFPI leads to delayed lag times under static conditions as well. van't Veer and Mann performed thrombin generation assays with and without TFPI and with varying levels of TF (46). In comparing the lag times with TFPI with those without, they found that it was always increased and that the increases were more prominent for lower TF levels. Although these assays were performed with lipid vesicles and not platelets, the surface-dependent mechanism could still be at play.

Our mathematical model gives as output the concentration of every model species at every point in time, and also gives us the freedom to turn on and turn off specific pathways. These capabilities allowed us to investigate TFPIα binding with FXa and FV-h to characterize their individual and combined inhibitory behavior. In turning off these pathways separately and together, we found that TFPIα binding with both FXa and FV-h has a strong inhibitory role. When TFPIα could bind with FV-h but not with FXa in either plasma or on platelet surfaces, the inhibitory effect of TFPIα saturated at about a 3 nM TFPIα concentration. With the FXa inhibition pathway on but without TFPIα/FV-h binding, the inhibitory effects of TFPIα increased with increasing TFPIα concentration up to the maximum that we simulated (5 nM). These results can be explained by considering what constitutes prothrombinase in the system. In this new model, there are two forms of prothrombinase, FXa:FV-h and FXa:FVa, both of which can actively convert prothrombin to thrombin. In our model, to form either type of prothrombinase complex, FV must first be converted to FV-h by FXa or to FVa by thrombin. Only FXa is present in the initial stage of coagulation, so FV-h is available first. This allows formation of FV-h:FXa, which generates the first thrombin. Once a sufficient level of thrombin is reached, thrombin becomes the primary activator of FV, fully activating it to FVa and leading to FXa:FVa formation, which is protected from TFPIα inhibition and further supports propagation of thrombin. This is in line with the proposed scheme of Schuijt et al. (14) suggesting that FXa-dependent FV activation is pivotal to the initiation phase of coagulation. Essentially, FV-h is needed early to generate the first thrombin and start the positive feedback, then FVa is the primary cofactor for FXa. In other words, the prothrombinase concentration is limited by the amount of FXa and not by the amount of FV-h, and this explains the observed differences between the two inhibitory pathways.

The composition of platelet-released FV forms was important in the new model. Increasing the amount of FV-h relative to FV within the platelets resulted in acceleration of thrombin generation, with the most significant effects at low TF and effects that are mostly washed out at higher TF. At low TF, if all platelet-released FV was FV-h there would be no need for FXa to activate it first, thus removing a reaction step and accelerating coagulation. Additionally, the released FV-h would be able to immediately bind to FXa on activated platelet surfaces to form active prothrombinase (FV-h:FXa) during the early stages of coagulation. Our simulations in this study were performed under the assumption of normal healthy blood, and it is possible that these effects are magnified in the case of hemophilia A. In our previous study (28), in which the model did not account for FV-h, we found that lowering the FV levels in plasma and platelets could enhance thrombin generation in hemophilia A, where there is a deficiency in FVIII. In that study, the model suggested that the reason for this is that FV and FVIII compete for FXa in the early stage of coagulation and that lowering FV weakens this competition so that more of the albeit small quantity of FVIII can be activated; this leads to more tenase, more prothrombinase, and ultimately to more thrombin. In our new model we have introduced a new species that also competes for FXa, namely FV-h. Thus there is now competition between three species for FXa: FV, FVIII, and FV-h. It will be interesting to see how this changes our results for hemophilia A blood, and this is a topic of immediate future research.

It seems plausible, then, that a reduction or modulation of inhibitors could offset complications associated with bleeding disorders. For example, TFPIα levels have been shown to affect clotting in individuals with hemophilia A and B, the bleeding disorders characterized by deficiencies in clotting factors VIII (FVIII) and IX (FIX), respectively. Several biochemical experiments have revealed relationships between TFPIα and the early stages of coagulation in hemophilia blood (47). One study showed that TFPIα modulates the generation of FXa by inhibiting TF:VIIa in the presence of FVIII and FIX (48), suggesting that TFPIα itself could be inhibited to enhance coagulation. This hypothesis was examined in various animal models as well: a recent mouse study demonstrated that an anti-TFPIα antibody used in mice under hemophilic conditions decreased the hemoglobin lost over 20 min following tail transection. This indicated that direct inhibition of TFPIα effectively suppressed tail bleeding in mice with hemophilia (49). Another study showed that rabbits made temporarily hemophilic with anti-FVIII antibodies had reduced mean bleeding times after injection with anti-TFPIα antibodies (50). This study demonstrated that partial inhibition of TFPIα mitigates bleeding under hemophilia conditions. Together with our previous findings regarding FV and hemophilia, these studies suggest the potential for TFPIα and FV manipulation in the treatment of hemophilia. Further investigation of interactions between TFPIα and FV and their effects on coagulation in hemophilia is thus warranted. As a first step, we have developed a mathematical model of coagulation under flow that includes the relevant TFPIα and FV interactions with the goal of making possible future studies focused on hemophilia.

The reason we studied TFPIα at 0.5 and 2.5 nM is because it is still not clear how much free TFPIα is in the blood. Although TFPI is often reported to be 2.5 nM in plasma, TFPIα has been suggested to account for only 10%–30% of the total TFPI pool in the blood (15), with platelet TFPI accounting for about 7%–8% of this total (5). Approximately 80% of plasma TFPI is a C-terminus truncated form (cannot bind to FV-h) and is thought to be bound to lipoprotein (51). Although one biochemical study showed that the lipoprotein-bound form of TFPI can actively inhibit thrombin generation (52), it is not entirely clear how inhibitory this form is in vivo. The remaining 20% is free in the plasma and consists of a mixture of a full-length TFPIα form and the truncated form. Thus, the 0.5 nM levels studied here represent that 20%.

One limitation of our model is the absence of explicit inclusion of protein S in the coagulation reactions. Protein S is known to be a critical regulator of coagulation, playing the role of cofactor for both activated protein C and TFPIα in the inactivation of FVa and inhibition of FXa, respectively (53). Protein S can bind directly to lipid surfaces, and thus could localize TFPIα bound to the protein S near the lipid surface. This is likely part of a mechanism that enhances the rate of encounter between platelet-bound FXa and TFPIα. FV-short and protein S have recently been shown to be synergistic cofactors for TFPIα, leading to much stronger inhibition of FXa together than when TFPIα is bound to only one of FV-h or protein S (54). This synergy seems to occur via formation of a trimolecular complex of TFPIα, FV-short, and protein S (55, 56), and it was hypothesized that these complexes are present in circulating plasma at subnanomolar concentrations (56). Considering the high concentrations of protein S in plasma, it was further suggested that nearly all of the TFPIα in plasma may be bound within such trimolecular complexes and that no or very little free FV-short or free TFPIα exists in plasma (55). However, data supporting that hypothesis are sparse and, as mentioned above, it is still unclear how much free TFPIα exists in circulating plasma. While we do not include protein S explicitly in our model, some of our simulation results may still shed light on its potential effects. For example, our simulations with high levels of plasma TFPIα can be thought of as corresponding to lower levels of the protein S-FV short-TFPIα complex which has 10-fold higher power to inhibit FXa than does TFPIα alone (53). Similarly, if almost all plasma TFPIα is in complex with protein S and FV-short, little TFPIα would be available to bind with FV-h produced by FXa or released from platelets, while FXa-inhibiting capability would still be present. Our simulations in

which we "turned off" TFPIα binding to FV-h would correspond, at least approximately, to that situation. Thus, even in scenarios in which TFPIα circulates in complex with protein S and FV-short, our model provides strong evidence that direct inhibition of platelet-bound FXa is an important mechanism for regulating thrombin generation under flow. In future research, we plan to explicitly include in the model protein S and its cofactor activity for TFPIα and activated protein C.

Finally, it is also known that platelets secrete TFPIα upon activation with thrombin (5,57). The exact location of these TFPIα molecules within the platelet is unknown, but it is known that it is not the α-granules (57) where FV is stored. It is possible that this stored and released TFPIα pool could play an important role in regulating thrombin generation, especially if protein S can quickly localize it to the platelet surface. This is another topic of immediate future research.

CONCLUSION

In this study, we extended a mathematical model of flow-mediated coagulation to explore the effects of TFPIα-mediated inhibitory reactions that take place on activated platelet surfaces. Results from our new model show that the surface-dependent TFPI inhibition is much stronger than the TFPI inhibition on the subendothelium and, as such, the TF threshold density is shifted to higher values in our new model compared with our old one. Furthermore, these reactions could lead to significant delays in thrombin generation at low TF density if TFPIα levels were increased. Ultimately, the new model was sensitive to changes in TFPIα levels, especially at low TF density, and gave TFPIα potential to be a significant modifier of thrombin generation. There are still some additional limitations in this model that we need to address in future work: 1) we do not include TFPIα secretion from platelets; 2) we do not consider inhibition by TFPIβ in the endothelial region; and 3) some reaction kinetics are unknown and we thus made assumptions about their values, and more experimental data would be useful for defining more precise values. Nevertheless, we developed an updated version of an experimentally validated mathematical model of flow-mediated coagulation that is sensitive to TFPIα and successfully exhibits the experimentally observed inhibitory effects of TFPIα under flow. More importantly, this model revealed the importance of the platelet surface as a platform for efficient inhibition. It is known that the platelet-surface dependence of procoagulant enzyme reactions is key to localizing coagulation to the site of injury. Thus, it makes sense that the inhibition of these key enzymes should also be most effective where they are needed most. Finally, TFPIα may be a potential therapeutic target to rescue thrombin generation in various bleeding disorders, and the current model can serve as a foundational tool to assess the effectiveness of TFPIα as a modifier of thrombin generation in these cases.

SUPPORTING MATERIAL

Supporting material can be found online at https://doi.org/10.1016/j.bpj.2022.11.023.

AUTHOR CONTRIBUTIONS

K.M. carried out all simulations. K.M., A.L.F., and K.L. designed the research, analyzed the data, and wrote the article.

ACKNOWLEDGMENTS

This work was, in part, supported by the National Institutes of Health (R01 HL120728, R01 HL151984) and the National Science Foundation CAREER (DMS-1848221).

DECLARATION OF INTERESTS

K.L. received research support from Novo Nordisk.

REFERENCES

1. Camerer, E., A. B. Kolstø, and H. Prydz. 1996. Cell biology of tissue factor, the principal initiator of blood coagulation. *Thromb. Res.* 81:1–41. https://linkinghub.elsevier.com/retrieve/pii/0049384895002096X.
2. Furie, B., and B. C. Furie. 1992. Molecular and cellular biology of blood coagulation. *N. Engl. J. Med.* 326:800–806.
3. Maroney, S. A., P. E. Ellery, and A. E. Mast. 2010. Alternatively spliced isoforms of tissue factor pathway inhibitor. *Thromb. Res.* 125:S52–S56. https://linkinghub.elsevier.com/retrieve/pii/S0049384810000915.
4. Maroney, S. A., and A. E. Mast. 2015. New insights into the biology of tissue factor pathway inhibitor. *J. Thromb. Haemostasis.* 13:S200–S207. https://doi.org/10.1111/jth.12897.
5. Novotny, W. F., T. J. Girard, …, G. J. Broze. 1988. Platelets secrete a coagulation inhibitor functionally and antigenically similar to the lipoprotein associated coagulation inhibitor. *Blood.* 72:2020–2025. https://ashpublications.org/blood/article/72/6/2020/166184/Platelets-secrete-a-coagulation-inhibitor.
6. Broze, G. J. 1995. Tissue factor pathway inhibitor and the revised theory of coagulation. *Annu. Rev. Med.* 46:103–112.
7. Sandset, P. M. 1996. Tissue factor pathway inhibitor (TFPI) – an update. *Haemostasis.* 26:154–165. https://www.karger.com/Article/FullText/217293.
8. Duga, S., R. Asselta, and M. L. Tenchini. 2004. Coagulation factor V. *Int. J. Biochem. Cell Biol.* 36:1393–1399. https://linkinghub.elsevier.com/retrieve/pii/S1357272503002863.
9. Segers, K., B. Dahlbäck, and G. A. F. Nicolaes. 2007. Coagulation factor V and thrombophilia: background and mechanisms. *Thromb. Haemostasis.* 98:530–542. http://www.thieme-connect.de/DOI/DOI?10.1160/TH07-02-0150.
10. Kuang, S.-Q., S. Hasham, …, D. M. Milewicz. 2001. Characterization of a novel autosomal dominant bleeding disorder in a large kindred from east Texas. *Blood.* 97:1549–1554. https://ashpublications.org/blood/article/97/6/1549/107333/Characterization-of-a-novel-autosomal-dominant.
11. Vincent, L. M., S. Tran, …, B. Dahlbäck. 2013. Coagulation factor VA2440G causes east Texas bleeding disorder via TFPI. *J. Clin. Invest.* 123:3777–3787. http://www.jci.org/articles/view/69091.
12. Broze, G. J., and T. J. Girard. 2013. Factor V, tissue factor pathway inhibitor, and east Texas bleeding disorder. *J. Clin. Invest.* 123:3710–3712. http://www.jci.org/articles/view/71220.

13. Wood, J. P., M. W. Bunce, …, A. E. Mast. 2013. Tissue factor pathway inhibitor-alpha inhibits prothrombinase during the initiation of blood coagulation. *Proc. Natl. Acad. Sci. USA.* 110:17838–17843.
14. Schuijt, T. J., K. Bakhtiari, …, C. van 't Veer. 2013. Factor Xa activation of factor V is of paramount importance in initiating the coagulation system: lessons from a tick salivary protein. *Circulation.* 128:254–266. https://doi.org/10.1161/CIRCULATIONAHA.113.003191.
15. Wood, J. P., P. E. R. Ellery, …, A. E. Mast. 2014. Biology of tissue factor pathway inhibitor. *Blood.* 123:2934–2943. https://ashpublications.org/blood/article/123/19/2934/32640/Biology-of-tissue-factor-pathway-inhibitor.
16. Foster, W. B., M. E. Nesheim, and K. G. Mann. 1983. The factor Xa-catalyzed activation of factor V. *J. Biol. Chem.* 258:13970–13977.
17. Thorelli, E., R. J. Kaufman, and B. Dahlbäck. 1997. Cleavage requirements for activation of factor V by factor Xa. *Eur. J. Biochem.* 247:12–20.
18. Nicolaes, G. A. F., and B. Dahlbäck. 2002. Factor V and thrombotic disease: description of a janus-faced protein. *Arterioscler. Thromb. Vasc. Biol.* 22:530–538. https://doi.org/10.1161/01.ATV.0000012665.51263.B7.
19. Mann, K. G., and M. Kalafatis. 2003. Factor V: a combination of dr. Jekyll and mr. Hyde. *Blood.* 101:20–30. https://ashpublications.org/blood/article/101/1/20/88938/Factor-V-a-combination-of-Dr-Jekyll-and-Mr-Hyde.
20. Petrillo, T., F. Ayombil, …, R. M. Camire. 2021. Regulation of factor V and factor V-short by TFPI: relationship between B-domain proteolysis and binding. *J. Biol. Chem.* 296:100234. https://linkinghub.elsevier.com/retrieve/pii/S002192582000349X.
21. Mast, A. E. 1996. Physiological Concentrations of Tissue Factor Pathway Inhibitor Do Not Inhibit Prothrombinase 1:1845–1850.
22. Wood, J. P., H. H. Petersen, …, A. E. Mast. 2017. TFPIa interacts with FVa and FXa to inhibit prothrombinase during the initiation of coagulation. *Blood Adv.* 1:2692–2702.
23. Kuharsky, A. L., and A. L. Fogelson. 2001. Surface-mediated control of blood coagulation: the role of binding site densities and platelet deposition. *Biophys. J.* 80:1050–1074. https://linkinghub.elsevier.com/retrieve/pii/S0006349501760857.
24. Fogelson, A. L., and N. Tania. 2005. Coagulation under flow: the influence of flow-mediated transport on the initiation and inhibition of coagulation. *Pathophysiol. Haemostasis Thrombosis.* 34:91–108. https://www.karger.com/Article/FullText/89930.
25. Fogelson, A. L., Y. H. Hussain, and K. Leiderman. 2012. Blood clot formation under flow: the importance of factor XI depends strongly on platelet count. *Biophys. J.* 102:10–18. https://linkinghub.elsevier.com/retrieve/pii/S0006349511013142.
26. Leiderman, K., W. C. Chang, …, A. L. Fogelson. 2016. Synergy between tissue factor and exogenous factor XIa in initiating coagulation. *Arterioscler. Thromb. Vasc. Biol.* 36:2334–2345. https://doi.org/10.1161/ATVBAHA.116.308186.
27. Link, K. G., M. T. Stobb, …, K. Leiderman. 2018. A local and global sensitivity analysis of a mathematical model of coagulation and platelet deposition under flow. *PLoS One.* 13:e0200917. https://dx.plos.org/10.1371/journal.pone.0200917.
28. Link, K. G., M. T. Stobb, …, K. B. Neeves. 2020. A mathematical model of coagulation under flow identifies factor V as a modifier of thrombin generation in hemophilia A. *J. Thromb. Haemostasis.* 18:306–317. https://doi.org/10.1111/jth.14653.
29. Hockin, M. F., K. C. Jones, …, K. G. Mann. 2002. A model for the stoichiometric regulation of blood coagulation. *J. Biol. Chem.* 277:18322–18333.
30. Danforth, C. M., T. Orfeo, …, K. E. Brummel-Ziedins. 2012. Defining the boundaries of normal thrombin generation: investigations into hemostasis. *PLoS One.* 7:e30385. https://dx.plos.org/10.1371/journal.pone.0030385.
31. Brummel-Ziedins, K. E., T. Orfeo, …, K. G. Mann. 2009. Empirical and theoretical phenotypic discrimination. *J. Thromb. Haemostasis.* 7:181–186.
32. Miyazawa, K., A. L. Fogelson, and K. Leiderman. 2022. Inhibition of platelet-surface-bound proteins during coagulation under flow II: the role of antithrombin and heparin. *Biophys. J.*
33. Tracy, P. B., L. L. Eide, …, K. G. Mann. 1982. Radioimmunoassay of factor V in human plasma and platelets. *Blood.* 60:59–63.
34. Steen, M., and B. Dahlbäck. 2002. Thrombin-mediated proteolysis of factor V resulting in gradual B-domain release and exposure of the factor xa-binding site. *J. Biol. Chem.* 277:38424–38430. https://linkinghub.elsevier.com/retrieve/pii/S0021925818363233.
35. Monković, D. D., and P. B. Tracy. 1990. Functional characterization of human platelet-released factor V and its activation by factor Xa and thrombin. *J. Biol. Chem.* 265:17132–17140. https://linkinghub.elsevier.com/retrieve/pii/S0021925817448794.
36. Mann, K. G. 1987. The assembly of blood clotting complexes on membranes. *Trends Biochem. Sci.* 12:229–233. https://www.sciencedirect.com/science/article/pii/0968000487901150.
37. Krishnaswamy, S., K. C. Jones, and K. G. Mann. 1988. Prothrombinase complex assembly. Kinetic mechanism of enzyme assembly on phospholipid vesicles. *J. Biol. Chem.* 263:3823–3834. https://linkinghub.elsevier.com/retrieve/pii/S0021925818689999.
38. Jesty, J., T.-C. Wun, and A. Lorenz. 1994. Kinetics of the inhibition of factor Xa and the tissue factor-factor VIIa complex by the tissue factor pathway inhibitor in the presence and absence of heparin. *Biochemistry.* 33:12686–12694. https://doi.org/10.1021/bi00208a020.
39. Solymoss, S., M. M. Tucker, and P. B. Tracy. 1988. Kinetics of inactivation of membrane-bound factor Va by activated protein C. Protein S modulates factor Xa protection. *J. Biol. Chem.* 263:14884–14890. https://linkinghub.elsevier.com/retrieve/pii/S0021925818681219.
40. Thomassen, S., T. G. Mastenbroek, …, J. W. M. Heemskerk. 2018. Suppressive role of tissue factor pathway inhibitor-α in platelet-dependent fibrin formation under flow is restricted to low procoagulant strength. *Thromb. Haemostasis.* 118:502–513.
41. Saltelli, A., P. Annoni, …, S. Tarantola. 2010. Variance based sensitivity analysis of model output. Design and estimator for the total sensitivity index. *Comput. Phys. Commun.* 181:259–270. https://linkinghub.elsevier.com/retrieve/pii/S0010465509003087.
42. Saltelli, A., S. Tarantola, …, M. Ratto. 2004. Sensitivity Analysis in Practive: A Guide to Assessing Scientific Models.
43. Baugh, R. J., G. J. Broze, and S. Krishnaswamy. 1998. Regulation of extrinsic pathway factor Xa formation by tissue factor pathway inhibitor. *J. Biol. Chem.* 273:4378–4386. https://linkinghub.elsevier.com/retrieve/pii/S0021925818925603.
44. Panteleev, M. A., V. I. Zarnitsina, and F. I. Ataullakhanov. 2002. Tissue factor pathway inhibitor: a possible mechanism of action. *Eur. J. Biochem.* 269:2016–2031.
45. Shibeko, A. M., E. S. Lobanova, …, F. I. Ataullakhanov. 2010. Blood flow controls coagulation onset via the positive feedback of factor VII activation by factor Xa. *BMC Syst. Biol.* 4:5–12.
46. van't Veer, C., and K. G. Mann. 1997. Regulation of tissue factor initiated thrombin generation by the stoichiometric inhibitors tissue factor pathway inhibitor, antithrombin-III, and heparin cofactor-II. *J. Biol. Chem.* 272:4367–4377.
47. Peterson, J. A., S. A. Maroney, and A. E. Mast. 2016. Targeting TFPI for hemophilia treatment. *Thromb. Res.* 141:S28–S30. https://linkinghub.elsevier.com/retrieve/pii/S0049384816303590.
48. Repke, D., C. H. Gemmell, …, Y. Nemerson. 1990. Hemophilia as a defect of the tissue factor pathway of blood coagulation: effect of factors VIII and IX on factor X activation in a continuous-flow reactor. *Proc. Natl. Acad. Sci. USA.* 87:7623–7627.
49. Maroney, S. A., B. C. Cooley, …, A. E. Mast. 2012. Absence of hematopoietic tissue factor pathway inhibitor mitigates bleeding in mice with hemophilia. *Proc. Natl. Acad. Sci. USA.* 109:3927–3931.
50. Erhardtsen, E., M. Ezban, …, O. Nordfang. 1995. Blocking of tissue factor pathway inhibitor (TFPI) shortens the bleeding time in rabbits

with antibody induced hemophilia A. *Blood Coagul. Fibrinolysis.* 6:388–394.

51. Broze, G. J., Jr., G. W. Lange, …, L. MacPhail. 1994. Heterogeneity of plasma tissue factor pathway inhibitor. *Blood Coagul. Fibrinolysis.* 5:551–559. https://europepmc.org/article/med/7841311.

52. Augustsson, C., I. Hilden, and L. C. Petersen. 2014. Inhibitory effects of LDL-associated tissue factor pathway inhibitor. *Thromb. Res.* 134:132–137.

53. Gierula, M., and J. Ahnström. 2020. Anticoagulant protein S—new insights on interactions and functions. *J. Thromb. Haemostasis.* 18:2801–2811.

54. Dahlbäck, B., L. J. Guo, …, S. Tran. 2018. Factor V-short and protein S as synergistic tissue factor pathway inhibitor (TFPI α) cofactors. *Res. Pract. Thromb. Haemost.* 2:114–124.

55. Dahlbäck, B., and S. Tran. 2022. The preAR2 region (1458–1492) in factor V-Short is crucial for the synergistic TFPIα-cofactor activity with protein S and the assembly of a trimolecular factor Xa-inhibitory complex comprising FV-Short, protein S, and TFPIα. *J. Thromb. Haemostasis.* 20:58–68.

56. Dahlbäck, B., and S. Tran. 2022. A hydrophobic patch (PLVIVG; 1481–1486) in the B-domain of factor V-short is crucial for its synergistic TFPIα-cofactor activity with protein S and for the formation of the FXa-inhibitory complex comprising FV-short, TFPIα, and protein S. *J. Thromb. Haemostasis.* 20:1146–1157.

57. Maroney, S. A., and A. E. Mast. 2008. Expression of tissue factor pathway inhibitor by endothelial cells and platelets. *Transfus. Apher. Sci.* 38:9–14. https://linkinghub.elsevier.com/retrieve/pii/S1473050207001759.

Biophysical Journal, Volume *122*

Supplemental information

Inhibition of platelet-surface-bound proteins during coagulation under flow I: TFPI

Kenji Miyazawa, Aaron L. Fogelson, and Karin Leiderman

Manuscript submitted to **Biophysical** *Journal*

Article

Supplementary Information for: Inhibition of platelet-surface-bound proteins during coagulation under flow

Kenji Miyazawa, Aaron L. Fogelson, Karin Leiderman

S1 MODEL SCHEMATIC

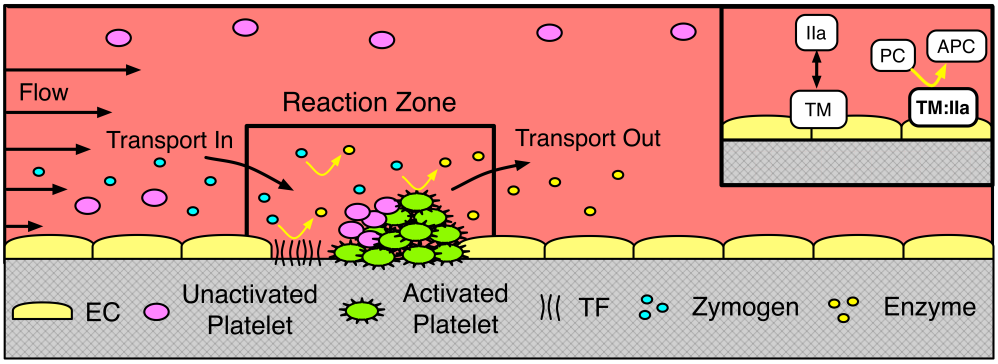

Figure S1: Schematic of the model reaction zone (main figure) and endothelial zone (inset).

S2 MODEL EQUATIONS

Below we have listed the full model equations for all species. The model detailed here includes extensions of our previous work (1–3). In total, the model consists of 130 species (and their corresponding ordinary differential equations) and 239 parameters including kinetic rates and initial/upstream concentrations. The solution of the model equations was carried out with our in-house fortran code that uses DLSODE for the numerical solution of the differential equations; each run of the model that simulates 40 minutes of clotting activity takes less than 10 seconds on a linux-based laptop. Simulations of this model (in the absence of heparin) can be performed with our online coagulation simulator: ClotSims. Below, blue text indicates the additional terms we added for the TFPI-mediated reactions, and purple text indicates the additional terms we added for the AT-mediated reactions. Strikeouts shows the terms we have removed from our previous version of the model.

$$
\begin{aligned}
\frac{d}{dt}z_7 &= -k_7^{on} z_7 [TF]^{avail} + k_7^{off} z_7^m && (1)\\
&\quad -k^+_{z_7:e_2} z_7 e_2 + k^-_{z_7:e_2}[Z_7:E_2]\\
&\quad -k^+_{z7:e_{10}} z_7 e_{10} + k^-_{z_7:e_{10}}[Z_7:E_{10}]\\
&\quad +k_{flow}(z_7^{up} - z_7)\\
&\quad -k^+_{z_7:e_9} z_7 e_9 + k^-_{z_7:e_9}[Z_7:E_9]\\
\frac{d}{dt}e_7 &= -k_7^{on} e_7 [TF]^{avail} + k_7^{off} e_7^m && (2)\\
&\quad +k^{cat}_{z_7:e_2}[Z_7:E_2] + k^{cat}_{z_7:e_{10}}[Z_7:E_{10}]\\
&\quad k_{flow}(e_7^{up} - e_7) + k^{cat}_{z7:e_9}[Z_7:E_9]\\
\frac{d}{dt}z_{10} &= -k_{10}^{on} z_{10} p_{10}^{avail} + k_{10}^{off} z_{10}^m && (3)\\
&\quad -k^+_{z_{10}:e_7^m} e_7^m + k^-_{z_{10}:e_7^m}[Z_{10}:E_7^m]\\
&\quad k_{flow}(z_{10}^{up} - z_{10})\\
\frac{d}{dt}e_{10} &= -k_{10}^{on} e_{10} p_{10}^{avail} + k_{10}^{off} e_{10}^m && (4)\\
&\quad +k^{cat}_{z_{10}:e_7^m}[Z_{10}:E_7^m]\\
&\quad +(k^{cat}_{z_7:e_{10}} + k^-_{z_7:e_{10}})[Z_7:E_{10}] - k^+_{z_7:e_{10}} e_{10} z_7\\
&\quad +(k^{cat}_{z_7^m:e_{10}} + k^-_{z_7^m:e_{10}})[Z_7^m:E_{10}] - k^+_{z_7^m:e_{10}} e_{10} z_7^m\\
&\quad -k^+_{TFPI:e_{10}} e_{10}[TFPI] + k^-_{TFPI:e_{10}^m}[TFPI:E_{10}]\\
&\quad k_{flow}(e_{10}^{up} - e_{10})\\
&\quad \cancel{-k^{in}_{AT:e_{10}} e_{10}}\\
&\quad -k_{diff}(e_{10} - e_{10}^{ec})\\
&\quad -k^+_{TFPI:e_5^h:e_{10}}[TFPI:E_5^h]e_{10}\\
&\quad -k^-_{TFPI:e_5^h:e_{10}}[E_{10}:TFPI:E_5^h]\\
&\quad -k^+_{TFPI:e_5^{hm}:e_{10}}[TFPI:E_5^{hm}]e_{10}\\
&\quad +k^-_{TFPI:e_5^{hm}:e_{10}}[E_{10}:TFPI:E_5^{hm}]\\
&\quad -k^{AT}_{e_{10}} e_{10}[AT]\\
&\quad +k^{ATH}_{e_{10}} e_{10}[AT:Hep]
\end{aligned}
$$

$$\frac{d}{dt}z_{10}^m = k_{10}^{on} z_{10} p_{10}^{avail} - k_{10}^{off} z_{10}^m \quad (5)$$
$$k^+_{z_{10}^m:TEN} z_{10}^m [TEN] + k^-_{z_{10}^m:TEN} [Z_{10}^m : TEN]$$
$$-k^+_{z_{10}^m:TEN} z_{10}^m [TEN^*] + k^-_{z_{10}^m:TEN} [Z_{10}^m : TEN^*]$$

$$\frac{d}{dt}e_{10}^m = k_{10}^{on} e_{10} p_{10}^{avail} - k_{10}^{off} e_{10}^m \quad (6)$$
$$+k^{cat}_{z_{10}^m:TEN} [Z_{10}^m : TEN] + (k^{cat}_{z_5^m:e_{10}^m} + k^-_{z_5^m:e_{10}^m})[Z_5^m : E_{10}^m]$$
$$-k^+_{z_5^m:e_{10}^m} e_{10}^m z_5^m + (k^{cat}_{z_8^m e_{10}^m} + k^-_{z_8^m e_{10}^m})[Z_8^m : E_{10^m}]$$
$$-k^+_{z_8^m:e_{10}^m} e_{10}^m z_8^m$$
$$+k^-_{e_5^m:e_{10}^m} [PRO] - k^p_{e_5^m:e_{10}^m} e_{10}^m e_5^m$$
$$+k^{cat}_{z_{10}^m:TEN} [Z_{10}^m : TEN^*]$$
$$-k^+_{e_5^{hm}:e_{10}^m} e_{10}^m e_5^{hm} + k^-_{e_5^{hm}:e_{10}^m} PRO^h$$
$$-k^+_{TFPI:e_{10}^m} e_{10}^m TFPI + k^-_{TFPI:e_{10}^m} [TFPI : E_{10}^m]$$
$$-k^+_{TFPI:e_5^{hm}:e_{10}^m} [TFPI : E_5^{hm}] e_{10}^m$$
$$+k^-_{TFPI:e_5^{hm}:e_{10}^m} [E_{10}^m : TFPI : E_5^{hm}]$$
$$-k^+_{TFPI:e_{10}:e_5^{hm}} [TFPI : E_5^{hm}] e_{10}^m$$
$$+k^-_{TFPI:e_{10}:e_5^{hm}} [TFPI : PRO^h]^{v5}$$
$$-k^{AT}_{e_{10}^m} e_{10}^m [AT]$$
$$-k^{ATH}_{e_{10}^m} e_{10} [AT : Hep]$$

$$\frac{d}{dt}z_5 = -k_5^{on} z_5 p_5^{avail} + k_5^{off} z_5^m \quad (7)$$
$$-k^+_{z_5:e_2} z_5 e_2 + k^-_{z_5:e_2} [Z_5 : E_2]$$
$$k_{flow}(z_5^{up} - z_5)$$
$$+n_5 (k^+_{adh} p^{avail}_{PLAS} + k^{act}_{plt}([PL_a^v] + [PL_a^s]) + k^{act}_{e2} \frac{e_2}{e_2 + 0.001})[PL]$$

$$\frac{d}{dt}e_5 = -k_5^{on} e_5 p_5^{avail} + k_5^{off} e_5^m \quad (8)$$
$$+k^{cat}_{z_5:e_2} [Z_5 : E_2]$$
$$+k_{flow}(e_5^{up} - e_5)$$
$$k^-_{e_5:APC} [APC : E_5] - k^+_{e_5:APC} e_5 [APC]$$
$$+k^{cat}_{e_5^h:e_2} [E_5^h : E_2]$$

$$\frac{d}{dt}z_5^m = k_5^{on} z_5 p_5^{avail} - k_5^{off} z_5^m \quad (9)$$
$$-k^+_{z_5^m e_{10}^m} z_5^m e_{10}^m + k^-_{z_5^m:e_{10}^m} [Z_5^m : E_{10}^m]$$
$$-k^+_{z_5^m:e_2^m} z_5^m e_2^m + k^-_{z_5^m e_2^m} [Z_5^m : E_2^m]$$

$$\frac{d}{dt}e_5^m = k_5^{on}e_5p_5^{avail} - k_5^{off}e_5^m \quad (10)$$
$$+k^{cat}_{z_5^m:e_2^m}[Z_5^m : E_2^m]$$
$$+k^{-}_{e_5^m:APC}[APC : E_5^m]$$
$$-k^{+}_{e_5^m:APC}e_5^m[APC]$$
$$-k^{+}_{e_5^m:e_{10}^m}e_5^m e_{10}^m + k^{-}_{e_5^m:e_{10}^m}[PRO]$$
$$+k^{cat}_{e_5^{hm}:e_2^m}[E_5^{hm} : E_2^m]$$

$$\frac{d}{dt}z_8 = -k_8^{on}z_8p_8^{avail} + k_8^{off}z_8^m \quad (11)$$
$$+k_{flow}(z_8^{up} - z_8)$$
$$-k^{+}_{z_8:e_2}z_8e_2 + k^{-}_{z_8:e_2}[Z_8 : E_2]$$

$$\frac{d}{dt}e_8 = -k_8^{on}e_8p_8^{avail} + k_8^{off}e_8^m \quad (12)$$
$$k_{flow}(e_8^{up} - e_8)$$
$$+k^{cat}_{z_8:e_2} - 0.005e_8$$
$$+k^{-}_{e_8:APC}[APC : E_8] - k^{+}_{e_8:APC}e_8[APC]$$

$$\frac{d}{dt}z_8^m = k_8^{on}z_8p_8^{avail} - k_8^{off}z_8^m \quad (13)$$
$$-k^{+}_{z_8^m:e_{10}^m}z_8^m e_{10}^m + k^{-}_{z_8^m:e_{10}^m}[Z_8^m : E_{10}^m]$$
$$-k^{+}_{z_8^m:e_2^m}z_8^m e_2^m$$
$$+k^{-}_{z_8^m:e_2^m}[Z_8^m : E_2^m]$$

$$\frac{d}{dt}e_8^m = k_8^{on}e_8p_8^{avail} - k_8^{off}e_8^m \quad (14)$$
$$k^{cat}_{z_8^m:e_{10}^m}[Z_8^m : E_{10}^m] + k^{cat}_{z_8^m:e_2^m}[Z_8^m : E_2^m]$$
$$-k^{+}_{e_8^m:APC}e_8^m[APC] + k^{-}_{e_8^m:APC}[APC : E_8^m]$$
$$-k^{+}_{e_8^m:e_9^m}e_9^m e_8^m + k^{-}_{e_8^m:e_9^m}[TEN] - 0.005e_8^m$$
$$-k^{+}_{e_8^m:e_9^m}e_8^m e_9^m + k^{-}_{e_8^m:e_9^m}[TEN]$$

$$\frac{d}{dt}z_9 = k_{flow}(z_9^{up} - z_9) - k_9^{on}p_9^{avail}z_9 + k_9^{off}z_9^m \quad (15)$$
$$-k^{+}_{z_9:e_7^m}z_9e_7^m + k^{-}_{z_9:e_7^m}[Z_9 : E_7^m]$$
$$-k^{+}_{z_9:e_{11}^h}e_{11}^h + k^{-}_{z_9:e_{11}^h}[Z_9 : E_{11}^h]$$
$$-k^{+}_{z_9:e_11}z_9e_{11} + k^{-}_{z_9:e_{11}}[Z_9 : E_{11}]$$

$$\frac{d}{dt}e_9 = f_{flow}(e_9^{up} - e_9) \tag{16}$$
$$-k_9^{on} p_9^{avail} e_9 + k_9^{off} e_9^m$$
$$k_{z_9:e_7^m}^{cat}[Z_9 : E_7^m]$$
$$\cancel{-k_{AT:e_9}^{in} e_9} - k_{z_7:e_9}^{+} z_7 e_9$$
$$+(k_{z_7:e_9}^{cat} + k_{z_7:e_9}^{-})[Z_7 : E_9]$$
$$+(k_{z_7^m:e_9}^{cat} + k_{z_7^m:e_9}^{-})[Z_7^m : E_9] - k_{z_7^m:e_9}^{+} z_7^m e_9$$
$$-k_9^{on} p_9^{*,avail} e_9 + k_9^{off} e_9^{m*}$$
$$-k_{diff}(e_9 - e_9^{ec})$$
$$+k_{z_9:e_{11}^h}^{cat}[Z_9 : E_{11}^h] + k_{z_9:e_{11}}^{cat}[Z_9 : E_{11}]$$
$$-k_{e_9}^{AT} e_9[AT]$$
$$-k_{e_9}^{ATH} e_9[AT : Hep]$$

$$\frac{d}{dt}z_9^m = k_9^{on} p_9^{avail} z_9 - k_9^{off} z_9^m \tag{17}$$
$$-k_{z_9^m:e_{11}^{h,m}}^{+} z_9^m e_{11}^{h,m} + k_{z_9^m e_{11}^{h,m}}^{-}[Z_9^m : E_{11}^{h,m}]$$
$$-k_{z_9^m:e_{11}^{m*}}^{+} z_9^m e_{11}^{m*} + k_{z_9^m e_{11}^{m*}}^{-}[Z_9^m : E_{11}^{m*}]$$

$$\frac{d}{dt}e_9^m = k_9^{on} p_9^{avail} e_9 - k_9^{off} e_9^m \tag{18}$$
$$-k_{e_8^m:e_9^m}^{+} e_8^m e_9^m + k_{e_8^m:e_9^m}^{-}[TEN]$$
$$+k_{z_9^m:e_{11}^{h,m}}^{cat}[Z_9^m : E_{11}^{h,m}]$$
$$+k_{z_9^m:e_{11}^{m*}}^{cat}[Z_9^m : E_{11}^{m*}]$$
$$-k_{e_9^m}^{AT} e_9^m[AT]$$
$$-k_{e_9^m}^{ATH} e_9^m[AT : Hep]$$

$$\frac{d}{dt}z_2 = -k_2^{on} p_2^{avail} z_2 + k_2^{off} z_2^m + k_{flow}(z_2^{up} - z_2) \tag{19}$$

$$\frac{d}{dt}e_2 = k_{flow}(e_2^{up} - e_2) \tag{20}$$
$$-k_{2*}^{on} p_2^{*,avail} e_2 + k_{2*}^{off} e_2^m + k_{z_2^m:PRO}^{cat}[Z_2^m : PRO]$$
$$\cancel{-k_{AT:e_2}^{in} e_2} - k_{z_5:e_2^p} z_5 e_2 + (k_{z_5:e_2}^{cat} + k_{z_5:e_2}^{-})[Z_5 : E_2]$$
$$-k_{z_8:e_2}^{+} z_8 e_2 + (k_{z_8:e_2}^{cat} + k_{z_8:e_2}^{-})[Z_8 : E_2]$$
$$-k_{z_7:e_2}^{+} z_7 e_2 + (k_{z_7^m:e_2}^{cat} + k_{z_7:e_2}^{-})[Z_7 : E_2]$$
$$-k_{z_7^m e_2}^{+} z_7^m e_2 + (k_{z_7^m:e_2}^{cat} + k_{z_7^m:e_2}^{-})[Z_7^m : E_2]$$
$$-k_{diff}(e_2 - e_2^{ec})$$
$$-k_{z_{11}:e_2}^{+} z_{11} + (k_{z_{11}:e_2}^{-} + k_{z_{11}:e_2}^{cat})[Z_{11} : E_2]$$
$$-k_{e_{11}^h:e_2}^{+} e_{11}^h e_2 + (k_{e_{11}^h:e_2}^{-} + k_{e_{11}^h} : e_2)^{cat}[E_{11}^h : E_2]$$
$$+k_{z_2^m:PRO^h}^{cat}[Z_2^m : PRO^h] - k_{e_5^h:e_2}^{+} e_2 e_5^h$$
$$+k_{e_5^h:e_2}^{-}[E_5^h : E_2] + k_{e_5^h:e_2}^{cat}[E_5^h : E_2]$$
$$-k_{e_2}^{AT} e_2[AT]$$
$$-k_{e_2}^{ATH} e_2[AT : Hep]$$

$$\begin{aligned}
\frac{d}{dt}z_2^m &= k_2^{on}p_2^{avail}z_2 - k_2^{off}z_2^m \\
&\quad -k^+_{z_2^m:PRO}z_2^m[PRO] + k^-_{z_2^m:PRO}[Z_2^m:PRO] \\
&\quad -k^+_{z_2^m:PRO^h}z_2^m PRO^h + k^-_{z_2^m:PRO^h}[Z_2^m:PROh]
\end{aligned} \tag{21}$$

$$\begin{aligned}
\frac{d}{dt}e_2^m &= k_{2*}^{on}p_2^{avail}e_2 - k_{2*}^{off}e_2^m \\
&\quad +(k^{cat}_{z_5^m:e_2^m} + k^-_{z_5^m:e_2^m})[Z_5^m:E_2^m] \\
&\quad -k^+_{z_5^m:e_2^m}z_5^m e_2^m \\
&\quad +(k^{cat}_{z_8^m:e_2^m} + k^-_{z_8^m:e_2^m})[Z_8^m:E_2^m] - k^+_{z_8^m:E_2^m}z_8^m e_2^m \\
&\quad -k^+_{z_{11}^m:e_2^m}z_{11}^m e_2^m \\
&\quad +(k^-_{z_{11}^m:e_2^m} + k^{cat}_{z_{11}^m:e_2^m})[Z_{11}^m:E_2^m] \\
&\quad -k^+_{e_{11}^{h,m*}e_2^m}e_{11}^{h,m*}e_2^m \\
&\quad +(k^-_{e_{11}^{h,m*}e_2^m} + k^{cat}_{e_{11}^{h,m*}:e_2^m})[E_{11}^{hms}:E_2^m] \\
&\quad -k^+_{e_5^{hm}:e_2^m}e_2^m e_5^{hm} + k^-_{e_5^{hm}:e_2^m}[E_5^{hm}:E_2^m] \\
&\quad +k^{cat}_{e_5^{hm}:e_2^m}[E_5^{hm}:E_2^m] \\
&\quad -k^+_{PRO^h:e_2^m}PRO^h e_2^m + k^-_{PRO^h:e_2^m}[PRO^h:E_2^m] \\
&\quad +k^{cat}_{PRO^h:e_2^m}[PRO^h:E_2^m] \\
&\quad -k^{AT}_{e_2^m}e_2^m[AT] \\
&\quad -k^{ATH}_{e_2^m}e_2^m[AT:Hep]
\end{aligned} \tag{22}$$

$$\begin{aligned}
\frac{d}{dt}[TEN] &= -k^-_{e_8^m:e_9^m}[TEN] + k_{e_8^m:e_9^m}e_8^m e_9^m \\
&\quad +(k^{cat}_{z_{10}^m:TEN} + k^-_{z_{10}^m:TEN})[Z_{10}^m:TEN] - k^+_{z_{10}^m:TEN}z_{10}^m[TEN]
\end{aligned} \tag{23}$$

$$\begin{aligned}
\frac{d}{dt}[PRO] &= -k^-_{e_5^m:e_{10}^m}[PRO] + k^+_{e_5^m:e_{10}^m}e_{10}^m e_5^m \\
&\quad +(k^{cat}_{z_2^m:PRO} + k^-_{z_2^m:PRO})[Z_2^m:PRO] - k^+_{z_2^m:PRO}z_2^m[PRO] \\
&\quad +k^{cat}_{PRO^h:e_2^m}[PRO^h:E_2^m]
\end{aligned} \tag{24}$$

$$\begin{aligned}
\frac{d}{dt}[PL_a^s] &= k^+_{adh}p^{avail}_{PLAS}[PL] - k^-_{adh}[PL_a^s] \\
&\quad +k^+_{adh}[PL_a^v] * p^{avail}_{PLAS}
\end{aligned} \tag{25}$$

$$\begin{aligned}
\frac{d}{dt}[PL] &= k^p_{flow}([PL]^{up} - [PL]) \\
&\quad -k^+_{adh}p^{avail}_{PLAS} + (k^{act}_{plt}([PL_a^v] + [PL_a^s]) + k^{act}_{e2}\frac{e_2}{e_2 + 0.001})[PL]
\end{aligned} \tag{26}$$

$$\begin{aligned}
\frac{d}{dt}[PL_a^v] &= k^-_{adh}[PL_a^s] - k^+_{adh}[PL_a^v]p^{avail}_{PLAS} \\
&\quad +(k^{act}_{plt}([PL_a^v] + [PL_a^s]) + k^{act}_{e2}\frac{e_2}{e_2 + 0.001})[PL]
\end{aligned} \tag{27}$$

$$\begin{aligned}
\frac{d}{dt}z_7^m &= k_7^{on}z_7[TF]^{avail} - k_7^{off}z_7^m \\
&\quad -k^+_{z_7^m:e_{10}}z_7^m e_{10} - k^+_{z_7^m:e_2}z_7^m e_2 \\
&\quad +k^-_{z_7^m:e_{10}}[Z_7^m:E_{10}] + k^-_{z_7^m:e_2}[Z_7^m:E_2] \\
&\quad -k^+_{z_7^m:e_9}z_7^m e_9 + k^-_{z_7^m:e_9}[Z_7^m:E_9] \\
&\quad -z_7^m\frac{d}{dt}[PL_a^s]\frac{1}{p^{avail}_{PLAS}}
\end{aligned} \tag{28}$$

$$\frac{d}{dt}e_7^m = k_7^{on}e_7[TF]^{avail} - k_7^{off}e_7^m \tag{29}$$
$$k^+_{TFPI:e_{10}:e_7^m}e_7^m[TFPI:E_{10}] + k^-_{TFPI:e_{10}:e_7^m}[TFPI:E_7^m]$$
$$+k^{cat}_{z_7^m:e_{10}}[Z_7^m:E_{10}] + k^{cat}_{z_7^m:e_2}[Z_7^m:E_2]$$
$$+(k^{cat}_{z_{10}:e_7^m} + k^-_{z_{10}:e_7^m})[Z_{10}:E_7^m]$$
$$-k^+_{z_{10}:e_7^m}e_7^m z_{10} - k^+_{z_9:e_7^m}e_7^m z_9$$
$$+(k^{cat}_{z_9:e_7^m} + k^-_{z_9:e_7^m})[Z_9:E_7^m]$$
$$+k^{cat}_{z_7^m:e_9}[Z_7^m:E_9] - e_7^m\frac{d}{dt}[PL_a^s]\frac{1}{p^{avail}_{PLAS}}$$

$$\frac{d}{dt}[TFPI] = -k^+_{TFPI:e_{10}}e_{10}[TFPI] + k^-_{TFPI:e_{10}}[TFPI:E_{10}] \tag{30}$$
$$k_{flow}([TFPI]^{up} - [TFPI])$$
$$-k^+_{TFPI:e_5^{hm}}e_5^{hm}[TFPI] + k^-_{TFPI:e_5^{hm}}[TFPI:E_5^{hm}]$$
$$-k^+_{TFPI:e_5^h}e_5^h[TFPI] + k^-_{TFPI:e_5^h}[TFPI:E_5^h]$$
$$-k^+_{TFPI:e_{10}^m}e_{10}^m[TFPI] + k^-_{TFPI:e_{10}^m}[TFPI:E_{10}^m]$$
$$-k^+_{TFPI:PRO^h:v_{10}}PRO^h[TFPI]$$
$$+k^-_{TFPI:PRO^h:v_{10}}[TFPI:PRO^h]^{v10}$$
$$-k^+_{TFPI:PRO^h:v_5}PRO^h[TFPI]$$
$$+k^-_{TFPI:PRO^h:v_5}[TFPI:PRO^h]^{v5}$$

$$\frac{d}{dt}[TFPI:E_{10}] = k^+_{TFPI:e_{10}}e_{10}[TFPI] - k^-_{TFPI:e_{10}}[TFPI:E_{10}] \tag{31}$$
$$+k^-_{TFPI:e_{10}:e_7^m}[TFPI:E_{10}:E_7^m]$$
$$-k^+_{TFPI:e_{10}:e_7^m}e_7^m[TFPI:E_{10}] + k_{flow}([TFPI:E_{10}]^{up} - [TFPI:E_{10}])$$
$$-k^+_{TFPI:e_{10}:e_5^h}[TFPI:E_{10}]e_5^h$$
$$+k^-_{TFPI:e_{10}:e_5^h}[E_{10}:TFPI:E_5^h]$$
$$-k_{10}^{on}[TFPI:E_{10}]p_{10}^{avail} + k_{10}^{off}[TFPI:E_{10}^m]$$

$$\frac{d}{dt}[TFPI:E_{10}:E_7^m] = -k^-_{TFPI:e_{10}:e_7^m}[TFPI:E_{10}:E_7^m] + k^+_{TFPI:e_{10}:e_7^m}e_7^m[TFPI:E_{10}] \tag{32}$$
$$-[TFPI:E_{10}:E_7^m]\frac{d}{dt}[PL_a^s]\frac{1}{p^{avail}_{PLAS}}$$

$$\frac{d}{dt}[APC] = (k^{cat}_{e_5^m:APC} + k^-_{e_5^m:APC})[APC:E_5^m] - k^{cat}_{e_5^m:APC}e_5^m \tag{33}$$
$$+(k^{cat}_{e_8^m:APC} + k^-_{e_8^m:APC})[APC:E_8^m] - k^+_{e_8^m:APC}e_8^m[APC]$$
$$+k_{flow}([APC]^{up} - [APC]) - k_{diff}([APC] - [APC^{ec}])$$
$$+(k^{cat}_{e_5:APC} + k^-_{e_5:APC})[APC:E_5] - k^+_{e_5:APC}e_5[APC]$$
$$+(k^{cat}_{e_8:APC} + k^-_{e_8:APC})[APC:E_8] - k^+_{e_8:APC}e_8[APC]$$
$$-k^+_{e_5^{hm}:APC}e_5^{hm}APC + k^-_{e_5^{hm}:APC}[APC:E_5^{hm}]$$
$$+k^{cat}_{e_5^{hm}:APC}[APC:E_5^{hm}] - k^+_{e_5^h:APC}e_5^hAPC$$
$$+k^-_{e_5^h:APC}[APC:E_5^h] + k^{cat}_{e_5^h:APC}[APC:E_5^h]$$

$$\frac{d}{dt}[Z_7 : E_2] = k_{flow}([Z_7 : E_2]^{up} - [Z_7 : E_2]) + k^+_{z_7:e_2} e_2 z_7 \quad (34)$$
$$-(k^{cat}_{z_7:e_2} + k^-_{z_7:e_2})[Z_7 : E_2]$$

$$\frac{d}{dt}[Z_7 : E_{10}] = k^+_{z_7:e_{10}} e_{10} z_7 - (k^{cat}_{z_7:e_{10}} + k^-_{z_7:e_{10}})[Z_7 : E_{10}] \quad (35)$$
$$+k_{flow}([Z_7 : E_{10}]^{up} - [Z_7 : E_{10}])$$

$$\frac{d}{dt}[Z^m_7 : E_{10}] = k^+_{z^m_7:e_{10}} e_{10} z^m_7 \quad (36)$$
$$-(k^{cat}_{z^m_7:e_{10}} + k^-_{z^m_7:e_{10}})[Z^m_7 : E_{10}] - [Z^m_7 : E_{10}]\frac{d}{dt}[PL^s_a]\frac{1}{p^{avail}_{PLAS}}$$

$$\frac{d}{dt}[Z^m_7 : E_2] = k^+_{z^m_7:e_2} e_2 z^m_7 - (k^{cat}_{z^m_7:e_2} + k^-_{z^m_7:e_2})[Z^m_7 : E_2] \quad (37)$$
$$-[Z^m_7 : E_2]\frac{d}{dt}[PL^s_a]\frac{1}{p^{avail}_{PLAS}}$$

$$\frac{d}{dt}[Z_{10} : E^m_7] = k^+_{z_{10}:e^m_7} e^m_7 z_{10} - (k^{cat}_{z_{10}:e^m_7} + k^-_{z_{10}:e^m_7})[Z_{10} : E^m_7] \quad (38)$$
$$-[Z_{10} : E^m_7]\frac{d}{dt}[PL^s_a]\frac{1}{p^{avail}_{PLAS}}$$

$$\frac{d}{dt}[Z^m_{10} : TEN] = k^+_{z^m_{10}:TEN} z^m_{10}[TEN] - (k^{cat}_{z^m_{10}:TEN} + k^-_{z^m_{10}:TEN})[Z_{10^m} : TEN] \quad (39)$$

$$\frac{d}{dt}[Z_5 : E_2] = k^+_{z_5:e_2} e_2 z_5 - (k^{cat}_{z_5:e_2} + k^-_{z_5:e_2})[Z_5 : E_2] \quad (40)$$
$$+k_{flow}([Z_5 : E_2]^{up} - [Z_5 : E_2])$$

$$\frac{d}{dt}[Z^m_5 : e^m_{10}] = k^+_{z^m_5:e^m_{10}} e^m_{10} z^m_5 - (k^{cat}_{z^m_5:e_{10}} + k^-_{z^m_5:e^m_{10}})[Z^m_5 : E^m_{10}] \quad (41)$$

$$\frac{d}{dt}[Z^m_5 : E^m_2] = k^+_{z^m_5:e^m_2} e^m_2 z^m_5 - (k^{cat}_{z^m_5:e^m_2} + k^-_{z^m_5:e^m_2})[Z^m_5 : E^m_2] \quad (42)$$

$$\frac{d}{dt}[Z^m_8 : E^m_{10}] = k^+_{z^m_8:e^m_{10}} e^m_{10} z^m_8 - (k^{cat}_{z^m_8:e^m_{10}} + k^-_{z^m_8:e^m_{10}})[Z^m_8 : E^m_{10}] \quad (43)$$

$$\frac{d}{dt}[Z^m_8 : E^m_2] = k^+_{z^m_8:e^m_2} e^m_2 z^m_8 - (k^{cat}_{z^m_8:e^m_2} + k^-_{z^m_8:e^m_2})[Z^m_8 : E^m_2] \quad (44)$$

$$\frac{d}{dt}[Z_8 : E_2] = k^+_{z_8:e_2} e_2 z_8 - (k^{cat}_{z_8:e_2} + k^-_{z_8:e_2})[Z_8 : E_2] \quad (45)$$
$$k_{flow}([Z_8 : E_2]^{up} - [Z_8 : E_2])$$

$$\frac{d}{dt}[APC : E^m_8] = k^+_{e^m_8:APC} e^m_8 [APC] - (k^{cat}_{e^m_8:APC} + k^-_{e^m_8:APC})[APC : E^m_8] \quad (46)$$

$$\frac{d}{dt}[Z_9 : E^m_7] = k^+_{z_9:e^m_7} e^m_7 z_9 - (k^{cat}_{z_9:e^m_7} + k^-_{z_9:e^m_7})[Z_9 : E^m_7] \quad (47)$$
$$-[Z_9 : E^m_7]\frac{d}{dt}[PL^s_a]\frac{1}{p^{avail}_{PLAS}}$$

$$\frac{d}{dt}[Z^m_2 : PRO] = k^+_{z^m_2:PRO} z^m_2 [PRO] - (k^{cat}_{z^m_2:PRO} + k^-_{z^m_2:PRO})[Z^m_2 : PRO] \quad (48)$$

$$\frac{d}{dt}[APC : E^m_5] = k^+_{e^m_5:APC} e^m_5 [APC] - (k^{cat}_{e^m_5:APC} + k^-_{e^m_5:APC})[APC : E^m_5] \quad (49)$$

$$\frac{d}{dt}[TF] = -[TF]\frac{d}{dt}[PL^s_a]\frac{1}{p^{avail}_{PLAS}} \quad (50)$$

$$\frac{d}{dt}[Z_7 : E_9] = k^+_{z_7:e_9} e_9 z_7 - (k^{cat}_{z_7:e_9} + k^-_{z_7:e_9})[Z_7 : E_9] \quad (51)$$

$$\frac{d}{dt}[Z^m_7 : E_9] = k^+_{z^m_7:e_9} e_9 z^m_7 - (k^{cat}_{z^m_7:e_9} + k^-_{z^m_7:e_9})[Z^m_7 : E_9] \quad (52)$$
$$-[Z^m_7 : E_9]\frac{d}{dt}[PL^s_a]\frac{1}{p^{avail}_{PLAS}}$$

$$\frac{d}{dt}e_9^{m*} = k_9^{on}p_9^{*,avail}e_9 - k_9^{off}e_9^{m*} + k^-_{e_8^m:e_9^m}[TEN^*] \quad (53)$$
$$-k^+_{e_8^m:e_9^m}e_8^m e_9^{m*}$$
$$-k^{AT}_{e_9^m}e_9^{m*}[AT]$$
$$-k^{ATH}_{E_9^m}e_9^{m*}[AT:Hep]$$

$$\frac{d}{dt}[TEN^*] = -k^-_{e_8^m:e_9^m}[TEN^*] + k^+_{e_8^m:e_9^m}e_8^m e_9^{m*} \quad (54)$$
$$+(k^{cat}_{z_{10}^m:TEN} + k^-_{z_{10}^m:TEN})[Z_{10}^m:TEN^*]$$
$$k^+_{z_{10}^m:TEN}[TEN^*]z_{10}^m$$

$$\frac{d}{dt}[Z_{10}^m:TEN^*] = k^+_{z_{10}^m:TEN}[TEN^*]z_{10}^m - (k^{cat}_{z_{10}^m:TEN} + k_{z_{10}^m}:TEN)^-[Z_{10}^m:TEN^*] \quad (55)$$

$$\frac{d}{dt}e_2^{ec} = k_{diff}(e_2 - e_2^{ec}) + k_{flow}(e_2^{ec,up} - e_2^{ec}) \quad (56)$$
$$-\cancel{k^{in}_{AT:e_2}e_2^{ec}}$$
$$-k^{on}_{TM}e_2^{ec}[TM]^{avail} + k^{off}_{TM}[TM:E_2^{ec}] - k^{AT}_{e_2^{ec}}e_2^{ec}[AT]$$

$$\frac{d}{dt}[APC^{ec}] = k_{flow}([APC]^{up} - [APC^{ec}]) + k_{diff}([APC] - [APC^{ec}]) \quad (57)$$
$$+k^{cat}_{PC:TM:e_2}[TM:E_2^{ec}:APC]$$

$$\frac{d}{dt}[TM:E_2^{ec}] = k^+_{TM}[E_2^{ec}](1 - [TM:E_2^{ec}] - [TM:E_2^{ec}:APC]) \quad (58)$$
$$-k^-_{TM}[TM:E_2^{ec}] - k^+_{PC:TM:e_2}[TM:E_2^{ec}]$$
$$+(k^-_{PC:TM:e_2} + k^{cat}_{PC:TM:e_2})[TM:E_2^{ec}:APC]$$

$$\frac{d}{dt}[TM:E_2^{ec}:APC] = k^+_{PC:TM:e_2}[TM:E_2^{ec}] \quad (59)$$
$$-(k^-_{PC:TM:e_2} + k^{cat}_{PC:TM:e_2})[TM:E_2^{ec}:APC]$$

$$\frac{d}{dt}e_9^{ec} = k_{diff}(e_9 - e_9^{ec}) + k_{flow}(e_9^{up} - e_9^{ec}) \quad (60)$$
$$-\cancel{k^{in}_{AT:e_9}e_9^{ec}} - k^{AT}_{e_9^{ec}}e_9^{ec}[AT]$$

$$\frac{d}{dt}e_{10}^{ec} = k_{diff}(e_{10} - e_{10}^{ec}) + k_{flow}(e_{10}^{up} - e_{10}^{ec}) \quad (61)$$
$$-\cancel{k^{in}_{AT:e_{10}}e_{10}^{ec}} - k^{AT}_{e_{10}^{ec}}e_{10}^{ec}[AT]$$

$$\frac{d}{dt}[APC:E_5] = -(k^{cat}_{e_5:APC} + k^-_{e_5:APC})[APC:E_5] + k^+_{e_5:APC}e_5[APC] \quad (62)$$

$$\frac{d}{dt}[APC:E_8] = -(k^{cat}_{e_8:APC} + k^-_{e_8:APC})[APC:E_8] + k^+_{e_8:APC}e_8[APC] \quad (63)$$

$$\frac{d}{dt}z_{11} = k_{flow}(z_{11}^{up} - z11) - k^{on}_{z_{11}}z_{11}p_{11}^{avail} \quad (64)$$
$$k^{off}_{z_{11}}z_{11}^m - k^+_{z_{11}:e_{11}^h}z_{11}e_{11}^h$$
$$k^-_{z_{11}:e_{11}^h}[Z_{11}:E_{11}^h] - k^+_{z_{11}:e_{11}}z_{11}e_{11}$$
$$k^-_{z_{11}:e_{11}}[Z_{11}:E_{11}] - k^+_{z_{11}:e_2}z_{11}e_2$$
$$k^-_{z_{11}:e_2}[Z_{11}:E_2]$$

$$\begin{aligned}
\frac{d}{dt}e_{11} &= k_{flow}(e_{11}^{up} - e_{11}) \\
&\quad -k_{e_{11}^{on,s}} e_{11} p_{111}^{avail} + k_{e_{11}^{off,s}} e_{11}^{m*} \\
&\quad -k^{+}_{z_9:e_{11}} z_9 e_{11} + (k^{-}_{z_9:e_{11}} + k^{cat}_{z_9:e_{11}})[Z_9 : E_{11}] \\
&\quad -k^{+}_{z_{11}:e_{11}} z_{11} e_{11} + (k^{-}_{z_{11}:e_{11}} + k^{cat}_{z_{11}:e_{11}})[Z_{11} : E_{11}] \\
&\quad +k^{cat}_{e_{11}^h:e_{11}^h}[E_{11}^h : E_{11}^h] - k^{+}_{e_{11}^h:e_{11}} e_{11}^h e_{11} \\
&\quad +(k^{-}_{e_{11}^h:e_{11}} + 2 * k^{cat}_{e_{11}^h:e_{11}})[E_{11}^h : E_{11}] \\
&\quad +k^{cat}_{e_{11}^h:e_2}[E_{11}^h : E_2] \\
&\quad -k^{AT}_{e_{11}} e_{11}[AT] \\
&\quad -k^{ATH}_{e_{11}} e_{11}[AT : Hep] \qquad (65) \\
\frac{d}{dt}z_{11}^m &= k^{on}_{z_{11}} z_{11} p_{11}^{avail} - k^{off}_{z_{11}} z_{11}^m \\
&\quad -k^{+}_{z_{11}^m:e_{11}^{h,m}} z_{11}^m e_{11}^{h,m} + k^{-}_{z_{11}^m:e_{11}^{h,m}}[Z_{11}^m : E_{11hm}] \\
&\quad -k^{+}_{z_{11}^m:e_{11}^{m*}} z_{11}^m e_{11}^{m*} + k^{-}_{z_{11}^m:e_{11}^{m*}}[Z_{11}^m : E_{11}^{m*}] \\
&\quad -k^{+}_{z_{11}^m:E_2^m} z_{11}^m e_2^m + k^{-}_{z_{11}^m:e_2^m}[Z_{11}^m : E_2^m] \qquad (66) \\
\frac{d}{dt}e_{11}^{m*} &= k^{on*}_{e_{11}} e_{11} p_{111}^{avail} - k^{off*}_{e_{11}} e_{11}^{m*} \\
&\quad -k^{+}_{z_9^m:e_{11}^{m*}} e_{11}^{m*} z_9^m \\
&\quad +(k^{-}_{z_9^m:e_{11}^{m*}} + k^{cat}_{z_9^m:e_{11}^{m*}})[Z_9^m : E_{11}^{m*}] \\
&\quad -k^{+}_{z_{11}^m:e_{11}^{m*}} z_{11}^m e_{11}^{m*} \\
&\quad +(k^{-}_{z_{11}^m:e_{11}^{m*}} + k^{cat}_{z_{11}^m:e_{11}^{m*}})[Z_{11}^m : E_{11}^{m*}] \\
&\quad +k^{+}_{e_{11}^{h,m*}:e_{11}^{m*}} e_{11}^{h,m*} e_{11}^{m*} \\
&\quad +(k^{-}_{e_{11}^{h,m*}:e_{11}^{m*}} + 2 * k^{cat}_{e_{11}^{h,m*}:e_{11}^{m*}})[E_{11}^{hms} : E_{11}^{h,m}] \\
&\quad +k^{cat}_{e_{11}^{h,m*}:e_2^m}[E_{11}^{hms} : E_2^m] \\
&\quad +k^{AT}_{e_{11}} e_{11}^{m*}[AT] \\
&\quad -k^{ATH}_{e_{11}} e_{11}^{m*}[AT : Hep] \qquad (67) \\
\frac{d}{dt}[Z_{11}^m : E_2^m] &= k^{+}_{z_{11}^m:e_2^m} z_{11}^m e_2^m - (k^{-}_{z_{11}^m:e_2^m} + k^{cat}_{z_{11}^m:e_2^m})[Z_{11}^m : E_2^m] \qquad (68) \\
\frac{d}{dt}[Z_9^m : E_{11}^{m*}] &= k^{+}_{z_9^m:e_{11}^{m*}} z_9^m e_{11}^m s \qquad (69) \\
&\quad -(k^{-}_{z_9^m:e_{11}^{m*}} + k^{cat}_{z_9^m:e_{11}^{m*}})[Z_9^m : E_{11}^{m*}] \\
\frac{d}{dt}[Z_{11} : E_2] &= k_{flow}([Z_{11} : E_2]^{up} - [Z_{11} : E_2]) + k^{+}_{z_{11}:e_2} z_{11} e_2 \qquad (70) \\
&\quad -(k^{-}_{z_{11}:e_2} + k^{cat}_{z_{11}:e_2})[Z_{11} : E_2] \\
\frac{d}{dt}[Z_9 : E_{11}] &= k_{flow}([Z_9 : E_{11}]^{up} - [Z_9 : E_{11}]) + k^{+}_{z_9:e_{11}} z_9 e_{11} \qquad (71) \\
&\quad -(k^{-}_{z_9:E_{11}} + k^{cat}_{z_9:e_{11}})[Z_9 : E_{11}] \\
\frac{d}{dt}[Z_{11} : E_{11}] &= k_{flow}([Z_{11} : E_{11}]^{up} - [Z_{11} : E_{11}]) + k^{+}_{z_{11}:e_{11}} z_{11} e_{11} \qquad (72) \\
&\quad -(k^{-}_{z_{11}:e_{11}} + k^{cat}_{z_{11}:e_{11}})[Z_{11} : E_{11}]
\end{aligned}$$

$$\begin{aligned}
\frac{d}{dt}e^h_{11} &= k^{on*}_{e^h_{11}} e^h_{11} p^{avail}_{111} + k^{off*}_{e^h_{11}} e^{h,m*}_{11} \\
&\quad -k^{on}_{e^h_{11}} e^h_{11} p^{avail}_{11} + k^{off}_{e^h_{11}} e^{h,m}_{11} \\
&\quad -k^{+}_{z_9:e^h_{11}} z_9 e^h_{11} + (k^{-}_{z_9:e^{h,m}_{11}} + k^{cat}_{z_9:e^h_{11}})[Z_9 : E^h_{11}] \\
&\quad -k_{z_{11}:e^{hp}_{11}} z_{11} e^h_{11} + (k^{-}_{z_{11}:e^h_{11}m} + 2 * k^{cat}_{z_{11}:e^h_{11}})[Z_{11:E^h_{11}}] \\
&\quad +k^{cat}_{z_{11}:e_{11}}[Z_{11} : E_{11}] + k^{cat}_{z_{11}:e_2}[Z_{11} : E_2] \\
&\quad -2 * k^{+}_{e^h_{11}:e^h_{11}} e^h_{11} e^h_{11} \\
&\quad +(2 * k^{-}_{e^h_{11}:e^h_{11}} + k^{cat}_{e^g_{11}:e^h_{11}})[E^h_{11} : E^h_{11}] \\
&\quad -k^{+}_{e^h_{11}:e_{11}} e^h_{11} e_{11} + k^{-}_{e^h_{11}:e_{11}}[E^h_{11} : E_{11}] \\
&\quad -k^{+}_{e^h_{11}:e_2} e^h_{11} e_2 + k^{-}_{e^h_{11}:e_2}[E^h_{11} : E_2] \\
&\quad +k_{flow}(e^{h,up}_{11} - e^h_{11}) \\
&\quad -k^{AT}_{e^h_{11}} e^h_{11}[AT] \\
&\quad -k^{ATH}_{e_{11}} e^h_{11}[AT : Hep]
\end{aligned} \tag{73}$$

$$\begin{aligned}
\frac{d}{dt}e^{h,m}_{11} &= k^{on}_{e^h_{11}} e^h_{11} p^{avail}_{11} - k^{off}_{e^h_{11}} e^{h,m}_{11} \\
&\quad -k^{+}_{z^m_9:e^{h,m}_{11}} z^m_9 e^{h,m}_{11} \\
&\quad +(k^{-}_{z^m_9:e^{h,m}_{11}} + k^{cat}_{z^m_9:e^{h,m}_{11}})[Z^m_9 : E^{h,m}_{11}] \\
&\quad -k^{+}_{z^m_{11}:e^{h,m}_{11}} z^m_{11} e^{h,m}_{11} \\
&\quad +(k^{-}_{z^m_{11}:e^{h,m}_{11}} + 2 * k^{cat}_{z^m_{11}:e^{h,m}_{11}})[Z^m_{11} : E^{h,m}_{11}] \\
&\quad +k^{cat}_{z^m_{11}:e^{m*}_{11}}[Z^m_{11} : E^{m*}_{11}] + k^{cat}_{z^m_{11}:e^m_2}[Z^m_{11} : E^m_2] \\
&\quad -k^{+}_{e^{h,m*}_{11}:e^{h,m}_{11}} e^{h,m*}_{11} e^{h,m}_{11} \\
&\quad +(k^{-}_{e^{h,m*}_{11}:e^{h,m}_{11}} + k^{cat}_{e^{h,m*}_{11}:e^{h,m}_{11}})[E^{hms}_{11} : E^{h,m}_{11}] \\
&\quad -k^{AT}_{e_{11}} e^{hm}_{11}[AT] \\
&\quad -k^{ATH}_{e_{11}} e^{hm}_{11}[AT : Hep]
\end{aligned} \tag{74}$$

$$\begin{aligned}
\frac{d}{dt}e^{h,m*}_{11} &= k^{on*}_{e^h_{11}} e^h_{11} p^{avail}_{111} - k^{off*}_{e^h_{11}} e^{h,m*}_{11} \\
&\quad -k^{+}_{e^{h,m*}_{11}:e^{h,m}_{11}} e^{h,m*}_{11} e^{h,m}_{11} + k^{-}_{e^{h,m*}_{11}:e^{h,m}_{11}}[E^{hms}_{11} : E^{h,m}_{11}] \\
&\quad -k^{+}_{e^{h,m*}_{11}:e^{m*}_{11}} e^{h,m*}_{11} e^{m*}_{11} + k^{-}_{e^{h,m*}_{11}:e^m_{11}s}[E^{hms}_{11} : E^{m*}_{11}] \\
&\quad -k^{+}_{e^{h,m*}_{11}:e^m_2} e^{h,m*}_{11} e^m_2 + k^{-}_{e^{h,m*}_{11}:e^m_2}[E^{hms}_{11} : E^m_2]
\end{aligned} \tag{75}$$

$$\begin{aligned}
\frac{d}{dt}[Z_9 : E^h_{11}] &= k_{flow}([Z_9 : E^h_{11}]^{up} - [Z_9 : E^h_{11}]) \\
&\quad +k^{+}_{z_9:e^h_{11}} z_9 e^h_{11} - (k^{-}_{z_9:e^h_{11}} + k^{cat}_{z_9:e^h_{11}})[Z_9 : E^h_{11}]
\end{aligned} \tag{76}$$

$$\begin{aligned}
\frac{d}{dt}[Z^m_9 : E^{h,m}_{11}] &= k^{+}_{z^m_9:e^{h,m}_{11}} z^m_9 e^{h,m}_{11} \\
&\quad -(k^{-}_{z^m_9:e^h_{11}m} + k^{cat}_{z^m_9:e^h_{11}m})[Z^m_9 : E^{h,m}_{11}]
\end{aligned} \tag{77}$$

$$\frac{d}{dt}[Z_{11} : E_{11}^h] = k_{flow}([Z_{11} : E_{11}^h]^{up} - [Z_{11} : E_{11}^h]) \quad (78)$$
$$+k_{z_{11}:e_{11}^{hp}} z_{11} e_{11}^h$$
$$-(k^-_{z_{11}:e_{11}^h} + k^{cat}_{z_{11}:e_{11}^h})[Z_{11} : E_{11}^h]$$

$$\frac{d}{dt}[E_{11}^h : E_{11}^h] = k_{flow}([E_{11}^h : E_{11}^h]^{up} - [E_{11}^h : E_{11}^h]) \quad (79)$$
$$+k^+_{e_{11}^h:e_{11}^h} e_{11}^h e_{11}^h$$
$$-(k^-_{e_{11}^h:e_{11}^h} + k^{cat}_{e_{11}^h:e_{11}^h})[E_{11}^h : E_{11}^h]$$

$$\frac{d}{dt}[E_{11}^h : E_{11}] = k_{flow}([E_{11}^h : E_{11}]^{up} - [E_{11}^h : E_{11}]) \quad (80)$$
$$+k^+_{e_{11}^h:e_{11}} e_{11}^h - (k^-_{e_{11}^h:e_{11}} + k^{cat}_{e_{11}^h:e_{11}})[E_{11}^h : E_{11}]$$

$$\frac{d}{dt}[E_{11}^h : E_2] = k_{flow}([E_{11}^h : E_2]^{up} - [E_{11}^h : E_2]) \quad (81)$$
$$+k^+_{e_{11}^h:e_2} e_{11}^h e_2 - (k^-_{e_{11}^h:e_2} + k^{cat}_{e_{11}^h:e_2})[E_{11}^h : E_2]$$

$$\frac{d}{dt}[Z_{11}^m : E_{11}^{h,m}] = k^+_{z_{11}^m:e_{11}^{h,m}} z_{11}^m e_{11}^{h,m} \quad (82)$$
$$-(k^-_{z_{11}^m:e_{11}^{h,m}} + k^{cat}_{z_{11}^m:e_{11}^{h,m}})[Z_{11}^m : E_{11}^{h,m}]$$

$$\frac{d}{dt}[Z_{11}^m : E_{11}^{m*}] = k^+_{z_{11}^m:e_{11}^{m*}} z_{11}^m e_{11}^{m*} \quad (83)$$
$$-(k^-_{z_{11}^m:e_{11}^{m*}} + k^{cat}_{z_{11}^m:e_{11}^m s})[Z_{11}^m : E_{11}^{m*}]$$

$$\frac{d}{dt}[E_{11}^{hms} : E_{11}^{h,m}] = k^+_{e_{11}^{h,m*}:e_{11}^{h,m}} e_{11}^{h,m} \quad (84)$$
$$-(k^-_{e_{11}^{h,m*}:e_{11}^{h,m}} + k^{cat}_{e_{11}^{h,m*}:e_{11}^{h,m}})[E_{11}^{hms} : E_{11}^{h,m}]$$

$$\frac{d}{dt}[E_{11}^{hms} : E_{11}^{m*}] = k_{e_{11}^{h,m*}:e_{11}^{h,m*}} e_{11}^{m*} \quad (85)$$
$$-(k^-_{e_{11}^{h,m*}:e_{11}^{m*}} + k^{cat}_{e_{11}^{h,m*}:e_{11}^{m*}})[E_{11}^{hms} : E_{11}^{m*}]$$

$$\frac{d}{dt}[E_{11}^{hms} : E_2^m] = k^+_{e_{11}^{h,m*}:e_2^m} e_{11}^{h,m*} e_2^m \quad (86)$$
$$-(k^-_{e_{11}^{hms:e_2^m}} + k^{cat}_{e_{11}^{h,m*}:e_2^m}[E_{11}^{hms} : E_2^m])$$

$$\frac{d}{dt} e_5^{hm} = +k^{cat}_{z_5^m:e_{10}^m}[Z_5^m : E_{10}^m] + k_5^{on} e_5^h p_5^{avail} \quad (87)$$
$$-k_5^{off} e_5^{hm} - k^+_{e_5^{hm}:e_{10}^m} e_{10}^m e_5^{hm} + k^-_{e_5^{hm}:e_{10}^m} PRO^h$$
$$-k^+_{e_5^{hm}:e_2^m} e_2^m e_5^{hm} + k^-_{e_5^{hm}:e_2^m}[E_5^{hm} : E_2^m]$$
$$-k^+_{TFPI:e_5^{hm}} e_5^{hm} TFPI + k^-_{TFPI:e_5^{hm}}[TFPI : E_5^{hm}]$$
$$-k^+_{e_5^{hm}:APC} e_5^{hm} APC + k^-_{e_5^{hm}:APC}[APC : E_5^{hm}]$$
$$-k^+_{TFPI:e_{10}:e_5^{hm}}[TFPI : E_{10}^m] e_h^{hm}$$
$$+k^-_{TFPI:e_{10}:e_5^{hm}}[E_{10}^m : TFPI : E_5^{hm}]$$
$$-k^+_{TFPI:e_{10}:e_5^{hm}:e_{10}^m}[TFPI : E_{10}^m] e_5^{hm}$$
$$+k^-_{TFPI:e_{10}:e_5^{hm}:e_{10}^m}[TFPI : PRO^h_{v10}]$$

$$\frac{d}{dt}e_5^h = -k_{5on}e_5^h p_5^{avail} + k_5^{off}e_5^{hm} \tag{88}$$
$$+k_{flow}(e_5^{up} - e_5^h) + (1 - f_5)N_5 dpl \cdot p$$
$$-k^+_{e_5^h:e_2}e_5^h + k^-_{e_5^h:e_2}[E_5^h : E_2]$$
$$-k^+_{e_5^h:APC}APC \cdot e_5^h + k^-_{e_5^h:APC}[APC : E_5^h]$$
$$-k^+_{TFPI:e_5^h}e_5^h TFPI$$
$$+k^-_{TFPI:e_5^h}[TFPI : E_5^h]$$
$$-k^+_{TFPI:e_{10}:e_5^h}[TFPI : E_{10}]e_5^h$$
$$+k^-_{TFPI:e_{10}:e_5^h}[E_{10} : TFPI : E_5^h]$$
$$-k^+_{TFPI:e_{10}^m:e_5^h}[TFPI : E_{10}^m]e_5^h$$
$$+k^-_{TFPI:e_{10}^m:e_5^h}[E_{10}^m : TFPI : E_5^h]$$

$$\frac{d}{dt}PRO^h = +k^+_{e_5^{hm}:e_{10}^m}e_{10}^m e_5^{hm} - k^-_{e_5^{hm}:e_{10}^m}PRO^h \tag{89}$$
$$-k^+_{z_2^m:PRO^h}PRO^h z_2^m + k^-_{z_2^m:PRO^h}[Z_2^m : PRO^h]$$
$$+k^{cat}_{z_2^m:PRO^h}[Z_2^m : PRO^h]$$
$$-k^+_{TFPI:PRO^h:v_{10}}PRO^h TFPI + k^-_{TFPI:PRO^h:v_{10}}[TFPI : PRO^h_{v10}]$$
$$-k^+_{TFPI:PRO^h:v_5}PRO^h TFPI + k^-_{TFPI:PRO^h:v_5}[TFPI : PRO^h_{v5}]$$
$$-k^+_{PRO^h:e_2^m}PRO^h e_2^m + k^-_{PRO^h:e_2^m}[PRO^h : E_2^m]$$

$$\frac{d}{dt}[Z_2^m : PRO^h] = +k^+_{z_2^m:PRO^h}PRO^h z_2^m - k^-_{z_2^m:PRO^h}[Z_2^m : PRO^h] \tag{90}$$
$$-k^{cat}_{z_2^m:PRO^h}[Z_2^m PRO^h]$$

$$\frac{d}{dt}[E_5^{hm} : E_2^m] = +k^+_{e_5^{hm}:e_2^m}e_2^m e_5^{hm} - k^-_{e_5^{hm}:e_2^m}[E_5^{hm} : E_2^m] \tag{91}$$
$$-k^{cat}_{e_5^{hm}:e_2^m}[E_5^{hm} : E_2^m]$$

$$\frac{d}{dt}[E_5^h : E_2] = +k^+_{e_5^h:e_2}e_2 e_5^h - k^-_{TFPI:e_5^h}[E_5^h : E_2] \tag{92}$$
$$-k^{cat}_{e_5^h:e_2}[E_5^h : E_2] + k_{flow}([E_5^h : E_2]^{up} - [E_5^h : E_2])$$

$$\frac{d}{dt}[TFPI : E_5^{hm}] = +k^+_{TFPI:e_5^{hm}}e_5^{hm}TFPI - k^-_{TFPI:e_5^{hm}}[TFPI : E_5^{hm}] \tag{93}$$
$$-k^+_{TFPI:e_5^{hm}:e_{10}m}[TFPI : E_5^{hm}]e_{10}^m$$
$$+k^-_{TFPI:e_5^{hm}:e_{10}m}[E_{10}^m : TFPI : E_5^{hm}]$$
$$+k_5^{on}[TFPI : E_5^h]p_5^{avail} - k_5^{off}[TFPI : E_5^{hm}]$$
$$-k^+_{TFPI:e_{10}:e_5^{hm}}[TFPI : E_5^{hm}]e_{10}^m$$
$$+k^-_{TFPI:e_{10}:e_5^{hm}}[TFPI : PRO^h_{v5}]$$
$$-k^+_{TFPI:e_5^{hm}:e_{10}}[TFPI : E_5^{hm}]e_{10}$$
$$+k^-_{TFPI:e_5^{hm}:e_{10}}[E_{10} : TFPI : E_5^{hm}]$$

$$\frac{d}{dt}[APC : E_5^{hm}] = +k^+_{e_5^{hm}:APC}E_5^{hm}APC - k^-_{e_5^{hm}:APC}[APC : E_5^{hm}] \tag{94}$$
$$+k^{cat}_{e_5^{hm}:APC}[APC : E_5 hm]$$

$$\frac{d}{dt}[APC:E_5^h] = +k^+_{e_5^h:APC}e_5^h APC - k^-_{e_5^{hm}:APC}[APC:E_5^h] \quad (95)$$
$$-k^{cat}_{e_5^h:APC}[APC:E_5^h]$$
$$+k_{flow}([APC:E_5^h]^{up} - [APC:E_5^h])$$

$$\frac{d}{dt}[TFPI:E_5^h] = +k_{TFPI:e_5^h up}e_5^h TFPI - k^-_{kTFPI:e_5^h}[TFPI:E_5^h] \quad (96)$$
$$+k_{flow}([TFPI:E_5^h]^{up} - [TFPI:E_5^h])$$
$$-k^+_{TFPI:e_5^h:e_{10}}[TFPI:E_5^h]e_{10}$$
$$+k^-_{TFPI:e_5^h:e_{10}}[E_{10}:TFPI:E_5^h]$$
$$+k_5^{on}[TFPI:E_5^h]p_5^{avail} + k_5^{off}[TFPI:E_5^{hm}]$$

$$\frac{d}{dt}[TFPI:E_{10}^m] = +k^+_{TFPI:e_{10}^m}e_{10}^m TFPI - k^-_{TFPI:e_{10}^m}[TFPI:E_{10}^m] \quad (97)$$
$$-k^+_{TFPI:e_{10}:e_5^h m}[TFPI:E_{10}^m]e_5^{hm}$$
$$+k^-_{TFPI:e_{10}:e_5^{hm}}[E_{10}^m:TFPI:E_5^{hm}]$$
$$+k_{10}^{on}[TFPI:E_{10}]p_{10}^{avail}$$
$$-k_{10}^{off}[TFPI:E_{10}^m]$$
$$-k^+_{TFPI:e_{10}^m:e_5^{hm}}[TFPI:E_{10}^m]e_5^{hm}$$
$$+k^-_{TFPI:e_{10}^m:e_5^{hm}}[TFPI:PRO^h]^{v10}$$
$$-k^+_{TFPI:e_{10}^m:e_5^h}[TFPI:E_{10}^m]e_5^h$$
$$+k^-_{TFPI:e_{10}^m:e_5^h}[E_{10}^m:TFPI:E_5^h]$$

$$\frac{d}{dt}[TFPI:PRO^h]^{v10} = +k^+_{TFPI:PRO^h:v_{10}}PRO^h TFPI \quad (98)$$
$$-k^-_{TFPI:PRO^h:v_{10}}[TFPI:PRO^h]^{v10}$$
$$+k^+_{TFPI:e_{10}^m:e_5^{hm}}[TFPI:E_{10}^p][TFPI:E_{10}^m]e_5^{hm}$$
$$-k^-_{TFPI:e_{10}^m:e_5^{hm}}[TFPI:PRO^h]^{v10}$$

$$\frac{d}{dt}[TFPI:PRO^h]^{v5} = +k^+_{TFPI:PRO^h:v_5}PRO^h TFPI \quad (99)$$
$$-k^-_{TFPI:PRO^h:v_5}[TFPI:PRO^h]^{v5}$$
$$+k^+_{TFPI:e_{10}:e_5^{hm}}[TFPI:E_5^{hm}]e_{10}^m$$
$$-k^-_{TFPI:e_{10}:e_5^{hm}}[TFPI:PRO^h]^{v5}$$

$$\frac{d}{dt}[E_{10}^m:TFPI:E_5^{hm}] = +k^+_{TFPI:e_{10}:e_5^h m}[TFPI:E_{10}^m]e_5^{hm} \quad (100)$$
$$-k^-_{TFPI:e_{10}:e_5^h m}[E_{10}^m:TFPI:E_5^{hm}]$$
$$+k^+_{TFPI:e_5^{hm}:e_{10}m}[TFPI:E_5^{hm}]e_{10}^m$$
$$-k^-_{TFPI:e_5^{hm}:e_{10}m}[E_{10}^m:TFPI:E_5^{hm}]$$
$$+k_{10}^{ont}p_{10}^{avail} - k_{10}^{offt}[E_{10}^m:TFPI:E_5^{hm}]$$
$$+k_5^{ont}[E_{10}^m:TFPI:E_5^h]p_5^{avail}$$
$$-k_5^{offt}[E_{10}^m:TFPI:E_5^{hm}]$$

$$\frac{d}{dt}[E_{10}:TFPI:E_5^h] = +k_{flow}([E_{10}:TFPI:E_5^h]^{up} - [E_{10}:TFPI:E_5^h]) \quad (101)$$
$$+k^+_{TFPI:e_{10}:e_5^h}[TFPI:E_{10}]e_5^h$$
$$-k^-_{TFPI:e_{10}:e_5^h}[E_{10}:TFPI:E_5^h]$$
$$+k^+_{TFPI:e_5^h:e_{10}}[TFPI:E_5^h]e_{10}$$
$$-k^-_{TFPI:e_5^h:e_{10}}[E_{10}:TFPI:E_5^h]$$
$$-k_5^{ont}[E_{10}:TFPI:E_5^h]p_5^{avail}$$
$$+k_5^{offt}[E_{10}:TFPI:E_5^{hm}]$$
$$-k_{10}^{ont}[E_{10}:TFPI:E_5^h]p_{10}^{avail}$$
$$+K_{10}^{offt}[E_{10}^m:TFPI:E_5^h]$$

$$\frac{d}{dt}[E_{10}:TFPI:E_5^{hm}] = +k_5^{ont}[E_{10}:TFPI:E_5^h]p_5^{avail} \quad (102)$$
$$-k_5^{offt}[E_{10}:TFPI:E_5^{hm}]$$
$$-k_{10}^{ont}[E_{10}:TFPI:E_5^{[}hm]]p_{10}^{avail}$$
$$+k_{10}^{offt}[E_{10}^m:TFPI:E_5^{hm}]$$
$$+k^+_{TFPI:e_5^{hm}:e_{10}}[TFPI:E_5^{hm}]e_{10}$$
$$-k^-_{TFPI:e_5^{hm}:e_{10}}[E_{10}:TFPI:E_5^{hm}]$$

$$\frac{d}{dt}[E_{10}^m:TFPI:E_5^h] = +k_{10}^{ont}[E_{10}:TFPI:E_5^h]p_{10}^{avail} \quad (103)$$
$$-k_{10}^{offt}[E_{10}^m:TFPI:E_5^h]$$
$$-k_5^{ont}[E_{10}^m:TFPI:E_5^h]p_5^{avail}$$
$$+k_5^{offt}[E_{10}^m:TFPI:E_5^{hm}]$$
$$+k^+_{TFPI:e_{10}^m:e_5^h}[TFPI:E_{10}^m]e_5^h$$
$$-k^-_{TFPI:e_{10}^m:e_5^h}[E_{10}^m:TFPI:E_5^h]$$

$$\frac{d}{dt}[PRO^h:E_2^m] = +k^+_{PRO^h:e_2^m}PRO^hE_2^m - k^-_{PRO^h:e_2^m}[PRO^h:E_2^m] \quad (104)$$
$$-k^{cat}_{PRO^h:e_2^m}[PRO^h:E_2^m]$$

$$\frac{d}{dt}[E_9:AT] = -k_9^{on}p_9^{avail}[E_9:AT] \quad (105)$$
$$+k_9^{off}[E_9^m:AT] + k_{e_9}^{AT}e_9[AT]$$
$$+k_{flow}([E_9:AT]_{up} - [E_9:AT])$$
$$-k_9^{on}p_{91}^{avail}[E_9:AT] + k_9^{off}[E_9^{m*}:AT]$$

$$\frac{d}{dt}[E_9^m:AT] = +k_{e_9^m}^{AT}e_9^m[AT] \quad (106)$$
$$-k_9^{off}[E_9^m:AT] + k_9^{on}p_9^{avail}[E_9:AT]$$

$$\frac{d}{dt}[E_9^{m*}:AT] = +k_{e_9^m}^{AT}e_9^{m*}[AT] \quad (107)$$
$$-k_9^{off}[E_9^{m*}:AT] + k_9^{on}p_{91}^{avail}[E_9:AT]$$

$$\frac{d}{dt}[E_{10}:AT] = +k_{e_{10}}^{AT}e_{10}[AT] \quad (108)$$
$$+k_{flow}([E_{10}:AT]_{up} - [E_{10}:AT])$$
$$+k_{10}^{off}[E_{10}^m:AT] - k_{10}^{on}p_{10}^{avail}[E_{10}:AT]$$

$$\begin{aligned}
\frac{d}{dt}[E_{10}^{m} : AT] &= +k_{e_{10}^{m}}^{AT} e_{10}^{m}[AT] && (109)\\
&\quad -k_{10}^{off}[E_{10}^{m} : AT] + k_{10}^{on} p_{10}^{avail}[E_{10} : AT]\\
\frac{d}{dt}[E_{2} : AT] &= +k_{e_2}^{off}[E_{2}^{m} : AT] - k_{e_2}^{on} p_{2}^{avail}[E_{2} : AT] && (110)\\
&\quad +k_{e_2}^{AT} e_2 + k_{flow}([E_2 : AT]_{up} - [E_2 : AT])\\
\frac{d}{dt}[E_{2}^{m} : AT] &= +k_{e_2^m}^{AT} e_{2}^{m}[AT] && (111)\\
&\quad -k_{e_2}^{off}[E_{2}^{m} : AT] + k_{e_2}^{on} p_{2}^{avail}[E_{2} : AT]\\
\frac{d}{dt}[E_{11} : AT] &= +k_{e_{11}}^{AT} e_{11}[AT] && (112)\\
&\quad -k_{e_{11}}^{AT}[E_{11} : AT][AT]\\
&\quad +k_{11}^{off}[E_{11}^{m*} : AT] - k_{11}^{on} p_{111}^{avail}[E_{11} : AT]\\
&\quad +k_{e_{11}}^{ATH} e_{11}[AT : Hep] - k_{e_{11}}^{ATH}[E_{11} : ATH][AT : Hep]\\
&\quad +k_{flow}([E_{11} : ATH]_{up} - [E_{11} : ATH])\\
&\quad -k_{e_{11}}^{on} p_{111}^{avail}[E_{11} : ATH] + k_{e_{11}}^{off}[E_{11}^{m*} : ATH]\\
\frac{d}{dt}[AT : E_{11} : AT] &= +k_{e_{11}}^{AT}[E_{11} : AT][AT] && (113)\\
\frac{d}{dt}[E_{11}^{m*} : AT] &= +k_{e_{11}}^{AT} e_{11}^{m*}[AT] && (114)\\
&\quad -k_{11}^{off}[E_{11}^{m*} : AT] + k_{11}^{on} p_{111}^{avail}[E_{11} : AT]\\
\frac{d}{dt}[E_{11}^{h} : AT] &= +k_{e_{11}}^{AT} e_{11}^{h}[AT] && (115)\\
&\quad +k_{11}^{off}[E_{11}^{hm} : AT] - k_{11}^{on} p_{11}^{avail}[E_{11}^{h} : AT]\\
\frac{d}{dt}[E_{11}^{hm} : AT] &= +k_{e_{11}}^{AT} e_{11}^{hm}[AT] && (116)\\
&\quad -k_{11}^{off}[E_{11}^{hm} : AT] + k_{11}^{on} p_{11}^{avail}[E_{11}^{h} : AT]\\
\frac{d}{dt}[AT] &= -k_{e_9}^{AT} e_9[AT] - k_{e_9^m}^{AT} e_9^m[AT] && (117)\\
&\quad +k_{e_9^m}^{AT} e_9^{m*}[AT]\\
&\quad -k_{e_{10}}^{AT} e_{10}[AT] + k e_{10}^{m\,AT} e_{10}^{m}[AT]\\
&\quad -k_{e_2}^{AT} e_2[AT] - k_{e_2^m}^{AT} e_2^m[AT]\\
&\quad -k_{e_{11}}^{AT} e_{11}[AT] - k_{e_{11}}^{AT}[E_{11} : AT][AT]\\
&\quad -k_{e_{11}}^{AT} e_{11}^{m*}[AT] - k_{e_{11}}^{AT} e_{11}^{h}[AT]\\
&\quad -k_{e_{11}}^{AT} e_{11}^{h}[AT]\\
&\quad +k_{flow}([AT]_{up} - [AT])\\
&\quad -k_{[AT:Hep]}^{+}[Hep][AT] + k_{[AT:Hep]}^{-}[AT : Hep]\\
\frac{d}{dt}[Hep] &= -k_{[AT:Hep]}^{+}[Hep][AT] + k_{[AT:Hep]}^{-}[AT : Hep] && (118)
\end{aligned}$$

$$\frac{d}{dt}[AT:Hep] = +k^{+}_{[AT:Hep]}[Hep][AT] - k^{-}_{[AT:Hep]}[AT:Hep] \quad (119)$$
$$-k^{ATH}_{e_{10}} e_{10}[AT:Hep] - k^{ATH}_{e^m_{10}} e^m_{10}[AT:Hep]$$
$$-k^{ATH}_{e_2} e_2[AT:Hep] - k^{ATH}_{e^m_2} e^m_2[AT:Hep]$$
$$-k^{ATH}_{e_9} e_9[AT:Hep] - k^{ATH}_{e^m_9} e^m_9[AT:Hep]$$
$$-k^{ATH}_{e^m_9} e^{m*}_9[AT:Hep]$$
$$-k^{ATH}_{e_{11}} e_{11}[AT:Hep] - k^{ATH}_{e_{11}}[E_{11}:ATH][AT:Hep]$$
$$-k^{ATH}_{e_{11}} e^{m*}_{11}[AT:Hep] - k^{ATH}_{e_{11}} e^{h}_{11}[AT:Hep]$$
$$-k^{ATH}_{e_{11}} e^{hm}_{11}[AT:Hep]$$

$$\frac{d}{dt}[E_{10}:ATH] = +k^{ATH}_{e_{10}} e_{10}[AT:Hep] + k_{flow}([E_{10}:ATH]_{up} - [E_{10}:ATH]) \quad (120)$$
$$-k^{on}_{10} p^{avail}_{10}[E_{10}:ATH] + k^{off}_{10}[E^m_{10}:ATH]$$

$$\frac{d}{dt}[E^m_{10}:ATH] = +k^{ATH}_{e^m_{10}} e^m_{10}[AT:Hep] \quad (121)$$
$$+k^{on}_{10} p^{avail}_{10}[E_{10}:ATH] - k^{off}_{10}[E^m_{10}:ATH]$$

$$\frac{d}{dt}[E_2:ATH] = +k^{ATH}_{e_2} e_2[AT:Hep] + k_{flow}([E_2:ATH]_{up} - [E_2:ATH]) \quad (122)$$
$$-k^{on}_{e_2} p^{avail}_{2}[E_2:ATH] + k^{off}_{e_2}[E^m_2:ATH]$$

$$\frac{d}{dt}[E^m_2:ATH] = +k^{ATH}_{e^m_2} e^m_2[AT:Hep] \quad (123)$$
$$+k^{on}_{2} p^{avail}_{2}[E_2:ATH] - k^{off}_{e_2}[E^m_2:ATH]$$

$$\frac{d}{dt}[E_9:ATH] = +k^{ATH}_{e_9} e_9[AT:Hep] + k_{flow}([E_9:ATH]_{up} - [E_9:ATH]) \quad (124)$$
$$-k^{on}_{e_9} p^{avail}_{9}[E_9:ATH] + k^{off}_{e_9}[E^m_9:ATH]$$
$$-k^{on}_{e_9} p^{avail}_{91}[E_9:ATH] + k^{off}_{9}[E^{m*}_9:ATH]$$

$$\frac{d}{dt}[E^{m*}_9:ATH] = +k^{ATH}_{e^m_9} e^m_9[AT:Hep] \quad (125)$$
$$+k^{on}_{e_9} p^{avail}_{9}[E_9:ATH] - k^{off}_{e_9}[E^m_9:ATH]$$

$$\frac{d}{dt}[E^{m*}_9:ATH] = +k_{e^m_9:ATH} e^{m*}_9[AT:Hep] \quad (126)$$
$$+k^{on}_{e_9} p^{avail}_{91}[E_9:ATH] - k^{off}_{e_9}[E^{m*}_9:ATH]$$

$$\frac{d}{dt}[ATH:E_{11}:ATH] = +k^{ATH}_{e_{11}}[AT:Hep][E_{11}:ATH] \quad (127)$$
$$+k_{flow}([ATH:E_{11}:ATH]_{up} - [ATH:E_{11}:ATH])$$

$$\frac{d}{dt}[E^{m*}_{11}:ATH] = +k^{ATH}_{e_{11}} e^{m*}_{11}[AT:Hep] + k^{on}_{e_{11}} p^{avail}_{111}[E_{11}:ATH] \quad (128)$$
$$-k^{off}_{e_{11}}[E^{m*}_{11}:ATH]$$

$$\frac{d}{dt}[E^{h}_{11}:ATH] = +k^{ATH}_{e_{11}} e^{h}_{11}[AT:Hep] \quad (129)$$
$$+k_{flow}([E^h_{11}:ATH]_{up} - [E^h_{11}:ATH])$$
$$+k^{off}_{e_{11}}[E^{hm}_{11}:ATH] - k^{on}_{e_{11}} p^{avail}_{111}[E^h_{11}:ATH]$$

$$\frac{d}{dt}[E^{hm}_{11}:ATH] = +k^{ATH}_{e_{11}} e^{hm}_{11}[AT:Hep] \quad (130)$$
$$-k^{off}_{11}[E^{hm}_{11}:ATH]$$
$$+k^{on}_{11} p^{avail}_{111}[E^h_{11}:ATH]$$

S1 Table. INITIAL PLASMA LEVELS. Descriptions, notation and labels for each parameter associated with initial plasma levels are listed. The value of each parameter is found in the corresponding table listed above.

Description	Notation	Label	Table
Prothrombin	z_2	Z_2	S8
Factor V	z_5	Z_5	S8
Factor VII	z_7	Z_7	S8
Factor VIII	z_8	Z_8	S8
Factor IX	z_9	Z_9	S8
Factor X	z_{10}	Z_{10}	S8
Factor XI	z_{11}	Z_{11}	S8
TFPI	[TFPI]	TFPI	S8
AT	[AT]	AT	S8
Hep	[Hep]	Hep	S8

S2 Table. PLATELET CHARACTERISTICS. Descriptions, notation and labels for each parameter associated with platelet characteristics are listed. The value of each parameter is found in the corresponding table listed above.

Description	Notation	Label	Table
Platelet count	PL^{up}	PLup	S8
Binding site number for II	N_2	N2	S8
Binding site number for IIa	N_2^*	N2*	S8
Binding site number for V/Vh/Va	N_5	N5	S8
Binding site number for VIII/VIIIa	N_8	N8	S8
Binding site number for IX	N_9	N9	S8
Binding site number for IXa	N_9^*	N9*	S8
Binding site number for X/Xa	N_{10}	N10	S8
Binding site number for XI	N_{11}	N11	S8
Binding site number for XIa	N_{11}^*	N11*	S8
Rate of unactivated platelets adhering to SE	k_{adh}^+	kadh	S14
Rate of activated platelets adhering to SE	$k_{adh}^{+,*}$	kadh1	S14
Rate of platelet activation by platelet in solution	k_{plt}^{act}	$kact_{plt}$	S14
Rate of platelet activation on SE	$k_{plt}^{act,*}$	$kact^*_{plt}$	S14
Rate of platelet activation by thrombin	$k_{e_2}^{act}$	$kact_{e2}$	S14

S3 Table. KINETIC RATE CONSTANTS. Descriptions, notation and labels for each parameter associated with kinetic rate constants are listed. The value of each parameter is found in the corresponding table listed above.

Description	Notation	Label	Table
Rates of activation of TF:VII by fX	K_M	KZ7mE10M	S9
	$k^{cat}_{z_7^m:e_{10}}$	KZ7mE10CAT	S9
	$k^{-}_{z_7^m:e_{10}}$	KZ7mE10MI	S9
Rates of activation of fX by TF:VIIa	K_M	KZ10E7mM	S9
	$k^{cat}_{z_{10}:e_7^m}$	KZ10E7mCAT	S9
	$k^{-}_{z_{10}:e_7^m}$	KZ10E7mMI	S9
Rates of activation of fIX by TF:VIIa	K_M	KZ9E7mM	S9
	$k^{cat}_{z_9:e_7^m}$	KZ9E7mCAT	S9
	$k^{-}_{z_9:e_7^m}$	KZ9E7mMI	S9
Rates of binding of fVII/fVIIa to TF	k_7^{on}	K7ON	S9
	k_7^{off}	K7OFF	S10
Rates of activation of TF:VII by fXa	K_M	KZ7E10M	S10
	$k^{cat}_{z_7:e_{10}^m}$	KZ7E10CAT	S10
	$k^{-}_{z_7:e_{10}^m}$	KZ7E10MI	S10
Rates of activation of TF:VII by fIIa	K_M	KZ7E2M	S10
	$k^{cat}_{z_7:e_2}$	KZ7E2CAT	S10
	$k^{-}_{z_7:e_2}$	KZ7E2MI	S10
Rates of activation of TF:VII by fIXa	K_M	KZ7E9M	S10
	$k^{cat}_{z_7:e_9}$	KZ7E9CAT	S10
	$k^{-}_{z_7:e_9}$	KZ7E9MI	S10
Rates of activation of fV by fIIa	K_M	KZ5E2M	S10
	$k^{cat}_{z_5:e_2}$	KZ5E2CAT	S10
	$k^{-}_{z_5:e_2}$	KZ5E2MI	S10
Rates of activation of fVIII by fIIa	K_M	KZ8E2M	S10
	$k^{cat}_{z_8:e_2}$	KZ8E2CAT	S10
	$k^{-}_{z_8:e_2}$	KZ8E2MI	S10
Rates of activation of fIX by fXIa-fXIa	$k^{+}_{z_9:e_{11}}$	KZ9E11P	S10
	$k^{cat}_{z_9:e_{11}}$	KZ9E11CAT	S10
	$k^{-}_{z_9:e_{11}}$	KZ9E11MI	S10
Rates of activation of fIX by fXIa-fXI	$k^{+}_{z_9:e_{11}^h}$	KZ9E11P	S10
	$k^{cat}_{z_9:e_{11}^h}$	KZ9E11CAT	S10
	$k^{-}_{z_9:e_{11}^h}$	KZ9E11MI	S10
Rates of activation of fXI by fIIa	$k^{+}_{z_{11}:e_2}$	KZ11E2P	S10
	$k^{cat}_{z_{11}:e_2}$	KZ11E2CAT	S10
	$k^{-}_{z_{11}:e_2}$	KZ11E2MI	S11
Rates of binding of fX/fXa to plt. surface	k_{10}^{on}	K10ON	S11
	k_{10}^{off}	K10OFF	S11
Rates of binding of fV/fVa to plt. surface	k_5^{on}	K5ON	S11
	k_5^{off}	K5OFF	S1
Rates of binding of fVIII/fVIIIa to plt. surface	k_8^{on}	K8ON	S1
	k_8^{off}	K8OFF	S1
Rates of binding of fIX/fIXa to plt. surface	k_9^{on}	K9ON	S1
	k_9^{off}	K9OFF	S11
Rates of binding of fII/fIIa to plt. surface	k_2^{on}, $k_2^{on,*}$	K2ON, K2SON	S1
	k_2^{off}, $k_2^{off,*}$	K2OFF, K2SOFF	S11
Rates of binding of fXI/fXIa to plt. surface	k_{11}^{on}, $k_{11}^{on,*}$	K11ON, K11SON	S11
	k_{11}^{off}, $k_{11}^{off,*}$	K11OFF, K11SOFF	S12

S4 Table. KINETIC RATE CONSTANTS. Descriptions, notation and labels for each parameter associated with kinetic rate constants are listed. The value of each parameter is found in the corresponding table listed above.

Description	Notation	Label	Table
Rates of activation of fV by fXa on plt. surface	K_M	KZ5mE10mM	S12
	$k^{cat}_{z_5^m:e_{10}^m}$	KZ5mE10mCAT	S12
	$k^{-}_{z_5^m:e_{10}^m}$	KZ5mE10mMI	S12
Rates of activation of fV by fIIa on plt. surface	K_M	KZ5mE2mM	S12
	$k^{cat}_{z_5:e_2^m}$	KZ5mE2mCAT	S12
	$k^{-}_{z_5:e_2^m}$	KZ5mE2mMI	S12
Rates of activation of fVIII by fXa on plt. surface	K_M	KZ8ME10MM	S12
	$k^{cat}_{z_8:e_{10}^m}$	KZ8ME10MCAT	S12
	$k^{-}_{z_8:e_{10}^m}$	KZ8ME10MMI	S12
Rates of activation of fVIII by fIIa on plt. surface	K_M	KZ8ME2MM	S12
	$k^{cat}_{z_8:e_2^m}$	KZ8mE2mCAT	S12
	$k^{-}_{z_8:e_2^m}$	KZ8mE2mMI	S12
Rates of activation of fX by TEN on plt. surface	K_M	KZ10mTENM	S12
	$k^{cat}_{z_{10}^m:TEN}$	KZ10mTENCAT	S12
Rates of activation of fII by PRO on plt. surface	K_M	KZ2mPROM	S12
	$k^{cat}_{z_2^m:PRO}$	KZ2mPROCAT	S12
Rates of activation of fXI by fIIa on plt. surfaces	$k^{+}_{z_{11}^m:e_2^m}$	KZ11mE2mP	S12
	$k^{cat}_{z_{11}^m:e_2^m}$	KZ11mE2mCAT	S12
	$k^{-}_{z_{11}^m:e_2^m}$	KZ11mE2mMI	S12
Rates of activation of fIX by fXIa-fXIa on plt. surface	K_M	KZ9mE11mP	S12
	$k^{cat}_{z_9^m:e_{11}^m}$	KZ9mE11mCAT	S12
	$k^{-}_{z_9^m:e_2^m}$	KZ9mE11mMI	S12
Rates of formation of TEN on plt. surface	$k^{+}_{e_8^m:e_9^m}$	KE8mE9mP	S12
	$k^{-}_{e_8^m:e_9^m}$	KE8mE9mMI	S12
Rates of formation of PRO on plt. surface	$k^{+}_{e_5^m:e_{10}^m}$	KE5mE10mP	S12
	$k^{-}_{e_5^m:e_{10}^m}$	KE5mE10mMI	S12
Rates of inhibition of fXa by TFPI	$k^{+}_{tfpia:e_{10}}$	KTFPI_E10_P	S13
	$k^{-}_{tfpia:e_{10}}$	KTFPI_E10_M	S13
Rates of inhibition of TF:VIIa by TFPIa	$k^{+}_{tfpia:e_7^m}$	KTFPIa_E7m_P	S13
	$k^{-}_{tfpia:e_7^m}$	KTFPIa_E7m_M	S13
Rates of inhibition of fVa by APC on plt. surface	K_M	KE5mAPCM	S13
	$k^{cat}_{e_5^m:APC}$	KE5mAPCCAT	S13
	$k^{-}_{e_5^m:APC}$	KE5mAPCMI	S13
Rates of inhibition of fVIIIa by APC on plt. surface	K_M	KE8mAPCM	S13
	$k^{cat}_{e_8^m:APC}$	KE8mAPCCAT	S13
	$k^{-}_{e_8^m:APC}$	KE8mAPCMI	S13
Rates of inhibition of fIIa by TM on plt. surface	k^{on}_{TM}	KTMP	S13
	k^{off}_{TM}	KTMM	S14

S5 Table. NEW KINETIC RATE CONSTANTS ADDED IN TFPI EXTENSION. Descriptions, notation and labels for each parameter associated with kinetic rate constants are listed. The value of each parameter is found in the corresponding table listed above.

Description	Notation	Label	Table
Rates of binding of fV-h by fXa on plt. surface	$k^{+}_{e5hme10m}$	KE5HME10MP	S10
	$k^{-}_{e^m_5:e^m_{10}}$	KE5HME10MMI	S12
Rates of activation of II by PROh on plt. surface	K_M	KZ2MPROHM	S10
	$k^{cat}_{z^m_2:PRO^h}$	KZ2MPROHCAT	S12
	$k^{-}_{z^m_2:PRO^h}$	KZ2MPROHMI	S12
Rates of activation of fV-h by IIa on plt. surface	K_M	KE5HME2MM	S10
	$k^{cat}_{e^{hm}_5:e^m_2}$	KE5HME2MCAT	S12
	$k^{-}_{e^{hm}_5:e^m_2}$	KE5HME2MMI	S12
Rates of activation of fV-h by IIa in fluid	K_M	KE5HE2M	S10
	$k^{cat}_{e^h_5:e_2}$	KE5HE2CAT	S12
	$k^{-}_{e^h_5:e_2}$	KE5HE2MI	S12
Rates of binding of fV-h by TFPI on plt. surface	$k^{+}_{TFPI:e^{hm}_5}$	KTFPIE5HMP	S10
	$k^{-}_{TFPI:e^{hm}_5}$	KTFPIE5HMMI	S13
Rates of binding of fV-h by TFPI in fluid	$k^{+}_{TFPI:e^h_5}$	KTFPIE5HP	S10
	$k^{-}_{TFPI:e^h_5}$	KTFPIE5HMI	S13
Rates of binding of fXa by TFPI on plt. surface	$k^{+}_{TFPI:e^m_{10}}$	KTFPI_E10M_P	S10
	$k^{-}_{TFPI:e^m_{10}}$	KTFPI_E10M_MI	S13
Rates of binding of PROh by TFPI on plt. surface by binding fXa	$k^{+}_{TFPI:PRO^h:v_{10}}$	KTFPIPROHV10P	S10
	$k^{-}_{TFPI:PRO^h:v_{10}}$	KTFPIPROHV10MI	S13
Rates of binding of PROh by TFPI on plt. surface by binding fV-h	$k^{+}_{TFPI:PRO^h:v_5}$	KTFPIPROHV5P	S10
	$k^{-}_{TFPI:PRO^h:v_5}$	KTFPIPROHV5MI	S13
Rates of inactivation of fV-h by APC on plt. surface	K_M	KE5HMAPCM	S10
	$k^{cat}_{e^{hm}_5}$	KE5HMAPCCAT	S13
	$k^{-}_{e^{hm}_5:APC}$	KE5HMAPCMI	S13
Rates of inactivation of fV-h by APC in fluid	K_M	KE5HAPCM	S10
	$k^{cat}_{e^h_5}$	KE5HAPCCAT	S13
	$k^{-}_{e^h_5:APC}$	KE5HAPCMI	S13

S6 Table. NEW KINETIC RATE CONSTANTS ADDED IN AT EXTENSION. Descriptions, notation and labels for each parameter associated with kinetic rate constants are listed. The value of each parameter is found in the corresponding table listed above.

Description	Notation	Label	Table
Rates of inactivation of fIXa by AT on plt. surface	$k_{e_9^m}^{AT}$	KE9MATIII	S13
Rates of inactivation of fXa by AT on plt. surface	$k_{e_{10}^m}^{AT}$	KE10MATIII	S13
Rates of inactivation of IIa by AT on plt. surface	$k_{e_2^m}^{AT}$	KE2MATIII	S13
Rates of inactivation of fXIa by AT on plt. surface	$k_{e_{11}^m}^{AT}$	KE11MATIII	S13
Rates of inactivation of fIXa by AT in fluid	$k_{e_9}^{AT}$	KE9ATIII	S13
Rates of inactivation of fXa by AT in fluid	$k_{e_{10}}^{AT}$	KE10ATIII	S13
Rates of inactivation of IIa by AT in fluid	$k_{e_2 AT}$	KE2ATIII	S13
Rates of inactivation of fXIa by AT in fluid	$k_{e_{11}}^{AT}$	KE11ATIII	S13
Rates of binding of AT by Heparin on plt. surface	$k^{+}_{AT:Hep}$	KATBHEPMI	S13
	$k^{-}_{AT:Hep}$	KATBHEPMI	S13
Rates of inactivation of fIXa by ATH on plt. surface	$k_{e_9^m}^{ATH}$	KE9MATH	S13
Rates of inactivation of fXa by ATH on plt. surface	$k_{e_{10}^m}^{ATH}$	KE10MATH	S13
Rates of inactivation of IIa by ATH on plt. surface	$k_{e_2^m}^{ATH}$	KE2MATH	S13
Rates of inactivation of fXIa by AT on plt. surface	$k_{e_{11}^m}^{ATH}$	KE11MATH	S13
Rates of inactivation of fIXa by ATH in fluid	$k_{e_9}^{ATH}$	KE9ATH	S13
Rates of inactivation of fXa by ATH in fluid	$k_{e_{10}}^{ATH}$	KE10ATH	S13
Rates of inactivation of IIa by ATH in fluid	$k_{e_2}^{ATH}$	KE2ATH	S13
Rates of inactivation of fXIa by AT in fluid	$k_{e_{11}}^{ATH}$	KE11ATH	S13

Kinetic and Physical Parameter Values:

S7 Table. DIFFUSION COEFFICIENTS FOR PLATELETS AND FLUID-PHASE CHEMICAL SPECIES (a) From (4). (b) From (5).

Platelets	2.5×10^{-7} cm^2/s	a
Proteins	5×10^{-7} cm^2/s	b

S8 Table. NORMAL CONCENTRATIONS AND SURFACE BINDING SITE NUMBERS (a) From (6). (b) From (7). (c) (8) suggests that normal plasma concentration of fVIIa is about 1% of the normal fVII concentration. (d) From (9). (e) (f) From (10). (g) Estimated as described in the text of the Supplementary Information. (h) From (11). (i) From (12). (j) From (13). (k) From (14). (l) From (15, 16). (m) Number of fV molecules released per activated platelet (17). (n) Maximum concentration of platelets in a 2 μm high reaction zone assuming that 20 platelets can cover a 10μm-by-10μm injured surface (18). (o) From (19). (p) Refer to heparin dosage calculation in later section of supplemental material.

Prothrombin	1.4 μM	a
Factor V	0.01 μM	b
Factor VII	0.01 μM	a
Factor VIIa	0.1 nM	c
Factor VIII	1.0 nM	a
Factor IX	0.09 μM	a
Factor X	0.17 μM	a
Factor XI	30.0 nM	a
TFPI	0.5 nM	d
Protein C	65 nM	e
Platelet count	$2.5(10)^5/\mu$l	f
N_2	1000/plt	g
N_2^*	1000/plt	g
N_5	3000/plt	h
N_8	450/plt	i
N_9	250/plt	j
N_9^*	250/plt	j
N_{10}	2700/plt	k
N_{11}	1500/plt	l
N_{11}^*	250/plt	l
n_5	3000/plt	m
p_{PLAS}	0.167 nM	n
AT	2.4 nM	o
$LMWH$	253 nM	p
UFH	759 nM	p

S9 Table. REACTIONS ON SUBENDOTHELIUM (a) $k^{\text{cat}}_{z_7^m:e_{10}} = 5.0$ sec^{-1} and $K_M = 1.2 \cdot 10^{-6}$ M (20). (b) $k^{\text{cat}}_{z_7^m:e_2} = 6.1 \cdot 10^{-2}$ sec^{-1} and $K_M = 2.7 \cdot 10^{-6}$ M (20). (d) $k^{\text{cat}}_{z_{10}:e_7^m} = 1.15$ sec^{-1} and $K_M = 4.5 \cdot 10^{-7}$ M (6). (d) $k^{\text{cat}}_{z_9:e_7^m} = 1.15$ sec^{-1} and $K_M = 2.4 \cdot 10^{-7}$ M (21). (e) $K_d = 1.0 \cdot 10^{-10}$ M (22).

Activation (of -, by -)							
(TF:VII,fXa)	E_{10}, Z_7^m	$Z_7^m : E_{10}$	E_7^m	$k^+_{z_7^m:e_{10}}=5.0 \cdot 10^6$	$k^-_{z_7^m:e_{10}}=1.0$	$k^{\text{cat}}_{z_7^m:e_{10}}=5.0$	a
(TF:VII, fIIa)	E_2, Z_7^m	$Z_7^m : E_2$	E_7^m	$k^+_{z_7^m:e_2}=3.92 \cdot 10^5$	$k^-_{z_7^m:e_2}=1.0$	$k^{\text{cat}}_{z_7^m:e_2}=6.1 \cdot 10^{-2}$	b
(fX, TF:VIIa)	E_7^m, Z_{10}	$Z_{10} : E_7^m$	E_{10}	$k^+_{z_{10}:e_7^m}=5.0 \cdot 10^6$	$k^-_{z_{10}:e_7^m}=1.0$	$k^{\text{cat}}_{z_{10}:e_7^m}=1.15$	c
(fIX, TF:VIIa)	E_7^m, Z_9	$Z_9 : E_7^m$	E_9	$k^+_{z_9:e_7^m}=9.4 \cdot 10^6$	$k^-_{z_9:e_7^m}=1.0$	$k^{\text{cat}}_{z_9:e_7^m}=1.15$	d
Binding (of -, with -)							
(fVII, TF)	Z_7, TF		Z_7^m	$k_7^{\text{on}}=5.0 \cdot 10^7$	$k_7^{\text{off}}=5.0 \cdot 10^{-3}$		e
(fVIIa, TF)	E_7, TF		E_7^m	$k_7^{\text{on}}=5.0 \cdot 10^7$	$k_7^{\text{off}}=5.0 \cdot 10^{-3}$		e

S10 Table. REACTIONS IN THE PLASMA (a) $k^{\text{cat}}_{z_7:e_{10}} = 5.0\,\text{sec}^{-1}$ and $K_M = 1.2 \cdot 10^{-6}$ M (20). (b) $k^{\text{cat}}_{z_7:e_2} = 6.1 \cdot 10^{-2}\,\text{sec}^{-1}$ and $K_M = 2.7 \cdot 10^{-6}$ M (20) (c) $k^{\text{cat}}_{z_5:e_2} = 0.23\,\text{sec}^{-1}$ and $K_M = 7.17 \cdot 10^{-8}$ M (23). (d) $k^{\text{cat}}_{z_8:e_2} = 0.9\,\text{sec}^{-1}$ (24) and $K_M = 2 \cdot 10^{-7}$ M (25). (e) $k^{\text{cat}}_{z_{11}:e_2} = 1.3 \cdot 10^{-4}$, $K_M = 50$nM (26). Rate constants apply also for thrombin-activation of XIa-XI. (f) $k^{\text{cat}}_{z_9:e^h_{11}} = 0.21$, $K_M = 0.2\mu$M (27, 28). Rate constants apply also for activation of IX by XIa-XIa.

Reaction	Reactants	Complex	Product	$\text{M}^{-1}\text{sec}^{-1}$	sec^{-1}	sec^{-1}	Note
Activation (of -, by -)							
(fVII, fXa)	Z_7, E_{10}	$Z_7 : E_{10}$	E_7	$k^+_{z_7:e_{10}}$=5 $\cdot 10^6$	$k^-_{z_7:e_{10}}$=1.0	$k^{\text{cat}}_{z_7:e_{10}}$=5.0	a
(fVII, fIIa)	Z_7, E_2	$Z_7 : E_2$	E_7	$k^+_{z_7:e_2}$=3.92 $\cdot 10^5$	$k^-_{z_7:e_2}$=1.0	$k^{\text{cat}}_{z_7:e_2}$=6.1 $\cdot 10^{-2}$	b
(fV, fIIa)	Z_5, E_2	$Z_5 : E_2$	E_5	$k^+_{z_5:e_2}$= 1.73 $\cdot 10^7$	$k^-_{z_5:e_2}$=1.0	$k^{\text{cat}}_{z_5:e_2}$=0.23	c
(fVIII, fIIa)	Z_8, E_2	$Z_8 : E_2$	E_8	$k^+_{z_8:e_2}$=2.64 $\cdot 10^7$	$k^-_{z_8:e_2}$=1.0	$k^{\text{cat}}_{z_8:e_2}$=0.9	d
(fXI-fXI, fIIa)	Z_{11}, E_2	$Z_{11} : E_2$	E^h_{11}	$k^+_{z_{11}:e_2}$ = 2.0 $\cdot 10^7$	$k^-_{z_{11}:e_2}$ = 1.0	$k^{\text{cat}}_{z_{11}:e_2}$ = 1.3 $\cdot 10^{-4}$	e
(fIX, fXIa)	Z_9, E^h_{11}	$Z_9 : E^h_{11}$	E_9	$k^+_{z_9:e^h_{11}}$ = 0.6 $\cdot$ (10)^7	$k^-_{z_9:e^h_{11}}$ = 1.0	$k^{\text{cat}}_{z_9:e^h_{11}}$ = 0.21	f

S11 Table. BINDING TO PLATELET SURFACES (a) For fIX binding to platelets, $K_d = 2.5 \cdot 10^{-9}$ M (13), and for fX binding to platelets, K_d has approximately the same value (11). For fX binding to PCPS vesicles, the on-rate is about 10^7 $M^{-1}sec^{-1}$ and the off-rate is about 1.0 sec^{-1} (29) giving a dissociation constant of about 10^{-7} M. To estimate on- and off-rates for the higher-affinity binding of fX to platelets, we keep the on-rate the same as for vesicles and adjust the off-rate to give the correct dissociation constant. The rates for fIX binding with platelets are taken to be the same as for fX binding. (b) We assume binding constants for fIXa binding to the specific fIXa binding sites are the same as for shared sites. (c) fV binds with high-affinity to phospholipids (PCPS) (29) and we use the same rate constants reported there to describe fV binding to platelets. (d) The K_d for fVIII binding with platelets is taken from (12). We set the off-rate k_8^{off} for fVIII binding to platelets equal to that for fV binding to platelets, and calculate the on-rate k_8^{on}. (e) For prothrombin interactions with platelets, K_d is reported to be $5.9 \cdot 10^{-7}$ M (30). We choose k_2^{off} and set $k_2^{\text{on}} = k_2^{\text{off}}/K_d$. (f) Estimated as described in the text of the Supplementary Information. (g) K_d = 10 nM (31). (h) K_d = 1.7 nM (16).

Reaction	Reactants	Products	$M^{-1}sec^{-1}$	sec^{-1}	Note
Factor IX	Z_9, P_9	Z_9^m	k_9^{on}=$1.0 \cdot 10^7$	k_9^{off}=$2.5 \cdot 10^{-2}$	a
Factor IXa	E_9, P_9	E_9^m	k_9^{on}=$1.0 \cdot 10^7$	k_9^{off}=$2.5 \cdot 10^{-2}$	a
Factor IXa	E_9, P_9^*	$E_9^{m,*}$	k_9^{on}=$1.0 \cdot 10^7$	k_9^{off}=$2.5 \cdot 10^{-2}$	b
Factor X	Z_{10}, P_{10}	Z_{10}^m	k_{10}^{on}=$1.0 \cdot 10^7$	k_{10}^{off}=$2.5 \cdot 10^{-2}$	a
Factor Xa	E_{10}, P_{10}	E_{10}^m	k_{10}^{on}=$1.0 \cdot 10^7$	k_{10}^{off}=$2.5 \cdot 10^{-2}$	a
Factor V	Z_5, P_5	Z_5^m	k_5^{on}=$5.7 \cdot 10^7$	k_5^{off}=0.17	c
Factor Vh	E_5^h, P_5	E_5^{hm}	k_5^{on}=$5.7 \cdot 10^7$	k_5^{off}=0.17	c
Factor Va	E_5, P_5	E_5^m	$k_5^{\text{on}} = 5.7 \cdot 10^7$	k_5^{off}=0.17	c
Factor VIII	Z_8, P_8	Z_8^m	$k_8^{\text{on}} = 5.0 \cdot 10^7$	k_8^{off}=0.17	d
Factor VIIIa	E_8, P_8	E_8^m	$k_8^{\text{on}} = 5.0 \cdot 10^7$	k_8^{off}=0.17	d
Factor II	Z_2, P_2	Z_2^m	$k_2^{\text{on}} = 1.0 \cdot 10^7$	k_2^{off}=5.9	e
Factor IIa	E_2, P_2	E_2^m	$k_2^{*,\text{on}} = 1.0 \cdot 10^7$	$k_2^{*,\text{off}} = 0.2$	f
Factor XI	Z_{11}, P_{11}	Z_{11}^m	$k_{z_{11}}^{\text{on}} = 1.0 \cdot 10^7$	$k_{z_{11}}^{\text{off}}$=0.1	g
Factor XIa	E_{11}, P_{11}^*	E_{11}^m	$k_{e_{11}}^{\text{on}} = 1.0 \cdot 10^7$	$k_{e_{11}}^{\text{off}}$=0.017	h

S12 Table. REACTIONS ON PLATELET SURFACES (a) $k^{\text{cat}}_{z_5^m:e_{10}^m} = 0.046$ sec^{-1} and $K_M = 10.4 \cdot 10^{-9}$ M (32). (b) The rate constants for thrombin activation of fV on platelets are assumed to be the same as in plasma. (c) $k^{\text{cat}}_{z_8^m:e_{10}^m} = 0.023$ sec^{-1} and $K_M = 2.0 \cdot 10^{-8}$ M (25). (d) The rate constants for thrombin activation of fVIII on platelets are assumed to be the same as in plasma. (e) The formation of the tenase and prothrombinase complexes is assumed to be very fast with $K_d = 1.0 \cdot 10^{-10}$ M (33). (f) $k^{\text{cat}}_{z_{10}^m:ten} = 20$ sec^{-1} and $K_M = 1.6 \cdot 10^{-7}$ M (34). (g) $k^{\text{cat}}_{z_2^m:pro} = 30$ sec^{-1} and $K_M = 3.0 \cdot 10^{-7}$ M (35). (h) $k^{\text{cat}}_{z_{11}^m:e_2^m} = 1.3 \cdot 10^{-4}$, $K_M = 50$ nM (26). Rate constants apply also for thrombin-activation of Plt-XIa-XI. (i) $k^{\text{cat}}_{z_9^m:e_{11}^{h,m}} = 0.21$, $K_M = 0.2\mu$M (27, 28). Rate constants apply also for activation of platelet-bound IX by Plt-XIa-XIa.

Reaction	Reactants	Complex	Product	$M^{-1}sec^{-1}$	sec^{-1}	sec^{-1}	Note
Activation (of -, by -)							
(V, Xa)	Z_5^m, E_{10}^m	$Z_5^m : E_{10}^m$	E_5^{hm}	$k^+_{z_5^m:e_{10}^m}$=$1.0 \cdot 10^8$	$k^-_{z_5^m:e_{10}^m}$=1.0	$k^{\text{cat}}_{z_5^m:e_{10}^m}$=$4.6 \cdot 10^{-2}$	a
(V, IIa)	Z_5^m, E_2^m	$Z_5^m : E_2^m$	E_5^m	$k^+_{z_5^m:e_2^m}$=$1.73 \cdot 10^7$	$k^-_{z_5^m:e_2^m}$=1.0	$k^{\text{cat}}_{z_5^m:e_2^m}$= 0.23	b
(Vh, IIa)	E_5^{hm}, E_2^m	$E_5^{hm} : E_2^m$	E_5^m	$k^+_{z_5^m:e_2^m}$=$1.73 \cdot 10^7$	$k^-_{z_5^m:e_2^m}$=1.0	$k^{\text{cat}}_{z_5^m:e_2^m}$= 0.23	b
(VIII, Xa)	Z_8^m, E_{10}^m	$Z_8^m : E_{10}^m$	E_8^m	$k^+_{z_8^m:e_{10}^m}$=$5.1 \cdot 10^7$	$k^-_{z_8^m:e_{10}^m}$=1.0	$k^{\text{cat}}_{z_8^m:e_{10}^m}$=$2.3 \cdot 10^{-2}$	c
(VIII, IIa)	Z_8^m, E_2^m	$Z_8^m : E_2^m$	E_8^m	$k^+_{z_8^m:e_2^m}$=$2.64 \cdot 10^7$	$k^-_{z_8^m:e_2^m}$=1.0	$k^{\text{cat}}_{z_8^m:e_2^m}$= 0.9	d
(X, VIIIa:IXa)	Z_{10}^m, TEN	$Z_{10}^m : TEN$	E_{10}^m	$k^+_{z_{10}^m:ten}$=$1.31 \cdot 10^8$	$k^-_{z_{10}^m:ten}$=1.0	$k^{\text{cat}}_{z_{10}^m:ten}$=20.0	f
(X, VIIIa:IXa*)	Z_{10}^m, TEN^*	$Z_{10}^m : TEN^*$	E_{10}^m	$k^+_{z_{10}^m:ten}$=$1.31 \cdot 10^8$	$k^-_{z_{10}^m:ten}$=1.0	$k^{\text{cat}}_{z_{10}^m:ten}$=20.0	f
(II, Vh:Xa)	Z_2^m, $PROh$	$Z_2^m : PROh$	E_2^m	$k^+_{z_2^m:pro}$= $1.03 \cdot 10^8$	$k^-_{z_2^m:pro}$=1.0	$k^{\text{cat}}_{z_2^m:pro}$=30.0	g
(II, Va:Xa)	Z_2^m, PRO	$Z_2^m : PRO$	E_2^m	$k^+_{z_2^m:pro}$= $1.03 \cdot 10^8$	$k^-_{z_2^m:pro}$=1.0	$k^{\text{cat}}_{z_2^m:pro}$=30.0	g
(XI-XI, IIa)	Z_{11}^m, E_2^m	$Z_{11}^m : E_2^m$	E_{11}^{hm}	$k^+_{z_{11}^m:e_2^m}$ = $2.0 \cdot 10^7$	$k^-_{z_{11}^m:e_2^m}$ = 1.0	$k^{\text{cat}}_{z_{11}^m:e_2^m}$ = $1.3 \cdot 10^{-4}$	h
(IX, XIa)	Z_9^m, E_{11}^{hm}	$Z_9^m : E_{11}^{hm}$	E_9	$k^+_{z_9^m:e_{11}^m}$ = $0.6 \cdot 10^7$	$k^-_{z_9^m:e_{11}^m}$ = 1.0	$k^{\text{cat}}_{z_9^m:e_{11}^m}$ = 0.21	i
Binding (of -, with -)							
(VIIIa, IXa)	E_8^m, E_9^m		TEN	k^+_{ten}=$1.0 \cdot 10^8$	k^-_{ten}=0.01		e
(VIIIa, IXa*)	E_8^m, $E_9^{m,*}$		TEN^*	k^+_{ten}=$1.0 \cdot 10^8$	k^-_{ten}=0.01		e
(Vh, Xa)	E_5^{hm}, E_{10}^m		$PROh$	k^+_{pro}=$1.0 \cdot 10^8$	k^-_{pro}=0.01		e
(Va, Xa)	E_5^m, E_{10}^m		PRO	k^+_{pro}=$1.0 \cdot 10^8$	k^-_{pro}=0.01		e

S13 Table. INHIBITION REACTIONS (a) From (19). (b) From (36). (c) For inhibition of fVa by APC, $k^{\text{cat}}_{e_5^m:APC} = 0.5$ sec^{-1} and $K_M = 12.5 \cdot 10^{-9}$ (37). We assume the same reaction rates for the inhibition of fVIIIa by APC. (d) From (38). (e)From (39). (f) From (40). (g) $K_d = 0.5$ nM and $[PC] = 65$ nM (41). (h)From (42). (i) $k_{PC:TM:e_2^{ec}} = 0.167$ sec^{-1} , $K_M = 0.7 \cdot 10^{-6}$ M (43).

Reaction	Reactants	Product	$M^{-1}sec^{-1}$	sec^{-1}	sec^{-1}	Note
Inactivation (of -, by -)						
(IXa, AT-III)	E_9, AT	$E_9 : AT$		$k^{AT}_{e_9}$=4.8 · 10^2		a
(Xa, AT-III)	E_{10}, AT	$E_{10} : AT$		$k^{AT}_{e_{10}}$=3.5 · 10^3		a
(IIa, AT-III)	E_2, AT	$E_2 : AT$		$k^{AT}_{e_2}$=1.4 · 10^4		a
(XIa, AT-III)	E_{11}, AT	$E_{11} : AT$		$k^{AT}_{e_{11}}$=2.4 · 10^2		a
(XIa:AT, AT-III)	$E_{11} : AT$, AT	$AT : E_{11} : AT$		$k^{AT}_{e_{11}}$=2.4 · 10^2		a
(IXa, ATH)	E_9, ATH	$E_9 : ATH$		$k^{AT}_{e_9}$=5 · 10^5		b
(Xa, ATH)	E_{10}, ATH	$E_{10} : ATH$		$k^{AT}_{e_{10}}$=1.3 · 10^6		b
(IIa, ATH)	E_2, ATH	$E_2 : ATH$		$k^{AT}_{e_2}$=5.3 · 10^6		b
(XIa, ATH)	E_{11}, ATH	$E_{11} : ATH$		$k^{AT}_{e_{11}}$=1 · 10^4		b
(XIa:AT, ATH)	$E_{11} : AT$, ATH	$ATH : E_{11} : ATH$		$k^{in}_{AT:e_{11}}$=1 · 10^4		b
(APC, Va)	APC, E^m_5	none	$k^+_{e^m_5:APC}$ = 1.2 · 10^8	$k^-_{e^m_5:APC}$ = 1.0	$k^{cat}_{e^m_5:APC}$ = 0.5	c
(APC, VIIIa)	APC, E^m_8	none	$k^+_{e^m_8:APC}$ = 1.2 · 10^8	$k^-_{e^m_8:APC}$ = 1.0	$k^{cat}_{e^m_8:APC}$ = 0.5	c
Binding (of -, with -)						
(TFPI, Xa)	$TFPI$,E_{10}	$TFPIa$	$k^+_{tfpia:e_{10}}$=1.6 · 10^7	$k^-_{tfpia:e_{10}}$=3.3 · 10^{-4}		d
(TFPI, Vh)	$TFPI$, E^h_5	$TFPI : E^h_5$	$k^+_{tfpi:e5h}$ = 0.05 · 10^9	$k^-_{tfpi:e5h}$ = 0.0045		e
(TFPI:Xa, Vh)	$TFPIa$, E^h_5	$E^h_5 : TFPI : E_{10}$	$k^+_{tfpi:e5h}$ = 0.05 · 10^9	$k^-_{tfpi:e5h}$ = 0.0045		e
(TFPI:Vh, Xa)	$TFPI : E^h_5$, E_{10}	$E^h_5 : TFPI : E_{10}$	$k^+_{tfpia:e_{10}}$=1.6 · 10^7	$k^-_{tfpia:e_{10}}$=3.3 · 10^{-4}		d
(Xa:Vh, TFPI)	$E_{10} : E^h_5$, $TFPIa$	$E_{10} : E^h_5 : TFPI$	$k^+_{tfpibprohv5}$ = 0.05 · 10^9	$k^-_{tfpibprohv5}$ = 0.0045		e
(Xa:Vh, TFPI)	$E_{10} : E^h_5$, $TFPIa$	$TFPI : E_{10} : E^h_5$	$k^+_{tfpibprohv10}$ = 1.6 · 10^7	$k^-_{tfpibprohv10}$ = 3.3 · 10^-4		d
(TFPIa, TF:VIIa)	$TFPIa$,E^m_7	$TFPIa : E^m_7$	$k^+_{tfpia:e_{10}}$=1.6 · 10^7	$k^-_{tfpia:e_{10}}$=3.3 · 10^{-4}		f
(TM, Thrombin)	TM, E^{ec}_2	$TM : E^{ec}_2$	k^{on}_{TM} = 1.0 · 10^8	k^{off}_{TM} = 5.0 · 10^{-2}		g
(AT-III, Heparin)	AT, Hep	ATH	k^+_{ATH} = 1.0	k^-_{ATH} = 2.77 · 10^7		h
Activation (of -, by -)						
(PC, TM:E^{ec}_2)	$TM : E^{ec}_2$	APC	$k^+_{PC:TM:e^{ec}_2}$ = 1.7 · 10^6	$k^-_{PC:TM:e^{ec}_2}$ = 1.0	$k^{cat}_{PC:TM:e^{ec}_2}$ = 0.16	i

S14 Table. PLATELET TRANSITIONS (a) Estimated from data in (44, 45) as described in (46). (b) Estimated from data in (47) as described in (46). SE=subendothelium.

Reactants	Reactants	Products	$M^{-1}sec^{-1}$	sec^{-1}	Note
Unactivated platelet adhering to SE	PL, SE	PL_a^s	$k_{\text{adh}}^{+}=2\cdot 10^{10}$	$k_{\text{adh}}^{-}=0$	a
Activated platelet adhering to SE	PL_a^v, SE	PL_a^v	$k_{\text{adh}}^{+}=2\cdot 10^{10}$	$k_{\text{adh}}^{-}=0$	a
Platelet activation by platelet in solution	PL, PL_a^v	$2PL_a^v$	$k_{plt}^{\text{act}}=3\cdot 10^{8}$		b
Platelet activation on SE	PL, PL_a^s	PL_a^v, PL_a^s	$k_{plt}^{\text{act}}=3\cdot 10^{8}$		b
Platelet activation by thrombin	PL, E_2	PL_a^v		$k_{e_2}^{\text{act}}=0.50$	b

S3 CONVERSION OF HEPARIN POTENCY TO MOLAR CONCENTRATION

Based on the recommended dosage of heparin treatment (0.3-0.7 U/ml) (48), we use the value of 0.5 U/ml. Based on the information from second international standard for heparin by WHO, the conversion factor will be 130 U/mg (49). By using the mean molecular weight of heparin as 15kDa (50), we can get:

0.5 U/ml * 1/130 mg/U = 0.0038 mg/ml

$0.0038 g/L * 1/15000 mol/g = 2.53 * 10^{-}7M = 253nM$

For the LMWH, since the molecular weight of LMWH varies based on different product (51), we use 5kDa as its molecular weight. Therefore, the concentration of heparin at 100% is determined by:

$0.0038 g/L * 1/5000 mol/g = 2.53 * 10^{-}7M = 759nM$

Both concentrations were set as 100% baseline dosage concentration. For example, when we use 50% concentration of UFH and LMWH, we are using 126.5 nM and 379.5 nM respectively.

S4 LOCAL SENSITIVITY ANALYSIS - METHOD

As in our previous work (52), we again focus on the sensitivity of three special thrombin metrics:

1. Lag time: A measure of how fast the system is turned on, defined as the amount of time required for thrombin to reach 1 nM.

2. Maximum relative rate: A measure of how fast thrombin is produced once the system is turned on, defined as

$$\max_{t>t_{1nM}} \left(\frac{d[\text{thrombin}]}{dt} / [\text{thrombin}]\right).$$

3. Final concentration: The thrombin concentration after 20 minutes of clotting activity.

We examine the sensitivity of these metrics to two types of parameter variations: (i) the plasma levels of seven zymogens and two inhibitors, and (ii) the values of 24 new kinetic parameters that are related to TFPI reactions. We used a derivative-based approach to quantify the sensitivity of each metric with respect to centered difference in the parameters in a range of values (50%, 75%, 100%, 125% and 150% for the plasma level parameters, and 90%, 95%, 100%, 105% and 110% for kinetic parameters). The standard values for each plasma level parameters were set to the initial conditions. Similar to our previous SA results (52), we found that each of the metrics behaved monotonically with respect to varying each plasma level from 50% to 150% of the standard values, as shown in Fig. (S2A-C) and the kinetic parameters from 90% to 110% as shown in Fig. (S3A-C). The min/max values of these monotonic curves shows the change in the thrombin metric due to the factor change. Clotting factor variations had a significant effect on all three thrombin metrics but the largest change in the thrombin metrics due to variations in the kinetic parameters was less than 0.2% and therefore, we did not characterize the sensitivity of these parameters further. For the clotting factors and inhibitors, we quantified their sensitivity by the absolute difference they produced in each metric when considering their extremal values (i.e., 50% and 150%). For each metric, we ranked the parameters by considering their relative absolute difference. We define $x = (x_1, x_2, ..., x_p)$ to be the standard model parameter values and $m_i(x_{j,y\%})$ to be the values of the i-th metric when parameter j is chosen to be y% of its standard value and all other parameters are chosen to be at their standard value. The local sensitivity of the i-th metric to the j-th parameter is then:

$$LS_j^i = \frac{|m_i(x_{j,150\%} - m_i(x_{j,50\%}))|}{\max_k(|m_i(x_{k,150\%} - m_i(x_{k,50\%}))|)}$$

Each sensitivity score, LS, is then a number between 0 and 1 and we use these values to rank the input sensitivities. In our results, we denote LS scores higher than 0.75 with solid black triangles, LS scores from 0.25 to 0.75 as gray triangles, and for LS scores lower than 0.25 we use open triangles. In addition, because the response of the system outputs was monotonic throughout the entire range, we show separately the change in each metric for the 50% increase with the triangle upward and a 50% decrease with a triangle facing downward. Then the y-value of the triangle corresponds to its result on the output.

The local SA results in Fig. (S2D-I) reveal the most influential clotting factors and inhibitors, when perturbed one at a time for each of the three thrombin metrics. Fig. (S2D) shows that FVIII and FX have the greatest effect on the lag time, where an increase in either FVIII or FX levels by 50% leads to an approximately 10% decrease in the lag time from baseline. This is seen with the solid black (LS scores above 0.75), upward-facing (increase in factor level) triangles, with y-value near -10% showing the decrease in lag time. Comparing with sesitivity results from our old model((52)), we see an increased sensitivity to TFPI, where a decrease/increase by 50% leads to about a 8% decrease/5% increase in the lag time from baseline, respectively, although the TFPI LS score still does not reach 0.75. Fig. (S2E) shows that variations in FVIII, FIX, and FX have the largest effect on the maximum relative rate of thrombin generation, and this metric still has low sensitivity to TFPI. These findings are the same as in our previous results and make sense since these factors influence the rate of formation of the tenase complex on platelets, which affects the amplification stage of coagulation, and the inhibitory effect by TFPI does not alter such amplification process. It also indicates that new TFPI inhibitory reactions does not have significant influence towards the rate at which thrombin is being made. Fig. (S2F) shows that the final concentration metric is sensitive only to prothrombin (FII) as was found previously((52)). The corresponding LS scores are shown in Fig. (S2H-I).

Fig.(S3) demonstrates the local SA results for each of kinetic parameters that are related to TFPI reactions. Forward and reverse rate for each of the reaction are varied by 10% and change in lag time, maximum relative rate and final concentrations were observed. The results indicate that slight perturbation in reaction kinetics has minimal effect towards these three thrombin metrics, where none of the kinetic parameter caused more than 1% change from baseline in each cases. Such insensitiveness of the kinetic parameters, however, indicates the tolerance of the model towards the possible error in the kinetic parameters retrieved from experimental design.

S5 OTHER FIGURES

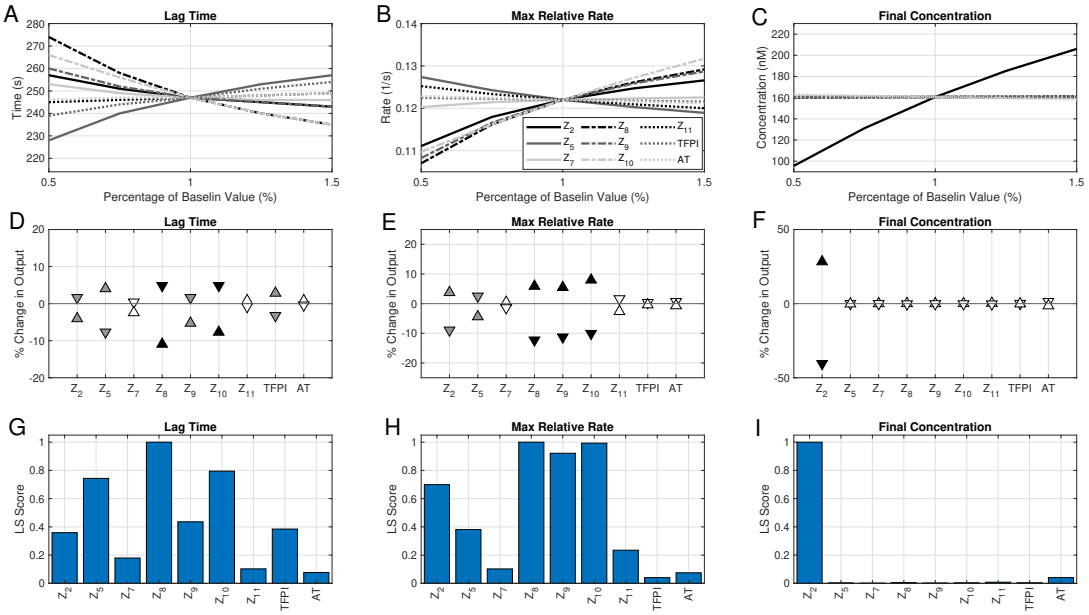

Figure S2: Local sensitivity analysis of clotting factor levels on thrombin metrics. The initial conditions of clotting factor and inhibitor levels were varied between 50% and 150% of their baseline values. Shown are (A,B,C) the amplitude change in lag time, maximum relative rate, and final thrombin concentration, (D,E,F) the percentage change in each of the metrics, and (G,H,I) the LS scores for each metric and for each species. Solid black triangles represent the species with LS score higher than 0.75, gray triangles for LS scores from 0.25 to 0.75, and open triangles for LS lower than 0.25. The arrow direction indicates if the variable was increased or decreased.

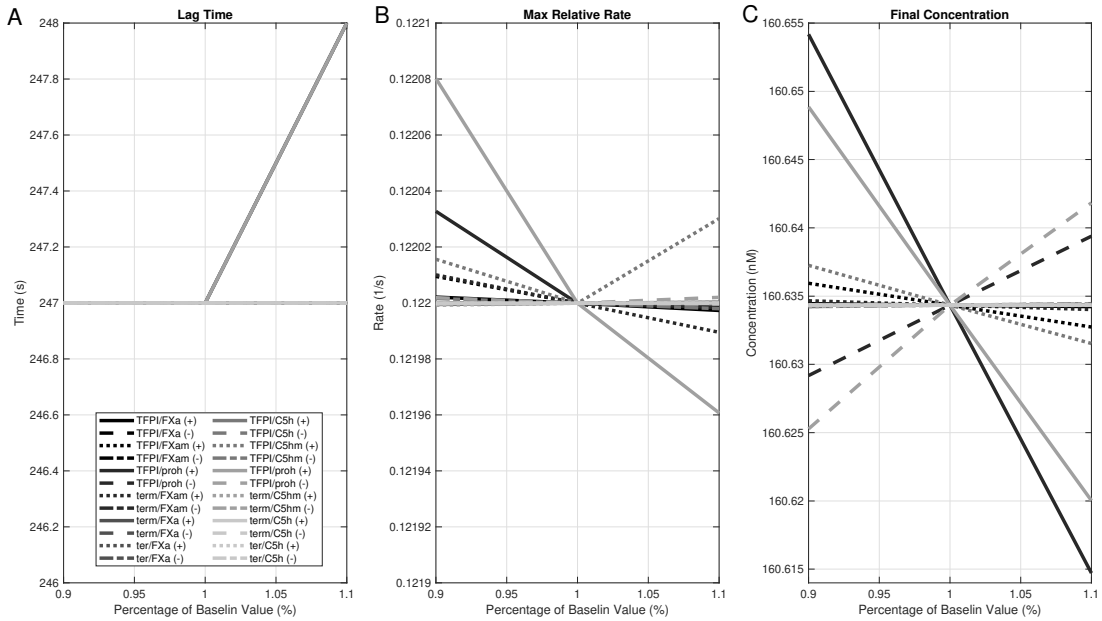

Figure S3: Local sensitivity analysis of TFPI-related kinetic rates on thrombin metrics. The new kinetic parameters were varied between 90% and 110% of their baseline values. Shown are (A,B,C) the amplitude of the changes in the lag time, maximum relative rate and final thrombin concentration due to the kinetic parameter variations. The plus/minus sign indicates the association/dissociation rate, respectively. Lower case *m* represents the components that are bound to platelet surface. The forward slash shows which two components are interacting each other, while the "ter" and "term" indicates interactions that involve a ternary complex and whether the species is in plasma or bound to the platelet surface, respectively. For example: term/FXa (+) indicates the rate of association between the platelet-bound TFPI:FV-h complex and the fluid phase FXa to form the ternary complex FXa:TFPI:FV-h.

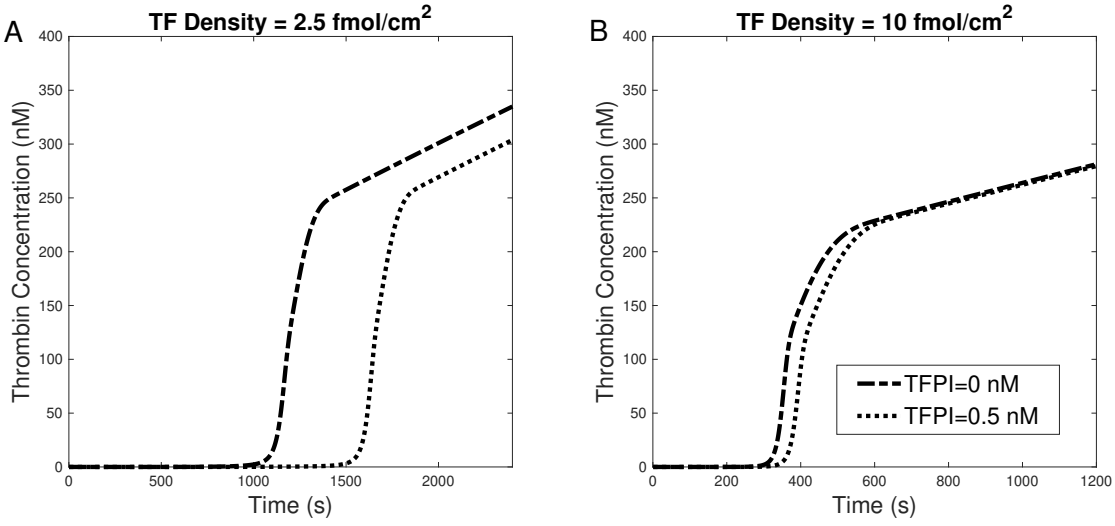

Figure S4: Thrombin generation time courses under different TFPI levels (0 nM and 0.5 nM) plotted in linear scale. TF level is varied by 2.5 fmol/cm^2 (A) and 10 fmol/cm^2 (B). Shear rate is fixed at 100/s.

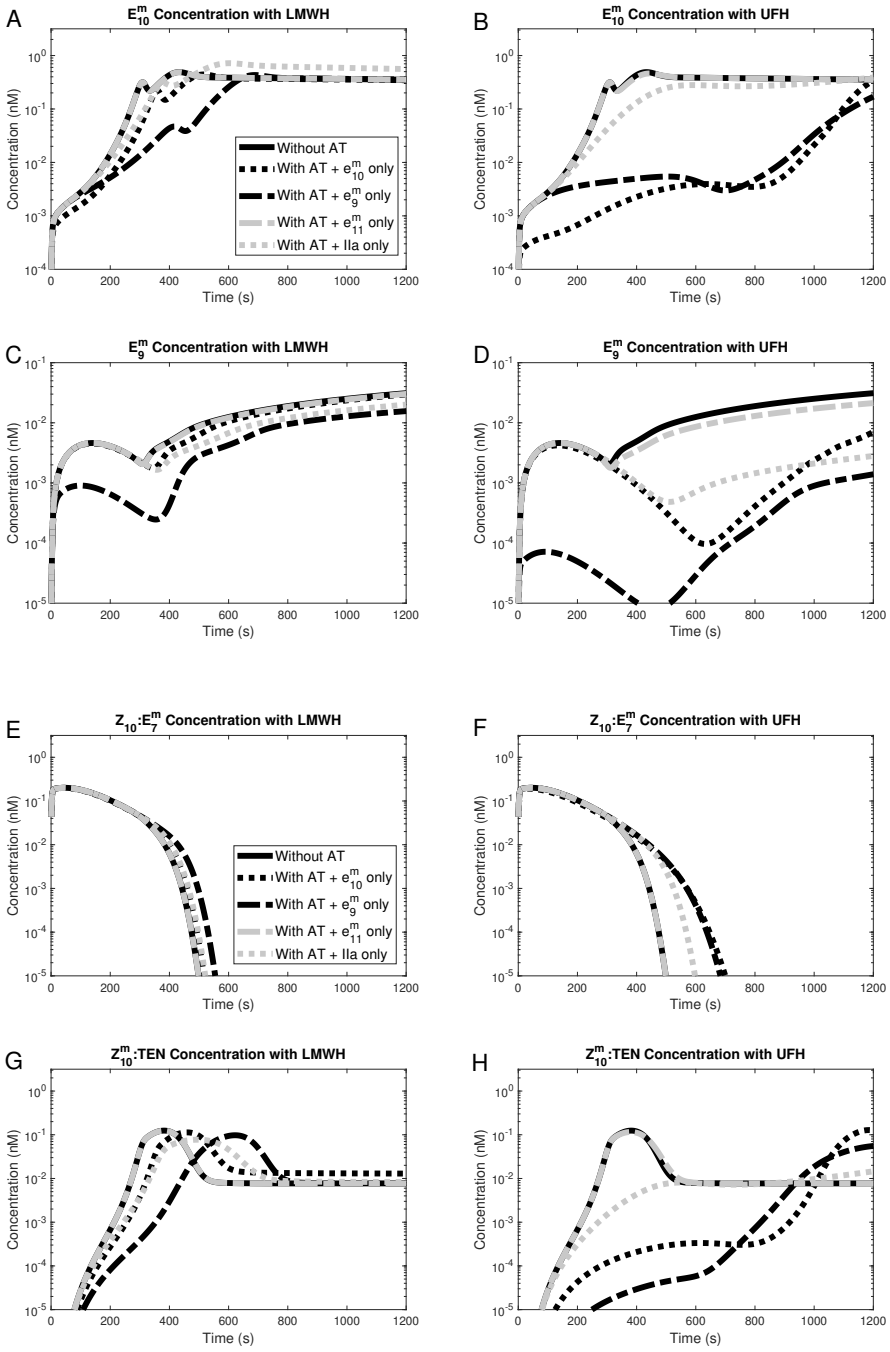

Figure S5: FXa concentration in the presence of LMWH (A) or UFH (B), FIXa concentration in the presence of LMWH (C) or UFH (D), FX:TF:VIIa concentration in the presence of LMWH (E) or UFH (F), and FX:tenase concentration in the presence of LMWH (G) or UFH (H). The time course is obtained from simulations in which we turn off all the AT-mediated inactivation reactions and then allow inhibition of FXa, FIXa, FXIa and thrombin, individually and one by one. Each curve thus shows thrombin/tenase generation when there is either no or only one inactivation reaction that exists in the system. TF density was set to 15 fmol/cm^2 and shear rate was set to 100/s. Heparin concentration is fixed to 100% of the standard therapeutic concentration.

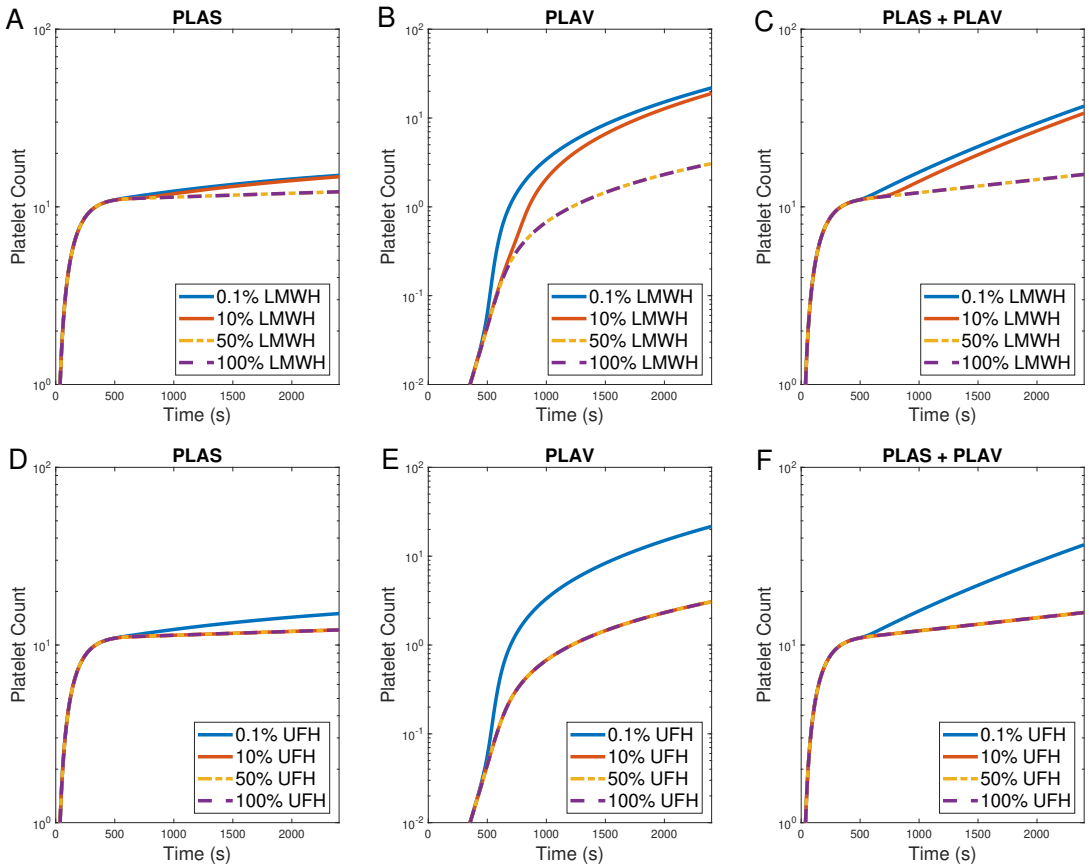

Figure S6: Subendothelium-attacehed platelet count (PLAS) and paltelet-attached-activated platelet count (PLAV) time course with varied LMWH treatmemnt (A-C) or UFH treatment (D-F). TF level is fixed to 6 $fmol/cm^2$. We examined how heparin in the system might affect platelet deposition. We specifically looked at two types of platelets: those that are activated and bound to subendothelium (PLAS), and those that are activated and bound to deposited platelets (PLAV), and their sum. The platelets accumulate on the subendothelium (SE) and PLAV eventually plateaus due to the limited space at the SE, whereas platelets above the injury site will continue to grow. Increasing the heparin concentrations led to decreases in both platelet species through time.This is because by increasing amount of heparin, it can greatly reduce the thrombin in the reaction zone, which leads to reduced amount of platelet to be activated by thrombin. Such a reduction can cause a shift from platelet-bound platelet to subendothelium-bound platelet. The increase in subendothelium-bound platelet will physically cover up the surface, which can negatively influence the initiation phase of coagulation.

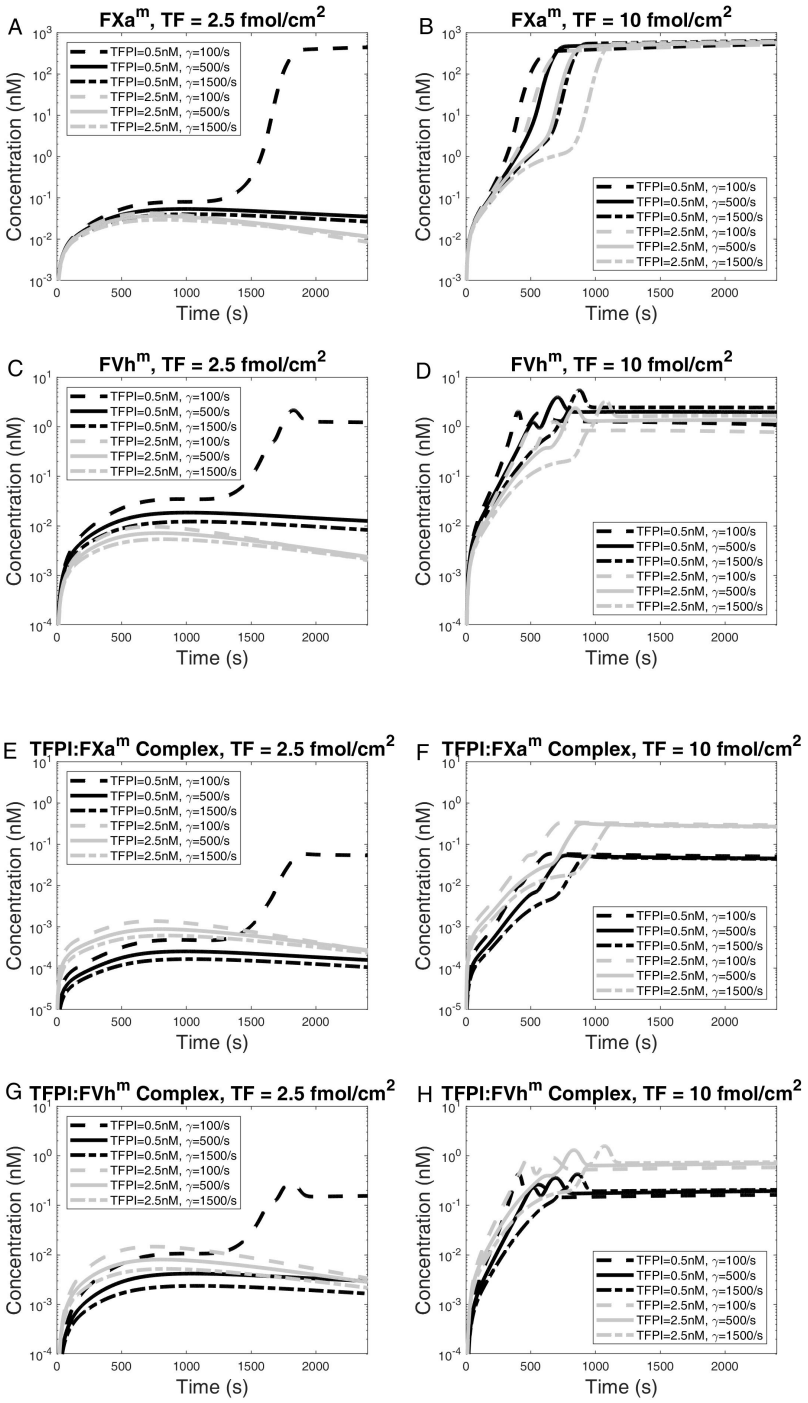

Figure S7: Concentration time course of platelet surface bound FXa, FV-h, and their complexes with TFPI. TF level is varied by 2.5 fmolcm% (A,C,E,G) and 10 fmol/cm^2 (B,D,F,H). Under each TF level, TFPI level is varied by 0.5 nM and 2.5 nM, and shear rate is varied by 100/s, 500/s and 1500/s.

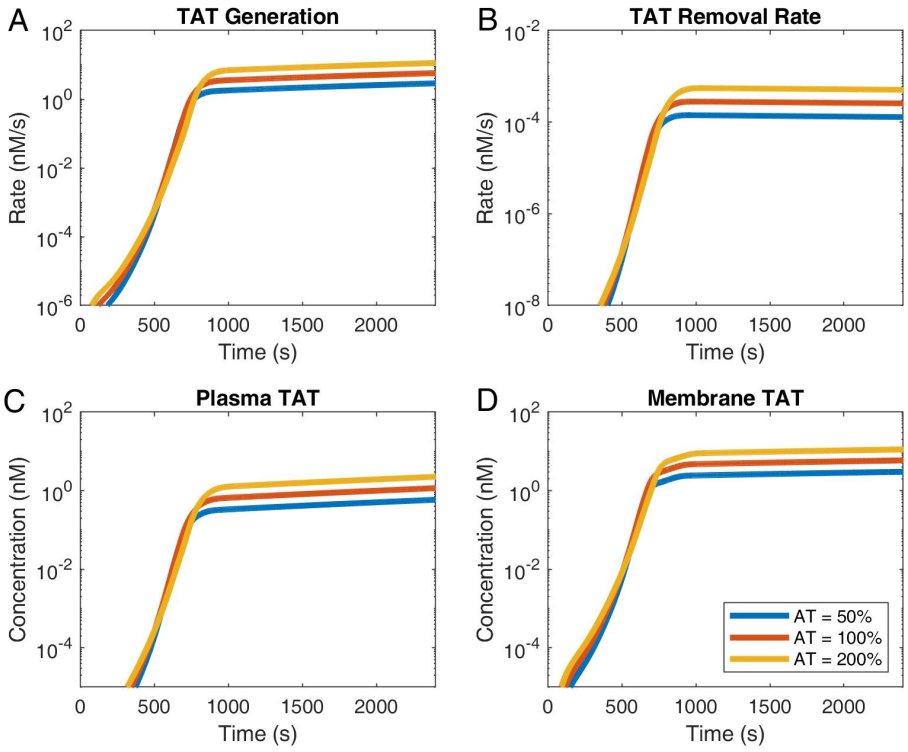

Figure S8: Instantaneous generation and removal of TAT (A,B), and accumulative concentration of TAT in plasma (C) and on the platelet membrane (D). TF level is fixed to 5 fmol/cm^2, and shear rate is fixed to 100/s.

REFERENCES

1. Kuharsky, A. L., and A. L. Fogelson, 2001. Surface-Mediated Control of Blood Coagulation: The Role of Binding Site Densities and Platelet Deposition. *Biophysical Journal* 80:1050–1074. https://linkinghub.elsevier.com/retrieve/pii/S0006349501760857.

2. Fogelson, A. L., and N. Tania, 2005. Coagulation under Flow: The Influence of Flow-Mediated Transport on the Initiation and Inhibition of Coagulation. *Pathophysiol Haemos Thromb* 34:91–108. https://www.karger.com/Article/FullText/89930.

3. Fogelson, A., Y. Hussain, and K. Leiderman, 2012. Blood Clot Formation under Flow: The Importance of Factor XI Depends Strongly on Platelet Count. *Biophysical Journal* 102:10–18. https://linkinghub.elsevier.com/retrieve/pii/S0006349511013142.

4. Turitto, V. T., and E. F. Leonard, 1972. Platelet adhesion to a spinning surface. *Trans. Amer. Soc. Artif. Int. Organs* 18:348–54.

5. Young, M., P. Carroad, and R. Bell, 1980. Estimation of diffusion coefficients of proteins. *Biotech and Bioeng* 22:947–955.

6. Mann, K., M. Nesheim, W. Church, P. Haley, and S. Krishnaswamy, 1990. Surface-dependent Reactions of the Vitamin K-dependent enzyme complexes. *Blood* 76:1–16.

7. Mann, K., E. Bovill, and S. Krishnaswamy, 1991. Surface-dependent reactions in the propagation phase of blood coagulation. *Ann. N. Y. Acad. Sci.* 614:63–75.

8. Morrissey, J. H., 1995. Tissue Factor Modulation of Factor VIIa Activity: Use in Measuring Trace Levels of Factor VIIa in Plasma,. *Thromb. Haemost.* 74:185–188.

9. Novotny, W., S. Brown, J. Miletich, D. Rader, and G. Broze, 1991. Plasma antigen levels of the lipoprotein-associated coagulation inhibitor in patient samples. *Blood* 78:387–93.

10. Weiss, H. J., 1975. Platelet Physiology and Abnormalities of Platelet Function (Part 1). *New Engl. J. Med.* 293:531–541.

11. Walsh, P. N., 1994. Platelet-Coagulant Protein Interactions. *In* R. W. Colman, J. Hirsh, V. J. Marder, and E. W. Salzman, editors, Hemostasis and Thrombosis: Basic Principles and Clinical Practice, J.B. Lippincott Company, Philadelphia, PA, 629–651. 3d edition.

12. Nesheim, M. E., D. D. Pittman, J. H. Wang, D. Slonosky, A. R. Giles, and R. J. Kaufman, 1988. The binding of S-labeled recombinant Factor VIII to activated and unactivated human platelets. *J Biol Chem* 263:16467.

13. Ahmad, S., R. Rawala-Sheikh, and P. Walsh, 1989. Comparative interactions of Factor IX and Factor IXa with human platelets. *Journal of Biological Chemistry* 264:3244–3251.

14. Mann, K., S. Krishnaswamy, and J. Lawson, 1992. Surface-dependent Hemostasis. *Semin Hematol* 29:213–26.

15. Baglia, F., B. Jameson, and P. Walsh, 1995. Identification and Characterization of a Binding Site for Platelets in the Apple 3 domain of coagulation Factor XI. *J Biol Chem* 270:6734–40.

16. Miller, T., D. Sinha, T. Baird, and P. Walsh, 2007. A Catalytic Domain Exosite (Cys^{527}-Cys^{542}) in Factor XIa mediates binding to a site on activated platelets. *Biochemistry* 46:14450–60.

17. Tracy, P., L. L. Eide, E. J. Bowie, and K. G. Mann, 1982. Radioimmunoassay of factor V in human plasma and platelts. *Blood* 60:59–63.

18. Hubbell, J. A., and L. V. McIntire, 1986. Platelet Active Concentration Profiles Near Growing Thrombi. A Mathematical Consideration. *Biophys J* 50:937–945.

19. Olson, S. T., I. Björk, and J. D. Shore, 1993. [30] Kinetic characterization of heparin-catalyzed and uncatalyzed inhibition of blood coagulation proteinases by antithrombin. *In* Methods in Enzymology, Elsevier, volume 222, 525–559. https://linkinghub.elsevier.com/retrieve/pii/007668799322033C.

20. Butenas, S., and K. Mann, 1996. Kinetics of Human Factor VII activation. *Biochemistry* 35:1904–1910.

21. Limentani, S. A., B. C. Furie, and B. Furie, 1994. The Biochemistry of Factor IX. *In* R. Colman, J. Hirsh, V. Marder, and E. Salzman, editors, Hemostasis and Thrombosis: Basic Principles and Clinical Practice, J.B. Lippincott Company, Philadelphia, PA, 94–108. 3d edition.

22. Nemerson, Y., 1992. The Tissue Factor Pathway of Blood Coagulation. *Semin Hematol* 29:170–176.

23. Monkovic, D. D., and P. B. Tracy, 1990. Functional Characterization of Human Platelet-released Factor V and its Activation by Factor Xa and Thrombin,. *J Biol Chem* 265:17132–40.

24. Hill-Eubanks, D., and P. Lollar, 1990. von Willibrand factor is a cofactor for thrombin-catalyzed cleavage of the Factor VIII light chain. *J Biol Chem* 265:17854–8.

25. Lollar, P., G. Knutson, and D. Fass, 1985. Activation of Porcine Factor VIII:C by Thrombin and Factor Xa. *Biochemistry* 24:8056–8064.

26. Gailani, D., and G. Broze Jr., 1991. Factor XI activation in a revised model of blood coagulation. *Science* 253:909–12.

27. Gailani, D., D. Ho, M. F. Sun, Q. Cheng, and P. N. Walsh, 2001. Model for a Factor IX activation complex on blood platelets: dimeric conformation of Factor XIa is essential. *Blood* 97:3117–22.

28. Sinha, D., M. Marcinkiewicz, D. Navaneetham, and P. Walsh, 2007. Macromolecular substrate-binding exosite on both the heavy and light chains of Factor XIa mediate the formation of the Michaelis Complex required for Factor IX activaiton. *Biochemistry* 46:9830–9.

29. Krishnaswamy, S., K. C. Jones, and K. G. Mann, 1988. Prothrombinase Complex Assembly. Kinetic Mechanism of Enzyme Assembly on Phospholipid Vesicles. *J Biol Chem* 263:3823–3834.

30. Mann, K. G., 1994. Prothrombin and thrombin. *In* R. Colman, J. Hirsh, V. Marder, and E. Salzman, editors, Hemostasis and Thrombosis: Basic Principles and Clinical Practice, J.B. Lippincott Company, Philadelphia, PA, 184–199. 3d edition.

31. Greengard, J., M. Heeb, E. Ersdal, P. Walsh, and J. Griffin, 1986. Binding of coagulation Factor XI to washed human platelets. *Biochemistry* 25:3884–90.

32. Monkovic, D., and P. Tracy, 1990. Activation of human Factor V by Factor Xa and thrombin. *Biochemistry* 29:1118.

33. Mann, K. G., 1987. The assembly of blood clotting complexes on membranes. *TIBS* 12:229–233.

34. Rawala-Sheikh, R., S. Ahmad, B. Ashby, and P. N. Walsh, 1990. Kinetics of coagulation Factor X activation by platelet-bound Factor IXa. *Biochemistry* 29:2606–11.

35. Nesheim, M. E., R. P. Tracy, P. B. Tracy, D. S. Boskovic, and K. G. Mann, 1992. Mathematical Simulation of Prothrominase. *Methods Enzymol.* 215:316–328.

36. Olson, S. T., R. Swanson, E. Raub-Segall, T. Bedsted, M. Sadri, M. Petitou, J.-P. Hérault, J.-M. Herbert, and I. Björk, 2004. Accelerating ability of synthetic oligosaccharides on antithrombin inhibition of proteinases of the clotting and fibrinolytic systems Comparison with heparin and low-molecular-weight heparin. *Thrombosis and haemostasis* 92:929–939.

37. Solymoss, S., M. Tucker, and P. Tracy, 1988. Kinetics of inactivation of membrane-bound Factor Va by activated protein C. Protein S modulates Factor Xa protection. *J Biol Chem* 263:14884–90.

38. Jesty, J., T.-C. Wun, and A. Lorenz, 1994. Kinetics of the Inhibition of Factor Xa and the Tissue Factor-Factor VIIa Complex by the Tissue Factor Pathway Inhibitor in the Presence and Absence of Heparin. *Biochemistry* 33:12686–12694. https://pubs.acs.org/doi/abs/10.1021/bi00208a020.

39. Maroney, S. A., and A. E. Mast, 2015. New insights into the biology of tissue factor pathway inhibitor. *J Thromb Haemost* 13:S200–S207. https://onlinelibrary.wiley.com/doi/10.1111/jth.12897.

40. Jesty, J., T. Wun, and A. Lorenz, 1994. Kinetics of the Inhibition of Factor Xa and the Tissue Factor-Factor VIIa Complex by the Tissue Factor Pathway Inhibitor in the Presence and Absence of Heparin. *Biochemistry* 33:12686–12694.

41. Griffin, J. H., 2001. Control of Coagulation Reactions. *In* E. Beutler, B. Coller, M. Lichtman, T. Kipps, and U. Seligsohn, editors, Williams Hematology, McGraw Hill, New York, 1435–1447.

42. Olson, S., I. Björk, R. Sheffer, P. Craig, J. Shore, and J. Choay, 1992. Role of the antithrombin-binding pentasaccharide in heparin acceleration of antithrombin-proteinase reactions. Resolution of the antithrombin conformational change contribution to heparin rate enhancement. *Journal of Biological Chemistry* 267:12528–12538. https://linkinghub.elsevier.com/retrieve/pii/S0021925818423095.

43. Broze, G., and J. Miletich, 1994. Biochemistry and Physiology of Protein C, Protein S, and Thrombomodulin. *In* R. W. Colman, J. Hirsh, V. J. Marder, and E. W. Salzman, editors, Hemostasis and Thrombosis: Basic Principles and Clinical Practice, Lippincott Company, Philadelpha, 259–276.

44. Turitto, V. T., and H. R. Baumgartner, 1979. Platelet Interaction with Subendothelium in Flowing Rabbit Blood: Effect of Blood Shear Rate. *Microvasc. Res.* 17:38–54.

45. Turitto, V. T., H. J. Weiss, and H. R. Baumgartner, 1980. The Effect of Shear Rate on Platelet Interaction with Subendothelium Exposed to Citrated Human Blood. *Microvasc. Res.* 19:352–365.

46. Kuharsky, A., and A. Fogelson, 2001. Surface-mediated Control of Blood Coagulation: The Role of Binding Site Densities and Platelet Deposition. *Biophys J* 80:1050–1074.

47. Gear, A. R. L., 1994. Platelet adhesion, shape change, and aggregation: rapid initiation and signal transduction events. *Can. J. Physiol. Pharmacol.* 72:285–94.

48. Byun, J.-H., I.-S. Jang, J. W. Kim, and E.-H. Koh, 2016. Establishing the heparin therapeutic range using aPTT and anti-Xa measurements for monitoring unfractionated heparin therapy. *Blood Research* 51:171. https://synapse.koreamed.org/DOIx.php?id=10.5045/br.2016.51.3.171.

49. Bangham, D., and M. V. Mussett, 1959. The Second International Standard for Heparin. *Bulletin of the World Health Organization* 20:1201.

50. Linhardt, R. J., 2016. Heparin and anticoagulation. *Frontiers in Bioscience* 21:1372–1392. https://imrpress.com/journal/FBL/21/7/10.2741/4462.

51. Hirsh, J., and M. Levine, 1992. Low molecular weight heparin. *Blood* 79:1–17. https://ashpublications.org/blood/article/79/1/1/173040/Low-molecular-weight-heparin.

52. Link, K. G., M. T. Stobb, J. Di Paola, K. B. Neeves, A. L. Fogelson, S. S. Sindi, and K. Leiderman, 2018. A local and global sensitivity analysis of a mathematical model of coagulation and platelet deposition under flow. *PLoS ONE* 13:e0200917. https://dx.plos.org/10.1371/journal.pone.0200917.